

Alma Mater Studiorum - Università di Bologna

Facoltà di Scienze Matematiche Fisiche e Naturali

Scuola di Dottorato in Scienze Biologiche, Biomediche e Biotecnologiche
Dottorato di Ricerca in Biologia Funzionale dei Sistemi Cellulari e Molecolari
Settore Disciplinare: BIO/19 – Microbiologia Generale

Caratterizzazione fisiologica di *Pseudomonas pseudoalcaligenes* KF707, crescita in biofilm e risposta a stress ambientali

(Physiological characterization of *Pseudomonas pseudoalcaligenes* KF707, biofilm and environmental stress response)

PhD Student:

Dott.ssa VALENTINA TREMAROLI

Tutor:

Chiar. mo Prof. DAVIDE ZANNONI

PhD Coordinator:

Chiar. mo Prof. VINCENZO SCARLATO

Alma Mater Studiorum - Università di Bologna

Facoltà di Scienze Matematiche Fisiche e Naturali

Scuola di Dottorato in Scienze Biologiche, Biomediche e Biotecnologiche
Dottorato di Ricerca in Biologia Funzionale dei Sistemi Cellulari e Molecolari
Settore Disciplinare: BIO/19 – Microbiologia Generale

Caratterizzazione fisiologica di *Pseudomonas pseudoalcaligenes* KF707, crescita in biofilm e risposta a stress ambientali

(Physiological characterization of *Pseudomonas pseudoalcaligenes* KF707, biofilm and environmental stress response)

PhD Student:

Dott.ssa VALENTINA TREMAROLI

Tutor:

Chiar. mo Prof. DAVIDE ZANNONI

PhD Coordinator:

Chiar. mo Prof. VINCENZO SCARLATO

Key words: Ps. pseudoalcaligenes KF707, biofilm, heavy metals, selenite, tellurite

Academic Years 2004/2006

Abbreviations

λ	wave length
2-DE	two-dimensional electrophoresis
ACN	acetonitrile
Amp	ampicillin
BSA	bovine serum albumine
BSO	buthionine sulfoximine
CBD	Calgary biofilm device
CFU	colony forming units
CLSM	confocal laser scanning microscopy
DCFH-DA	2',7'-dichlorodihydrofluorescein diacetate
DDTC	diethyldithiocarbamate
DEPC	di-ethyl-pyrocabonate
Diamide	diazenedicarboxylic acid bis-N,N-dimethylamide
DMSO	dimethylsulfoxide
DTT	dithiothreitol
EPS	esopolysaccharide
GSH/GSSG	reduced/oxidized glutathione
IEF	isoelectric focusing
Km	kanamycin
LB	Luria-Bertani medium
LC/MS/MS	liquid chromatography/mass spectroscopy/ mass spectroscopy
MALDI-TOF	matrix-assisted laser desorption ionization – time-of-flight
MBC	minimum bactericidal concentration
MBEC	minimum biofilm eradication concentration
MIC	minimum inhibitory concentration
MSM	minimal salt medium
OD₆₆₀	optical density at 660 nm
PAGE	polyacrylamide gel electrophoresis
PBS	phosphate buffered saline
PCB	polychlorinated biphenyl
PMSF	phenylmethyl-sulfonyl fluoride

PQ²⁺, paraquat	1,1'-4,4'-bipyridinium dichloride
ROS	reactive oxygen species
RSH	reduced thiols
SA	sucrose-asparagine medium
SDS	sodium dodecyl sulfate
sHsp	small heat shock protein
SOD	superoxide dismutase
tBH	tert-butyl hydroperoxide
Tc	tetracyclin
TEM	transmission electron microscopy
TF	trigger factor
TPM	thiopurine methyltransferase
X/Xox	xanthine/xanthine oxidase
X-Gal	5-bromo-4-chloro-3-indolyl- β -D-galactopyranoside

Table of contents

Preface	1
General material and methods	3
Bacterial strains, media and growth conditions	3
Genomic DNA extraction	6
RNA isolation	6
DNA manipulation and genetic techniques	7
Southern and Northern blot analyses	7
DNA sequencing and sequence analysis	8
Conjugation	8
Construction of <i>Ps. pseudoalcaligenes</i> KF707 genomic library	10
Construction of <i>Ps. pseudoalcaligenes</i> KF707 miniTn5 transposon mutant library	10
Protein extraction and two-dimensional gel electrophoresis (2-DE)	10
MALDI-TOF and LC/MS/MS analyses	11
Chapter 1	13
<i>Exploring biofilm formation in Pseudomonas pseudoalcaligenes</i> KF707: nutritional requirements and role of the CheA histidine kinase	13
Introduction	13
Material and methods	17
Bacterial strains and growth conditions	17
Molecular characterization of the <i>cheA::Tn5</i> and <i>cheA::Km</i> mutants	17
Biofilm growth conditions	18
Biofilm and planktonic growth curves	18
Confocal laser scanning microscopy (CLSM)	19
Motility assays	20
Chemotaxis assay	21
Transmission electron microscopy	21
Sample preparation for two-dimensional gel electrophoresis (2-DE) and MALDI-TOF analysis	21
Results	22
Characterization of <i>Ps. pseudoalcaligenes</i> KF707 biofilm development	22
Influence of media composition on biofilm formation	24
Characterization of biofilm formation in a <i>cheA::Tn5</i> mutant	26
Assessing the role of <i>cheA</i> in biofilm formation	29
The <i>cheA</i> mutants are impaired in chemotaxis	29
Motile behaviour in KF707 wild type and mutant strains	30
Tn5 transposon and Km insertion in the <i>cheA</i> gene do not affect flagellum number, position or structure	32
Proteome analysis of planktonic protein profiles of <i>Pseudomonas pseudoalcaligenes</i> KF707 wild type and <i>cheA</i> mutants	33
Discussion	36

Chapter 2	41
<i>Tolerance of Pseudomonas pseudoalcaligenes KF707 biofilm and planktonic cells to metals</i>	41
Introduction	41
Material and methods	46
Bacterial strains and growth conditions	46
Stock solutions of antibiotics and metals	46
Stock solution of neutralizer	46
Biofilm cultivation and metal susceptibility testing	47
Results	50
Biofilm formation	50
Definition of MIC, MBC and MBEC values for biocide susceptibility testing	51
Susceptibility of <i>Ps. pseudoalcaligenes</i> KF707 biofilm and planktonic cells to antibiotics and metal compounds	52
Selenite and tellurite transformation in <i>Ps. pseudoalcaligenes</i> KF707 biofilm and planktonic cells	62
Discussion	63
Chapter 3	71
<i>Evidence for the generation of reactive oxygen species and absence of a tellurite-mediated adaptive response to oxidative stress in cells of Pseudomonas pseudoalcaligenes KF707</i>	71
Introduction	71
Material and methods	74
Bacterial strains and growth conditions	74
Determination of basal resistance levels to tellurite and oxidants	74
Adaptation and cross-protection experiments	74
In vivo detection of ROS	75
Determination of reduced thiol (RSH) content	75
Detection of tellurite uptake	76
Preparation of cell lysates	76
Characterization of SOD activity by gel staining	76
Quantification of SOD activity by xanthine/xanthine oxidase-cytochrome <i>c</i> assay	77
Results	78
Effects of oxidants on ROS production	78
Adaptive and cross-protective responses against oxidative stress-induced killing	80
Effect of tellurite and diamide on RSH content	82
Effects of glutathione synthesis on tellurite toxicity	83
Effect of oxidants on SOD activity	84
Discussion	86
Chapter 4	91
<i>Global analysis of cellular factors and responses involved in Pseudomonas pseudoalcaligenes KF707 tolerance to tellurite</i>	91
Introduction	91
Material and methods	93
Growth of <i>Ps. pseudoalcaligenes</i> KF707 in the presence of potassium tellurite	93

Protection experiments	93
Northern blot analysis of <i>sodB</i> gene expression	94
Sample preparation for two-dimensional gel electrophoresis (2-DE) and matrix assisted laser desorption ionization-time of flight mass spectrometry	94
Results	95
Effects of tellurite on growth	95
Effects of selenite and arsenite on tellurite toxicity	96
Induction of <i>sodB</i> gene by tellurite and selenite	99
Proteomic response to tellurite adaptation	100
Discussion	103
Chapter 5	109
<i>Isolation and characterization of a tellurite-resistance genetic determinant from Pseudomonas pseudoalcaligenes KF707</i>	109
Introduction	109
Material and methods	114
Bacterial strains and growth conditions	114
MIC determination	114
Amplification of a <i>tpm</i> gene fragment from <i>Ps. pseudoalcaligenes</i> KF707 genome	114
Shotgun cloning strategy for the isolation of the <i>tpm</i> full-length gene	115
Screening of KF707 genomic DNA library and <i>tpm</i> subcloning	115
Northern blot analysis of <i>tpm</i> gene expression	116
Insertional mutagenesis of the <i>tpm</i> gene	116
Results	117
Isolation and characterization of <i>Ps. pseudoalcaligenes</i> KF707 <i>tpm</i> sequence	117
Role of <i>Ps. pseudoalcaligenes</i> KF707 TPM enzyme in tellurite resistance	121
Expression of <i>tpm</i> gene in <i>Ps. pseudoalcaligenes</i> KF707 cells exposed to tellurite and selenite	123
Discussion	124
Conclusions	127
References	133
Sitography	145

Preface

The release of organic and inorganic pollutants as a result of industrialization is an important environmental problem, which has an impact on both human health and economy. Remediation of soil and sediments often requires excavation and washing procedures that, although effective, are expensive and produce residual toxicity affecting the revegetation of treated sites. In this respect, remediation of polluted sites by living organisms, that is to say, bioremediation, may provide new cost-effective, sustainable and successful strategies as alternatives to chemical/physical procedures.

Numerous organic xenobiotic compounds have been found to be susceptible to microbial degradation and in most cases the catabolic pathways and their regulation have been characterized. Instead, removal of toxic metals is a particularly difficult task because metals cannot be degraded. Bacteria-based bioremediation requires that microorganisms are active in the presence of the target contaminant, as well as other contaminants. Toxic metals are known to influence biological remediation processes in both aerobic and anaerobic conditions, thus posing a limit to bioremediation efficacy. The presence of both organic xenobiotics and toxic metals, that is co-contamination, is a widespread environmental problem, corresponding to a high percentage of the hazardous waste sites. To improve biodegradation in co-contaminated sites, the use of metal-resistant bacteria has been proposed due to the fact that they can reduce bioavailability of metals (i.e. by immobilization) and/or protect indigenous bacterial communities from the noxious effects. The understanding of metal toxicity to strains with degradative abilities such as *Pseudomonas pseudoalcaligenes* KF707 is thus particularly appealing.

Numerous toxicological studies have revealed that bacteria possess a copious number of specific resistance determinants that enable them to cope with metal toxicity. However, existing knowledge of the mechanisms of metal toxicity and microbial responses is incomplete, as it mostly derives from the characterization of free-suspended (planktonic) microbial communities. Indeed, little is known about the mechanisms used by biofilms to counteract metal

toxicity, albeit biofilm is widely considered as the bacterial default mode of growth in natural environments (Costerton *et al.* 1994, Costerton *et al.* 1995).

Pseudomonas pseudoalcaligenes KF707 is a soil bacterium known for its ability to degrade polychlorinated biphenyls (PCBs), that are persistent environmental xenobiotics and the object of environmental and public health concerns. KF707 is a robust environmental microorganism, able to grow in the presence of high concentrations of the toxic metalloid tellurite. Information regarding the degradative abilities of *Ps. pseudoalcaligenes* KF707 is limited to studies in planktonic cultures. However, it is recognized that biofilms provide distinct physiological traits that enhance the degradation and/or removal of pollutants from the environment and increase the capability of adaptation and survival to environmental stresses. Bacterial properties such as chemotaxis, surface adherence and biofilm formation have not been addressed in previous studies concerning *Ps. pseudoalcaligenes* KF707 physiology, although these properties are likely to improve environmental fitness during colonization of favourable and polluted niches. Moreover, toxicological studies concerning the ability of this bacterium to survive metal toxicity have not been reported thus far.

The aim of this study was to investigate relevant properties of *Ps. pseudoalcaligenes* KF707 other than the ability to co-metabolize toxic organic xenobiotics. In particular, the mechanisms of biofilm development, the tolerance to toxic metals in both biofilm and free-suspended mode of growth and the global factors and cellular responses involved in tolerance to tellurite were investigated.

Note:

The results generated from this thesis have been divided into five chapters, each containing a brief introduction, a material and methods section relevant to the work described, a results and a discussion section. In order to avoid repetitions, all methods that were used generally throughout the study are described in a General material and methods chapter and references follow at the end of the manuscript.

General materials and methods

Bacterial strains, media and growth conditions

All strains, plasmids and primers used in this work are listed in Table 1.

Table 1. Bacterial strains and plasmids

Bacterial strains	Relevant genotype or characteristics	Reference
<i>Pseudomonas pseudoalcaligenes</i>		
KF707 (wild type)	Amp ^r	Taira <i>et al.</i> 1992
<i>cheA::Tn5</i>	<i>cheA::Tn5, lacZ, Km^r, Amp^r</i>	This study
<i>cheA::Km</i>	<i>cheA::km, Km^r, Amp^r</i>	This study
<i>Escherichia coli</i>		
LE392	<i>supF supE hsdR galK trpR metB lacY tonA</i>	Silhavy <i>et al.</i> 1984
S17- λ pir	Tp ^r Sm ^r <i>recA thi pro hsdR</i> RP4:2-Tc:Mu:Km λ pir	Simon <i>et al.</i> 1983
HB101	Sm ^r , <i>recA thi pro leu hsdR</i>	Boyer and Rolland-Dussoix 1969
DH5 α	<i>supE44 hsdR17 recA1 endA1 gyrA96 thi-1 relA1</i>	Hanahan 1983
Plasmids	Relevant genotype or characteristics	Reference
pUC18	Amp ^r , cloning vector	Sambrook <i>et al.</i> 1989
pLFR5	Tc ^r , conjugative plasmid and cosmid vector	Keen <i>et al.</i> 1988
pRK415	Tc ^r , conjugative plasmid	Keen <i>et al.</i> 1988
pUT mini-Tn5 Km	Amp ^r Km ^r , delivery plasmid for mini-Tn5 Km	de Lorenzo <i>et al.</i> 1990
pRK2013	Km ^r ori <i>colE1 RK2-Mob⁺ RK2-Tra⁺</i>	Figurski <i>et al.</i> 1979
pTPM	pUC18 <i>tpm</i>	This study
pTPMKO	pUC18 <i>tpm::Km</i>	This study

Table 1. *Continued*

Primers	Sequence (5' – 3')	Reference
M13 Forward	CGCCAGGGTTTTCCAGTCACGAC	Sigma
M13 Reverse	TCACACAGGAAACAGCTATGAC	Sigma
mini-Tn5 I-end	GGGAATTCGGCCTAGGCGG	This study
mini-Tn5 O-end	CGCCATTCGCCATTCAGG	This study
<i>sodA</i> Forward	CCTGCATTGCCATACGCCTACGA	Heim <i>et al.</i> 2003
<i>sodA</i> Reverse	GGTTGCCGCTACTCTCCACCATCA	Heim <i>et al.</i> 2003
<i>sodB</i> Forward	TACTTCGGACGCAGGTTGCGG	This study
<i>sodB</i> Reverse	TGAACCTGAACAACCTGRTCCC	This study
PTCF2 (tpmF)	GTGCCGYTRTGYYGGCAAGA	Favre-Bronté <i>et al.</i> 2005
PTCR2 (tpmR)	ATCAKYGGCGCGCGGT	Favre-Bronté <i>et al.</i> 2005

Liquid cultures of all bacterial strains were grown in agitation at 150 rpm at the optimum temperature (i.e. *E. coli* at 37 °C while *Ps. pseudoalcaligenes* KF707 at 30 °C). The compositions of the media used in this study are reported in Table 2.

Table 2. Composition of media. The asterisk (*) indicates medium components that were sterilized separately and then added to the autoclaved medium.

Rich media		
Luria-Bertani (LB) – pH 7	Trypton	10 g/l
	Yeast extract	5 g/l
	NaCl	10 g/l
Tryptic Soy Broth (TSB) – pH 7	Peptone	15 g/l
	Peptone Soy	5 g/l
	NaCl	5 g/l
Cation Adjusted Muller Hinton II Broth (CAMHB) – pH7	Beef Extract	3 g/l
	Casein acid hydrolysate	17.5 g/l
	Starch	1.5 g/l

Table 2. *Continued*

Defined Media		
Sucrose-Asparagine (SA) – pH 7	Sucrose	20 g/l
	Asparagine	2 g/l
	K ₂ HPO ₄	1 g/l
	MgSO ₄ 10 % (w/v) *	5 ml/l
Minimal Salt Dextrose (MSD) – pH 7	d-glucose (dextrose) *	1 g/l
	Na ₂ HPO ₄	7 g/l
	KH ₂ PO ₄	2 g/l
	Trisodium Citrate	0.5 g/l
	MgSO ₄	0.1 g/l
	(NH ₄) ₂ SO ₄	1 g/l
	FeSO ₄ 10 mM *	1 ml/l
	MnCl ₂ 10 mM *	1 ml/l

For growth on solid media, agar was added at the final concentration of 15 g/l. Antibiotic stock solutions were prepared as reported in Table 3. The solutions were stored at -20 °C in 1 ml aliquots until use.

Table 3. Antibiotic solutions and concentrations used for selective growth

Antibiotic stock solution	Concentration	
	<i>Ps. pseudoalcaligenes</i>	<i>E. coli</i>
Ampicillin, 50 mg/ml, water solution,	50 µg/ml	50 µg/ml
Kanamycin, 50 mg/ml, water solution,	50 µg/ml	25 µg/ml
Tetracycline, 20 mg/ml, 70 % ethanol in water	20 µg/ml	10 µg/ml

Genomic DNA extraction

Genomic DNA from *Ps. pseudoalcaligenes* KF707 was extracted as follows. 10 ml of an overnight grown culture was centrifuged at 4500 rpm at 4 °C for 10 minutes and washed with 10 ml of TES solution (50 mM Tris, 20 mM EDTA, 50 mM NaCl pH 8). The cell pellet was resuspended in 5 ml of TE (50 mM Tris, 20 mM EDTA pH 8) containing lysozyme at the concentration of 2 mg/ml. The solution was incubated at 30 °C for 30 minutes and mixed by inversion every 10 minutes. At the end of the incubation, 500 µl of a 10 % SDS solution and proteinase K at a final concentration of 0.5 mg/ml were added, followed by 1 h incubation at 37 °C. The reaction was stopped by adding a solution of 100 mM EDTA and 2 M sodium acetate. The lysate was incubated with RNase at 37 °C for 30 minutes after which 2.5 ml of a phenol-chloroform-isoamyl alcohol 25:24:1 v/v mixture was added and the sample was mixed by inversion at room temperature for 15 minutes. The water phase containing the genomic DNA was separated from the organic phase and cell debris by centrifugation at 3000 rpm at 4 °C for 10 minutes. The extraction was repeated twice and phenol traces were removed by adding 5 ml of a 24:1 v/v mixture of chloroform-isoamyl alcohol. The water phase was recovered after centrifugation at 3000 rpm at 4 °C for 10 minutes in a clean beacker. 1.5 volumes of cold ethanol were added to the extracted water phase and the genomic DNA was collected on a clean glass stick. The DNA was washed by immersing the glass stick in a 70 % ethanol solution and then air dried. The genomic DNA was immersed in a small volume of sterile milliQ water and left at 4 °C overnight to allow the DNA to suspend. The resuspended genomic DNA preparation was stored at – 20 °C.

RNA isolation

Ps. pseudoalcaligenes KF707 wild type and mutant cells were harvested at the desired growth phase (exponential phase, $OD_{660} \sim 0.6$; late exponential phase, $OD_{660} \sim 1.8$ for), collected in cold phenol-ethanol mixture (5 % phenol in ethanol) and spun down at 4 °C. Total RNA was extracted by using the RNeasy kit from QIAGEN (Milan, Italy). Residual DNA was removed by treatment with DNase I in the presence of RNA inhibitor (Invitrogen, Milan, Italy). The purity of the RNA

was determined by gel-electrophoresis and the quantification was carried out by spectrophotometry in a quartz cuvette at the $\lambda = 260$ nm. All solutions for RNA treatment were prepared in milliQ water treated with 1 % (v/v) DEPC (diethylpyrocarbonate, Sigma, Milan, Italy). All manipulations were carried out at 4 °C and the extracted RNA was stored in aliquots at – 80 °C.

DNA manipulations and genetic techniques

All restriction digests, ligations, cloning and DNA electrophoresis, were performed using standard techniques (Sambrook *et al.* 1989). Taq polymerase, the Klenow fragment of DNA polymerase, restriction endonucleases and T4 DNA ligase were used as specified by the vendors (Roche or Promega, Milan, Italy). The plasmid pUC18 was routinely used the cloning vector and recombinant plasmids were introduced into *E. coli* HB101 by transformation of chemically competent cells, prepared according to the CaCl₂ method (Sambrook *et al.* 1989). To detect the presence of insert DNA, X-Gal was added to agar media at a final concentration of 40 µg/ml. X-Gal stock solutions were prepared at a final concentration of 40 mg/ml in N-N-dimethylformamide and stored as 1 ml aliquots at - 20 °C protected from light. Kits for plasmid mini- and midi-preps, PCR purification and DNA gel extraction were obtained from QIAGEN (Milan, Italy) and used according to the manufacturer's instructions.

Southern and Northern blot analyses

Southern blot and Northern blot analyses were performed according to standard procedures (Sambrook *et al.* 1989). For Southern blot analyses, approximately 1 µg of digested genomic DNA or 500 ng of digested plasmid DNA were run on 1 % agarose gels and transferred onto nylon membrane (HybondTM-N⁺, GE Healthcare). For Northern blot analyses, 10-µg RNA samples were separated by electrophoresis in 1 % agarose-3.7 % formaldehyde gels and transferred onto nylon membrane. Hybridization was carried out overnight with radioactive-labelled probes at 65 °C or 50 °C, for Southern blot and Northern blot respectively. Hybridization solution for Southern blot assays contained 10 mg/ml blocking reagent (Boehringer), 0.1 % SDS, SSC 5× (added from 20× SSC stock solution: 3 M NaCl, 0.3 M sodium citrate). Hybridization solution for Northern

blot assays contained 1 % BSA (fraction V, Roche), 1 mM EDTA, 7 % SDS in 0.5 mM NaPO₄ buffer pH 7.2. For labelling reactions, approximately 100 ng of probe DNA were labelled with 5 µl of [α -³²P]dCTP (50 µCi) (GE Healthcare, Milan, Italy) using the Ready-To-GoTM DNA Labelling Beads kit (GE Healthcare, Milan, Italy) according to the manufacturer's instructions.

DNA sequencing and sequence analysis

Genomic DNA fragments of interest were cloned in the pUC18 cloning vector and positive plasmids were sent for sequencing to the BMR-genomics service of the University of Padova (Padova, Italy). Samples were prepared according to the recommended procedures (www.bmr-genomics.it). M13 Forward and Reverse primers (Table 1) were used for sequencing the extremities of DNA fragments cloned into the pUC18 vector from the M13 promoter. Mini-Tn5 I-end and O-end primers (Table 1) were used for the sequencing of the genomic DNA flanking the transposon insertions. Sequence identities were determined by DNA homology searches using the BLAST program to search both NCBI and TIGR databases.

Conjugation

Day I. Donor, receiver and helper strains were streaked out on LB agar plates added with the appropriate antibiotic. LB plates were incubated overnight at 37 °C and 30 °C for *E. coli* and *Ps. pseudoalcaligenes* KF707 optimal growth respectively. *E. coli* HB101 strain carrying the mobilization plasmid pRK2013 was commonly used as helper strain for tri-parental mating (see Table 1 for strain and plasmid features).

Day II. Donor, receiver and helper strains were inoculated in LB broth from single colonies grown on the agar plates. The appropriate antibiotics were added to LB medium in order to maintain selection. LB liquid cultures were grown overnight at the appropriate temperature under agitation at 150 rpm.

Day III. Donor, receiver and helper strains were inoculated with a 1 % inoculum in liquid LB medium without antibiotics from overnight grown liquid cultures. Cells were grown at the appropriate temperature and under shaking for 2.5 – 3 h, in order to obtain early exponential phase cultures (OD₆₆₀ ~ 0.2 – 0.3). 1

ml aliquot from each culture was collected in a sterile tube, spun down at room temperature and washed twice with 1 ml LB medium. Cells were suspended in 1 ml of fresh LB and then used for the preparation of conjugation mix by adding equal volumes (100 µl) of donor, receiver and helper suspensions to a sterile tube. The conjugation mix was incubated at 30 °C for 30 min and spot plated onto well dry LB agar plates without selection. Controls for each conjugation were carried out with 100 µl of the receiver, donor or helper cell suspensions alone added to sterile tubes and processed in the same way as conjugation mix. LB plates were incubated for 24 h at 30°C. The procedure is illustrated in Figure 1.

Day IV. The bacterial biomass was collected from each plate with a sterile loop and suspended in 2 ml of fresh LB in the presence of 20 % glycerol. 10 fold serial dilutions of cell suspensions of conjugation mix and controls were carried out in 0.9 % saline. The remaining part of the conjugation mix suspended in LB added with 20 % glycerol was stored at – 80 °C. Appropriate dilutions were plated on agar plates containing the antibiotics for transconjugants selection. For the selection of KF707 transconjugants, cells were plated on SA medium in the presence of appropriate antibiotics. SA medium was used to counter-select *E. coli* donor and helper strains, given that this medium does not support *E. coli* growth, thus resulting selective for *Ps. pseudoalcaligenes* KF707. Plates were incubated at the appropriate temperature until transconjugant growth was clearly visible (i.e. 24 h for *E. coli* transconjugants growing on LB and at least 36 h for KF707 growing on SA).

Day V. Transconjugants were streaked out on the appropriate agar media in the presence of antibiotic selection and incubated at the optimal temperature until growth was clearly visible. The selection was repeated at least twice, in order to obtain a pure culture and remove both donor and helper strain backgrounds.

Construction of Ps. pseudoalcaligenes KF707 genomic library

The construction of a representative genomic library of *Pseudomonas pseudoalcaligenes* KF707 was carried out with the Packagene Lambda DNA Packaging System (Promega) according to the manufacturer's instructions and using the plasmid pLFR5 as a lambda vector. *E. coli* LE392 was used as the host strain. KF707 genomic DNA was partially digested with *Sau3AI* restriction endonuclease and then fractionated by a 40 % - 10 % sucrose gradient centrifugation procedure. DNA fragments that were ~ 30 Kb long were purified by adding 2.5 volumes of ethanol and incubating at - 20 °C overnight to facilitate DNA precipitation. DNA fragments were washed twice with 70 % ethanol, dried and then cloned in the pLFR5 *BamHI* site. Cosmid packaging was carried out with the Packagene Lambda DNA Packaging System (Promega) according to the manufacturer's instructions. Library clones were selected on LB plates containing tetracycline (10 µg/ml). Cosmids containing DNA sequences of interest were extracted using the Midi-prep kit (QIAGEN).

Construction of Ps. pseudoalcaligenes KF707 miniTn5 transposon mutant library

Random mutagenesis was performed by inserting miniTn5 Km transposon into the chromosome of *Ps. pseudoalcaligenes* KF707 using tri-parental conjugation with *E. coli* S17- λ pir/ pUT-mini-Tn5 Km (donor strain), *E. coli* HB101/pRK2013 (helper strain) and *Ps. pseudoalcaligenes* KF707 (receiver strain) as previously described (de Lorenzo *et al.* 1990). Km resistant exconjugants were selected on SA plates supplemented with kanamycin (50 µg/ml) and X-Gal (40 µg/ml).

Protein extraction and two-dimensional gel electrophoresis (2-DE)

KF707 cells were grown in LB medium to the desired growth phase. Bacteria were harvested by centrifugation at 4000 rpm for 20 minutes at 4 °C and subsequently washed in 25 mM potassium phosphate buffer pH 7 containing 75 mM NaCl. Cell pellets were suspended in 25 mM potassium phosphate buffer pH 7 in the presence of 1mM PMSF and 0.1 mg/ml of RNase and DNase I and then disrupted by pressure shearing using a French pressure cell operated at 16000

KPsi. Unbroken cells and cell debris were removed by low speed centrifugation at 8000 rpm for 15 minutes at 4 °C and the supernatants were cleared by ultracentrifugation (32500 rpm, 1 h, 4 °C). The amount of total soluble protein content was estimated by the Peterson's Lowry method (Peterson 1977). Immobiline Drystrips of different pH ranges (GE Healthcare) were used for isoelectric focusing (IEF) in a Multiphor II electrophoresis system (GE Healthcare). After IEF, the strips were equilibrated for 15 minutes at room temperature in equilibration solution (40 % glycerol, 50 mM Tris pH 8.8, 8 M urea, 2 % SDS) containing 2 % DTT and then in equilibration solution containing 2.5 % iodoacetamide. Proteins were separated by 12 % sodium dodecyl sulfate-polyacrylamide gel electrophoresis (SDS-PAGE) in the second dimension using a MiniProtean gel electrophoresis unit (Biorad). For protein spots visualization, 2D gels were stained with Coomassie brilliant blue staining.

MALDI-TOF and LC/MS/MS analyses

Protein spots were excised from Coomassie brilliant blue-stained 2D gels and washed for 15 minutes first with water, then acetonitrile (ACN) and finally 50 mM NH₄HCO₃ (aq). The gel fragments were washed in 50:50 25 mM NH₄HCO₃/ACN for 1-2 hours to remove the dye and then the wash with ACN followed by 50 mM NH₄HCO₃ (aq) was repeated. Washed gel pieces were dehydrated with CAN, dried down and then rehydrated with 10 µl of 25 µg/ml modified trypsin (Roche) in 20 mM NH₄CO₃ on ice for 30 min. Excess trypsin was removed and the gel pieces covered with 10 µL of 20 mM NH₄CO₃ and incubated at 37 °C overnight. Peptides were extracted by three sequential extractions (70 % ACN for 1 hour, water for 30 minutes, 70 % ACN for 30 minutes) which were pooled together (Lauber *et al.* 2001) and dried down in a Speed vac concentrator.

MALDI-TOF spectra were obtained on a Voyager DE-STR (Applied Biosystems, Foster City, CA, USA) in the reflectron mode at the Southern Alberta Mass Spectrometry Center. Dried down peptides were dissolved in 50% ACN:water (vol/vol) 0.3% TFA (vol/vol) and analyzed with a standard dried-droplet method using 0.01% α -cyano-4-hydroxycinnamic acid. Peptides were

spotted with calibrants (angiotensin I 1296.685(M+H), ACTH clip 1-14 1680.795(M+H), and ACTH clip 18-39 2465.199 (M+H)) for high mass accuracy. In cases where no peptides were identified another spectra was obtained by first purifying the peptides with an OMIX C18 tip (Varian, Inc.) or C18 Ziptip (Millipore) according to manufacturers instructions.

Tandem mass spectra (LC/MS/MS) were obtained on an Agilent 1100 Series LC/MSD ion Trap XCT Plus at the SAMS facility. Samples were loaded in 3% ACN/0.05% formic acid and separated on a C18 column over a gradient of 0.05% formic acid (buffer A) and ACN/0.05% formic acid (buffer B) at a flow rate of 0.3 μ l/min. The gradient was 3% B for 0 to 5 min, 3% to 15% B for 3 min, 15% to 45% B for 42 min and 45% to 90% B for 5 min. Database searches were done with Mascot using the NCBI nr database for Proteobacteria (December 12, 2006). A fixed carbamidomethyl modification at cysteine, peptide tolerance of 100 ppm, MS/MS tolerance of 0.6 Da, 2+ and 3+ charged states and one missed cleavage site were selected for peptide fingerprinting searches.

Chapter 1

*Exploring biofilm formation in *Pseudomonas pseudoalcaligenes* KF707: nutritional requirements and role of the CheA histidine kinase*

Introduction

In natural environments, bacteria are commonly found in close association with surfaces. This mode of growth is known as a biofilm (Costerton *et al.* 1994, Costerton *et al.* 1995). Biofilms occur in every ecosystem at almost any solid-liquid interface in both industrial and clinical settings, where they are regarded as a source of noxious industrial and medical biofouling (Costerton *et al.* 1994, Costerton *et al.* 1987). Biofilm formation has been shown to be a relevant aspect of many bacterial diseases, principally because of their tolerance to antimicrobial agents and to immune host-defense responses (Donlan and Costerton 2002, Lewis 2001, Stewart 2002, Stewart and Costerton 2001). Therefore, in the attempt to develop novel antimicrobial therapies, the process of biofilm formation has received increasing attention and the molecular requirements and regulatory mechanisms behind biofilm development and dissolution have been thoroughly investigated.

From the environmental point of view, biofilms provide new degradative abilities for bioremediation of both xenobiotics (Carvalho *et al.* 2001, Puhakka 1995) and heavy metals (Diels *et al.* 2003, Travieso *et al.* 2002). Biofilm-mediated bioremediation is a proficient alternative to the environmental clean-up with planktonic microorganisms, not only because of the increased capability of adaptation and survival of biofilm cells but also because of the distinct physiological properties displayed by bacteria in a biofilm. These physiological traits may enhance the degradation and/or removal of pollutants from the environment (reviewed in Singh *et al.* 2006). Hence, the understanding of how

bacteria adapt and interact with surfaces in response to environmental cues is fundamental for developing successful bioremediation strategies.

Biofilm formation is a dynamic process that has been shown to occur as a defined series of steps (Figure 1.1). At least four distinct stages have been observed to characterize biofilm development, that are, reversible attachment, irreversible attachment, maturation and dispersion (O'Toole *et al.* 2000b). Each of these steps is highly regulated and involve different molecular requirements that may vary from one bacterial species to another (reviewed in O'Toole *et al.* 2000b and Stanley and Lazazzera 2004). Reversible attachment, that is, the transient interaction between the bacteria cell pole and the surface, is the first requisite for the colonization of the substratum. Flagellum-mediated motility and surface-associated proteins have been found to be necessary in different pseudomonads (O'Toole and Kolter 1998a-b, Hinsa *et al.* 2003). Irreversible attachment is realized when cells become attached via the long axis of the cell body (Marshall *et al.* 1971, Fletcher 1996). Other molecular requirements are necessary during this phase, such as an ABC transporter along with a secreted protein in *Ps. fluorescens* and a cytoplasmic protein of unknown function in *Ps. aeruginosa* (Hinsa *et al.* 2003, Caiazza and O'Toole 2004). Maturation proceeds first with microcolony formation, which is a process in which small clusters of cells are formed and that requires twitching motility, type IV pilus and GacA protein functions (O'Toole *et al.* 2000a, Parkins *et al.* 2001, O'Toole and Kolter 1998b). This is followed by the expansion of the formed microcolonies into the organized structure of a mature biofilm. Multiple factors are involved in this step of biofilm formation and quorum sensing-based signalling pathway seems to be required in some cases (Davies *et al.* 1998, Shrout *et al.* 2006, Kirisits and Parsek 2006). A key feature of mature biofilms is the formation of an esopolysaccharide (EPS) matrix (Danese *et al.* 2000, Hellmann *et al.* 1996, Watnick and Kolter 1999, Yildiz and Schoolnik 1999). The production of EPS matrix is activated by environmental signals such as surfaces, osmolarity, quorum sensing, and nutritional cues (Stanley and Lazazzera 2004). The last step in biofilm development is the bacterial dispersion from the biofilm structure back to the liquid phase. Dispersion has been shown to occur in response to environmental cues such as starvation, that seems to elicit a

reduction in bacterial adhesiveness (Gjermansen *et al.* 2005). The genes involved in biofilm dispersion are not as well defined as those required for biofilm formation but recent evidence suggests the involvement of the global regulator of carbon flux CsrA in *E. coli* (Jacson *et al.* 2002) and the chemotaxis regulator BdlA in *Ps. aeruginosa* (Morgan *et al.* 2006).

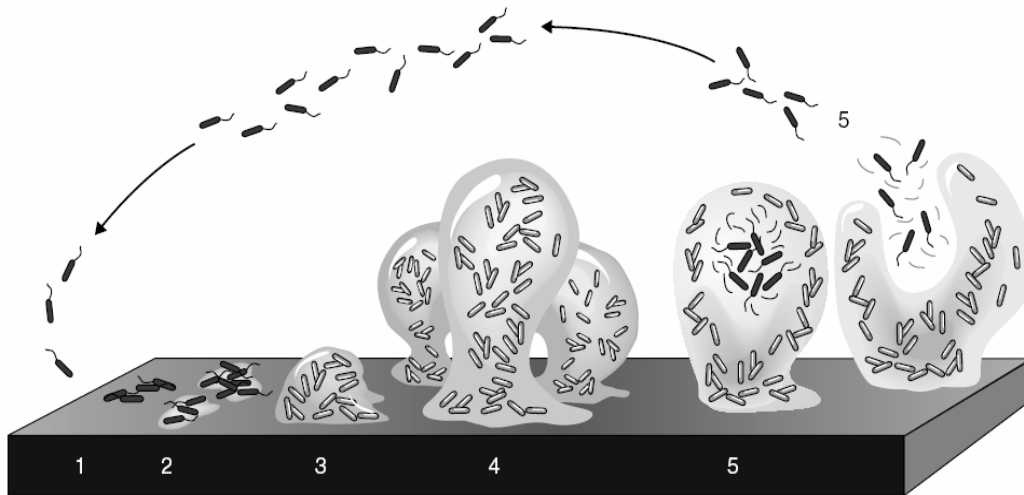


Figure 1.1. Schematic model of biofilm formation in bacteria. In their life cycle, bacteria alternate between free-suspended and sessile modes of growth in response to environmental cues. The formation of a sessile community, known as biofilm, is commonly described as a four-step model. At stage 1, bacterial cells adsorb to the substratum via cell pole during the so-called reversible attachment. At stage 2, cells attach irreversibly to the surface via their long axis and often lose their flagella-driven motility. Biofilm maturation occurs as a two-phase process (steps 3 and 4). At stage 3, small clusters of cells are formed as a result of clonal division of the attached cells, recruitment of planktonic cells from the medium or migration of irreversible cells on the surface by twitching motility. Cell clusters thus formed are known as microcolonies and represent the first phase of biofilm maturation. The second phase (step 4) is characterized by the expansion of microcolonies into a mature biofilm structure enclosed in an EPS matrix. At the dispersion phase (step 5), motile cells are shed from the mature structure back into the liquid, thus ending the cycle. This picture is from K. Sauer (2003).

Chemotaxis, that is, the migration of bacteria under the influence of a chemical gradient, is a well known microbial behavioural response that drives microorganisms to niches that are optimum for their growth and survival

(Wadhams and Armitage 2004). Common soil bacteria have been shown to be chemotactically attracted by many aromatic hydrocarbons and harmful pollutants (reviewed in Pandey and Jain 2002). In the case of highly hydrophobic chemicals adsorbed in the non-aqueous-phase liquid (NAPL), bacteria have been shown to gain access to the target contaminants by adhering directly to the NAPL-water interface, possibly through biofilm formation (Stelmach *et al.* 1999). Chemotaxis and/or motility might be required for the bacteria within the developing biofilm to move along the surface (Stelmach *et al.* 1999). Although chemotaxis is not a general requirement for biofilm formation (Pratt and Kolter 1998), a role for the chemosensory pathway has been shown in *H. pylori* colonization of the gastric mucosa (Foyne *et al.* 2000) and in *Aeromonas* adhesion to enterocyte and biofilm formation (Kirov *et al.* 2004). Moreover, the sensor histidine kinase protein CheA involved in signal transduction in chemotaxis, has been shown to be over-expressed in *Campilobacter jejuni* biofilms (Kalmokoff *et al.* 2006) and to be involved in the successful competitive colonization of root-tips by *Ps. fluorescens* WCS365 (de Weert *et al.* 2002).

In this chapter the basic characterization of biofilm development in *Pseudomonas pseudoalcaligenes* KF707 is described. *Pseudomonas pseudoalcaligenes* KF707 is a soil bacterium that is known for its ability to degrade recalcitrant pollutants such as polychlorinated biphenyls (PCBs) (Furukawa and Miyazaki 1986) and for its resistance to the toxic metalloid tellurite (Di Tomaso *et al.* 2002, Tremaroli *et al.* 2007). The specific nutritional requirements for *Pseudomonas pseudoalcaligenes* KF707 biofilm formation have been investigated. Biofilm formation was also studied in a *cheA::Tn5* chemotactic mutant and evidence is given for the involvement of the CheA-regulated signalling pathway in the formation of a mature biofilm structure.

Materials and methods

Bacterial strains and growth conditions

Ps. pseudoalcaligenes KF707 wild type, *cheA::Tn5* and *cheA::Km* mutants were used in this study. The bacterial strains were grown on either rich (LB, TSB and CAMHB) or defined (SA and MSD) media. The composition of the media is described in the general materials and methods chapter.

Molecular characterization of the cheA::Tn5 and cheA::Km mutants

The gene disrupted by the Tn5 transposon insertion was identified by sequencing the DNA regions flanking a cloned Tn5 fragment. The DNA sequences were compared with bacterial sequences available at the NCBI and TIGR databases and the transposon was found to have integrated into the *cheA* coding sequence, close to the 5' end of the gene. Southern blot analysis was performed to determine the uniqueness of transposon insertion. The kanamycin resistance cassette, derived from the Tn5 transposon as a *NotI* restriction fragment, was used to probe *PstI*-digested chromosomal DNA (no sites for *PstI* restriction endonuclease are present in Tn5, de Lorenzo and Timmis, 1994). This analysis revealed a single hybridizing band, consistent with the mutant having a single transposon insertion.

A 650 bp DNA sequence flanking the Tn5 transposon and harbouring a *cheZcheA* sequence was cloned in the pUC18 cloning vector and was *SacI*-digested. *SacI* restriction enzyme cleaves the *cheA* sequence ~ 250 bp downstream of the 5' end, thus cleaving the original 600 bp sequence to yield two fragments of 450 and 200 bp. A blunt-end kanamycin resistance cassette was ligated into the *SacI* digested plasmid treated with the Klenow enzyme (Promega) in order to produce blunt ends. The insertion cassette thus formed was ligated into the pRK415 conjugative plasmid and the resulting construct was conjugated into the KF707 wild type strain. Double cross-over recombinants were isolated that showed resistance to kanamycin. The integration of the Km cassette into the *cheA* sequence was verified by both southern blot analysis and sequencing.

Biofilm growth conditions

Biofilms were grown on the Calgary Biofilm Device (CBD, commercially available as MBECTM assay) as described by Ceri *et al.* (1999) as well as by the manufacturer (Innovotech, Edmonton, Canada). The CBD is a plastic device consisting of 96 conical pegs attached to a plastic lid and fitting into a 96 well microtitre plate, which contains the bacterial suspension. The procedure is illustrated in Figure 1.2 (A to C) and is briefly described here. From the corresponding cryogenic glycerol stock, each bacterial strain was streaked out twice on LB agar plates (supplemented with 50 µg/ml kanamycin for the growth of *cheA::Tn5* and *cheA::Km* mutants), avoiding antibiotic selection during the second subculture (Figure 1.2 A). Colonies from the secondary culture were suspended into fresh medium to match the optical density of a 1.0 McFarland standard and a 1:30 dilution from the bacterial suspension was prepared into the same medium (Figure 1.2 B). This standardized inoculum contained approximately 1.0×10^7 CFU ml⁻¹ and was used to inoculate the CBD by adding 150 µl of the inoculum to each well. The peg lid was then fitted on the top of the microtitre plate to assemble the CBD and the device was placed on a gyrorotary shaker at 100 rpm at 30 °C and 95 % humidity (Figure 1.2 C).

Biofilm and planktonic growth curves

For biofilm growth curve analysis, CFU per peg were determined by viable cell counts. At each time point, four pegs were removed from the lid and rinsed with 200 µl of 0.9 % saline to remove loose planktonic cells. After transferring to 200 µl of fresh saline, to which was added 0.1 % v/v Tween-20, the biofilms grown on the pegs were disrupted by sonication using an Aquasonic 250HT ultrasonic cleaner (VWR International, Mississauga, ON, Canada) set at 60 Hz for 5 minutes. The resulting cellular suspensions were serially diluted in 0.9 % saline in the presence of 0.1 % Tween-20. Aliquots of each dilution were plated onto LB agar medium and the agar plates were incubated at 30 °C for 24 h (Figure 1.2 D, E). As a control, viable cell counts of planktonic cell cultures were carried out by serial dilution in 0.9 % saline and appropriate dilutions were plated onto LB agar plates as described for biofilm cells.

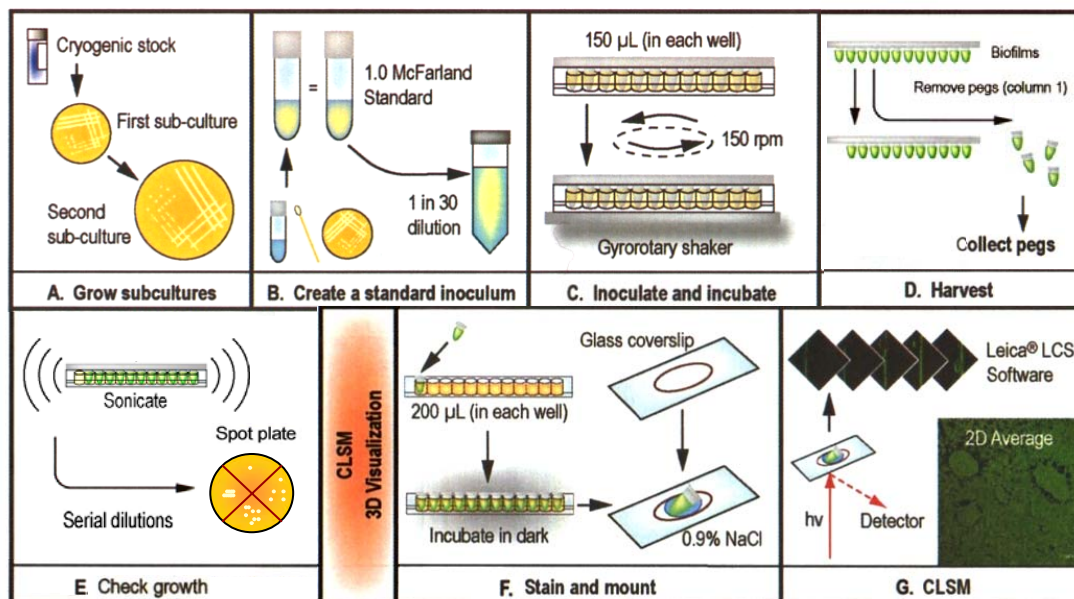


Figure 1.2. Biofilm cultivation on the CBD (A to E) and 3D visualization of microbial biofilms by CLSM (F, G). This picture has been adapted from Harrison *et al.* (2006).

Confocal laser scanning microscopy (CLSM)

For the examination by CLSM, biofilms formed on the pegs of the CBD were fluorescently stained with acridine orange (AO) as described by Harrison *et al.* (2006). AO is a membrane permeant nucleic acid stain that binds to both DNA and RNA, emitting fluorescence at 505-535 nm when excited at 488 nm (Bernas *et al.* 2005). AO functions as a general indicator of the biofilm bacterial biomass attached on the pegs. For the staining procedure, pegs were taken from the CBD, rinsed in 0.9 % saline in order to remove free swimming cells and stained in the dark with a solution of AO 0.1% w/v for 5 minutes at room temperature. The stained biofilms were placed on the top of a glass coverslip and immersed in 0.9 % saline (Figure 1.2 F). Microscopic visualization of the biofilms was carried out using a Leica DM IRE2 spectral confocal and multiphoton microscope with a Leica TCS SP2 acoustic optical beam splitter (AOBS) (Leica Microsystems, Richmond Hill, ON, Canada). Line averaging ($\times 2$) was used to capture images with reduced noise. A 63 x water immersion objective was used in all experiments. Image capture, 2D projections of z-stacks and 3D reconstructions

were performed using Leica Confocal Software (Leica Microsystem) as described by Harrison *et al.* (2006) (Figure 1.2 G).

Motility assays

The swimming, swarming and twitching behaviour of *Ps. pseudoalcaligenes* wild type and mutant cells were analysed as previously described by Rashid and Kornberg (2000). The assays are briefly described below.

Swimming. Tryptone swim plates [10 g/l tryptone, 5 g/l NaCl, 0.3 % (w/v) Difco bacto-agar] were inoculated with a sterile toothpick from cultures grown overnight on LB agar plates. The plates were wrapped in saran wrap to prevent dehydration and incubated at 30 °C for 24 h. Motility was qualitatively assessed by examining the circular turbid zone formed by the bacterial cells migrating away from the point of inoculation.

Swarming. Swarm plates consisted of 0.5 % (w/v) Difco bacto-agar with 8 g/l Difco nutrient broth (5 g/l bacto-beef extract, 3 g/l bacto-peptone extract) supplemented with 5g/l of dextrose. Swarm plates were allowed to dry at room temperature overnight before being used. Swarm plates were inoculated from both overnight LB agar plates and swim plates. The plates were incubated at 30 °C for at least 24 h.

Twitching. Twitch plates [10 g/l tryptone, 5 g/l yeast extract, 10 g/l NaCl, 1 % (w/v) Difco bacto-agar] were stab inoculated with a sharp toothpick to the bottom of a Petri dish from an overnight grown LB agar plate. After incubation for 24 to 48 h at 30 °C, a hazy zone of growth at the interface between the agar and the polystyrene surface was observed. The ability of bacteria to strongly adhere on the polystyrene surface was then examined by removing the agar, washing the unattached cells with a stream of water, and staining the attached cells with crystal violet [1 % (w/v) solution].

Chemotaxis assay

Agarose plug assays were carried out as previously described by Yu and Alam (1997) with slight modifications. Plugs contained 2 % low-melting-temperature agarose in chemotaxis buffer (40 mM potassium phosphate pH 7.0, 0.05 % glycerol, 10 mM EDTA) and the chemoattractant to be tested. A few crystals of Coomassie blue were added to provide contrast. 10 μ l of the melted agarose mixture was placed on a microscope slide, and a coverslip supported by two plastic strips was then placed on top to form a chamber. Cells were harvested in exponential phase ($OD_{660} \sim 0.7$), resuspended in chemotaxis buffer to the same OD_{660} , and flooded into the chamber to surround the agarose plug. Tryptone, glutamate and asparagine were assayed as chemoattractants and were provided at 0.1 % (wt/vol) in plug assays. Control plugs were assembled that contained 0.9 % saline instead of the attractant.

Transmission electron microscopy (TEM)

Bacteria were examined for general cell morphology and flagellum structure by TEM. Formvar-coated 100-mesh copper grids were placed on the top of a 20 μ l drop of exponentially growing cultures for 1 minute. The grids were rinsed twice with water and stained with 1 % uranyl acetate (w/v) for 1 minute. The negatively stained cells were air dried and then visualized with a Philips CM-100 transmission electron microscope at 80 keV.

Sample preparation for two-dimensional gel electrophoresis (2-DE) and MALDI-TOF analysis

KF707 wild-type, *cheA::Tn5* and *cheA::Km* cells were grown in LB to the exponential phase ($OD_{660} \sim 0.5$). Preparation of soluble protein fractions, 2-DE and identification of proteins differentially expressed are described in the General materials and methods chapter.

Results

Characterization of Ps. pseudoalcaligenes KF707 biofilm development

In order to obtain the first basic insights into the dynamics of biofilm development, we investigated the formation of biofilms of *Ps. pseudoalcaligenes* KF707 on the Calgary Biofilm Device (CBD). The CBD is a batch system that allows the formation of 96 statistically equivalent biofilms (Ceri *et al.* 1999). This system reproduces the bacterial lifestyle, in which free swimming (planktonic) bacteria attach to a biotic or abiotic surface and produce an organized multicellular structure (biofilm) in response to environmental signals. Cells forming a biofilm on the CBD are eventually released and colonize the surrounding medium, thus closing the planktonic-biofilm bacterial life cycle. Acridine orange (AO) staining and confocal laser scanning microscopy (CLSM) were used to visualize the evolution of biofilm organization. Figure 1.2 displays representative images of the time course of *Ps. pseudoalcaligenes* KF707 biofilms in LB medium at 4, 8, 16 and 24 h (A to D). In Figure 1.3 A, transiently attached cells are visible as green round spots and are indicated by a white arrow. At 16 h of biofilm development, *Ps. pseudoalcaligenes* KF707 cells are attached to the surface across the long axis of the cell body, which defines the occurrence of irreversible attachment (Marshall *et al.* 1971, Fletcher 1996) (Figure 1.3 B). The formation of a monolayer of irreversibly attached cells is followed by the production of microcolonies (Figure 1.3 C) that further develop into a mature biofilm. A mature biofilm structure is often characterized by macrocolonies separated by fluid-filled channels containing few adherent cells (Tolker-Nielsen *et al.* 2000). *Ps. pseudoalcaligenes* KF707 biofilms grown for 24 h in LB are characterized by dense and structured aggregates of an average thickness of approximately 21 μm , enclosed in an exopolysaccharide (EPS) matrix (Figure 1.3 D). The EPS matrix is a complex substance, composed of short oligonucleotides (Whitchurch *et al.* 2002), proteins (Branda *et al.* 2006) and polysaccharides (Branda *et al.* 2005, Sutherland *et al.* 2001). Due to the presence of DNA as an integral part of the matrix, in AO stained biofilms the EPS is visible as a diffuse

fluorescence sheltering the biofilm cells and linking adjacent cell aggregates (Figure 1.3 D).

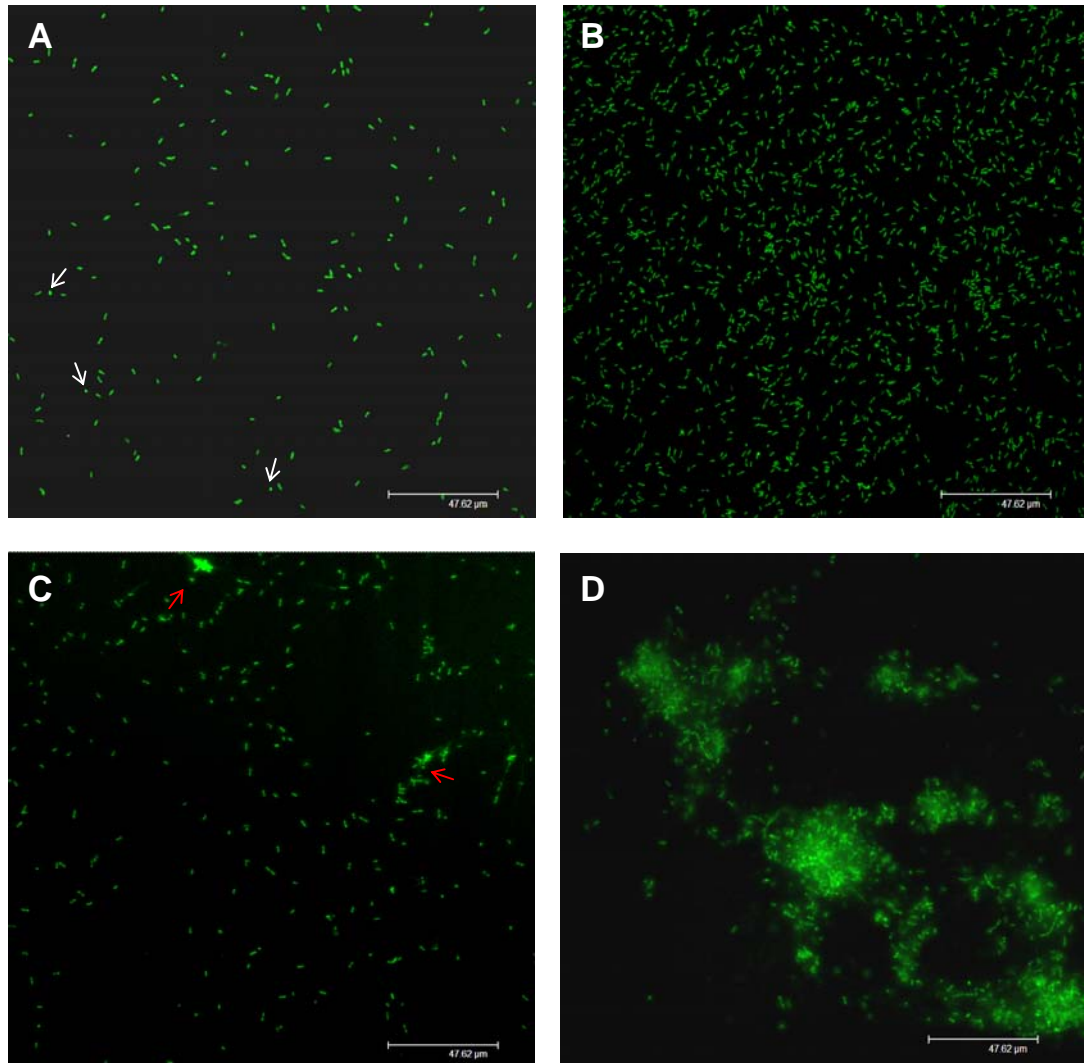


Figure 1.3. Time course of biofilm formation of *Ps. pseudoalcaligenes* KF707 in LB medium. Images display the 2D averages of z-stacks. Biofilms were grown in LB medium and the images displayed are representative of cell attachment and biofilm structure development at 4, 8, 16 and 24 h.

Overall, the observed development of *Ps. pseudoalcaligenes* KF707 biofilms is reminiscent of the biofilm progression described for other bacteria such as *Ps. aeruginosa* (Sauer *et al.* 2002, Tolker-Nielsen *et al.* 2000) and *E. coli* (Reisner *et al.* 2003).

Influence of media composition on biofilm formation

It has been reported that the type of carbon source influences the development and architecture of *Ps. aeruginosa* and *S. oneidensis* biofilms (Klausen *et al.* 2003, Thormann *et al.* 2004). In order to investigate the effect of medium composition on KF707 biofilm structure, biofilms were grown on other rich media (TSB and CAMHB, Figure 1.4) as well as minimal media (MSD and SA, Figure 1.5). Biofilms grown in different media were found to have a fundamentally different appearance.

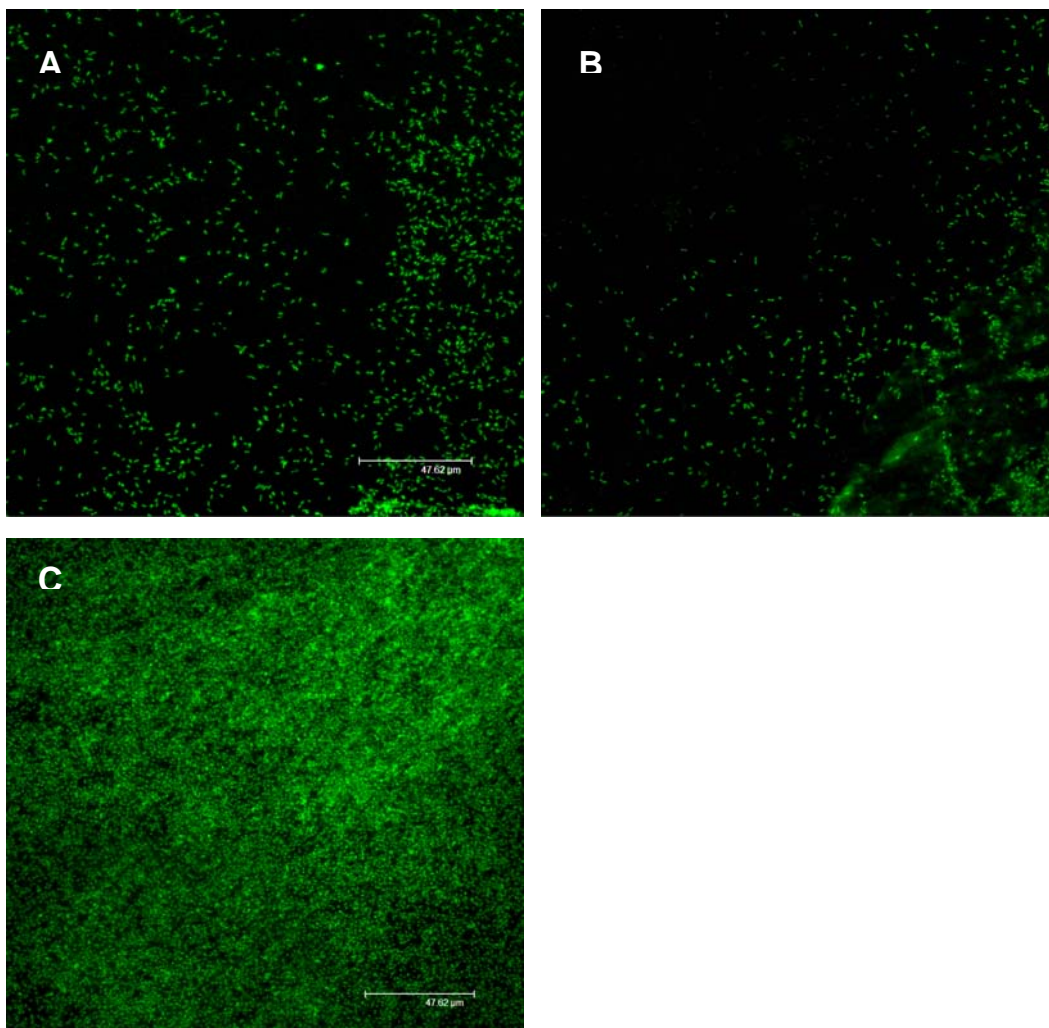


Figure 1.4. Structure of biofilms formed in rich media. Biofilms were grown for up to 64 h in TSB (A), CAMHB (B) or CAMHB to which 20 g/l NaCl was added (C). Images display the 2D averages of z-stacks representative of biofilm growth at 64 h.

In TSB and CAMHB rich media, KF707 cells formed biofilms of an average thickness of 10 and 13 μm respectively in which dense cell aggregates were not observed at prolonged times of growth (64 h, Figure 1.4). The main difference in composition among the three rich media used in this study is the presence of a higher NaCl concentration in LB as compared to TSB and CAMHB. By adding NaCl at a final concentration of 20 g/l to CAMHB medium, biofilm formation was shifted to a thick monolayer of cells covering the substratum (Figure 1.4 C).

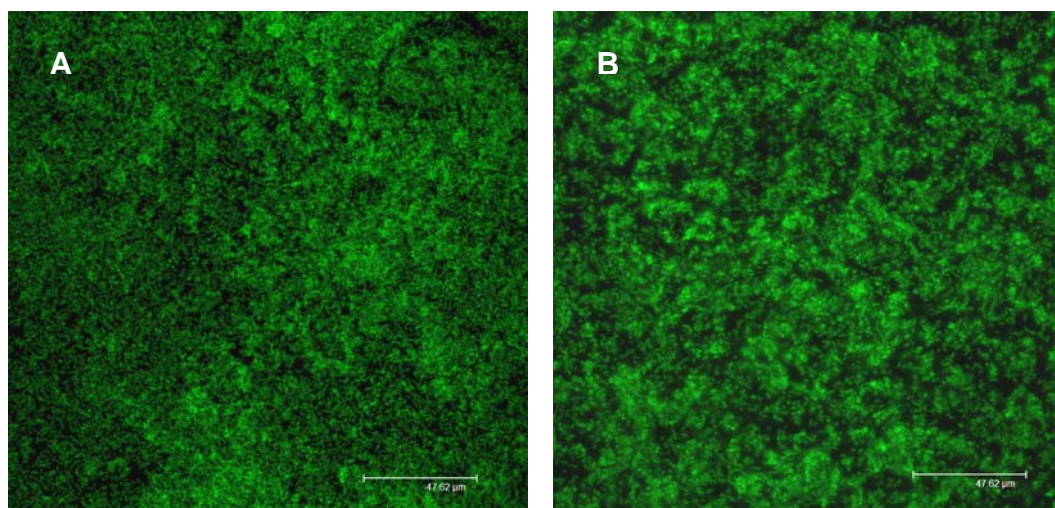


Figure 1.5. Structure of biofilms grown for 24 h in either SA (A) or MSD (B) minimal media. Images display the 2D averages of z-stacks.

In minimal media, a mat of cells, whose thickness was found to be approximately 17 μm after 24 h, was observed to uniformly cover the plastic surface (Figure 1.5 A, B). Finally, Figure 1.6 shows the evolution of biofilm architecture at prolonged times of growth (64 h) in LB (A) and SA (B). Few sparse cells were attached to the plastic surface in LB-grown biofilms (Figure 1.6 A), while a complex structure, around 23 μm thick, had formed when biofilms were grown in SA medium (Figure 1.6 B).

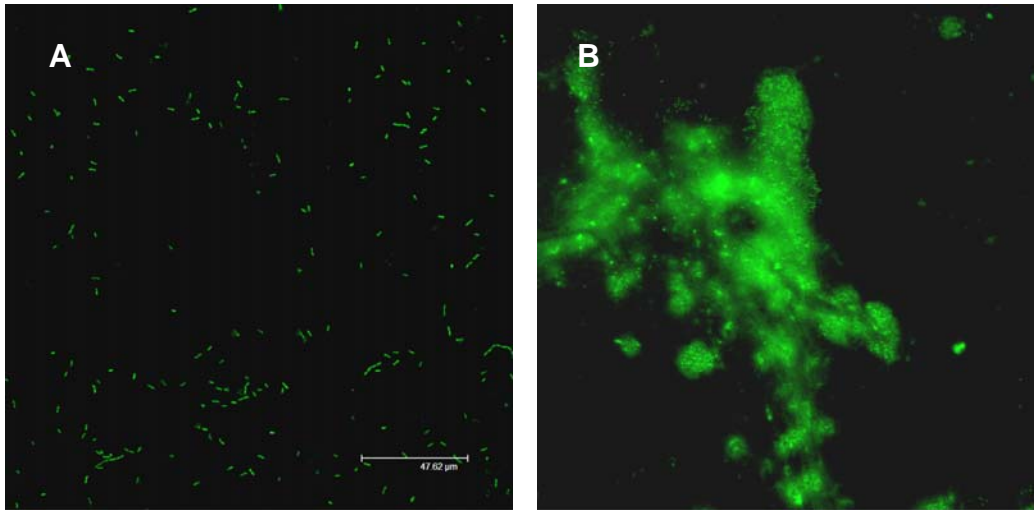


Figure 1.6. Development of biofilm structure in LB (A) and SA (B) media after 64 h of growth.

The results illustrated here show that *Ps. pseudoalcaligenes* KF707 biofilm structure and development depend on the medium used, suggesting that biofilm dynamics is probably metabolically controlled. Moreover, evidence is given that poor nutrient conditions and higher salinity result in a more robust biofilm for this soil bacterium.

Characterization of biofilm formation in a cheA::Tn5 mutant

It has been shown that the histidine kinase sensor CheA is required for the colonization of the gastric mucosa by *H. pylori* (Foyne *et al.* 2000) and for epithelial and intestinal cell adhesion and biofilm formation in *Aeromonas* (Kirov *et al.* 2004). On the other hand, chemotaxis was found to be dispensable for *E. coli* biofilm formation (Pratt and Kolter 1998). To define the role of the *cheA* gene in *Ps. pseudoalcaligenes* biofilm formation, we characterized the kinetics of biofilm formation in a *cheA::Tn5* mutant. The extent of biofilm formation was determined by both CLSM and viable cell counts, with the intent to give meaning to the microscopic observations. Figure 1.7 shows biofilm growth curves of the *cheA::Tn5* mutant (red lines) in comparison to the wild type strain (black lines) under three different conditions (i.e. growth in LB, SA and MSD). The wild type

strain reaches the maximum biofilm cell density in this assay by approximately 10 h in minimal medium (Figure 1.7 b, c) and 24 h in LB (Figure 1.7 a).

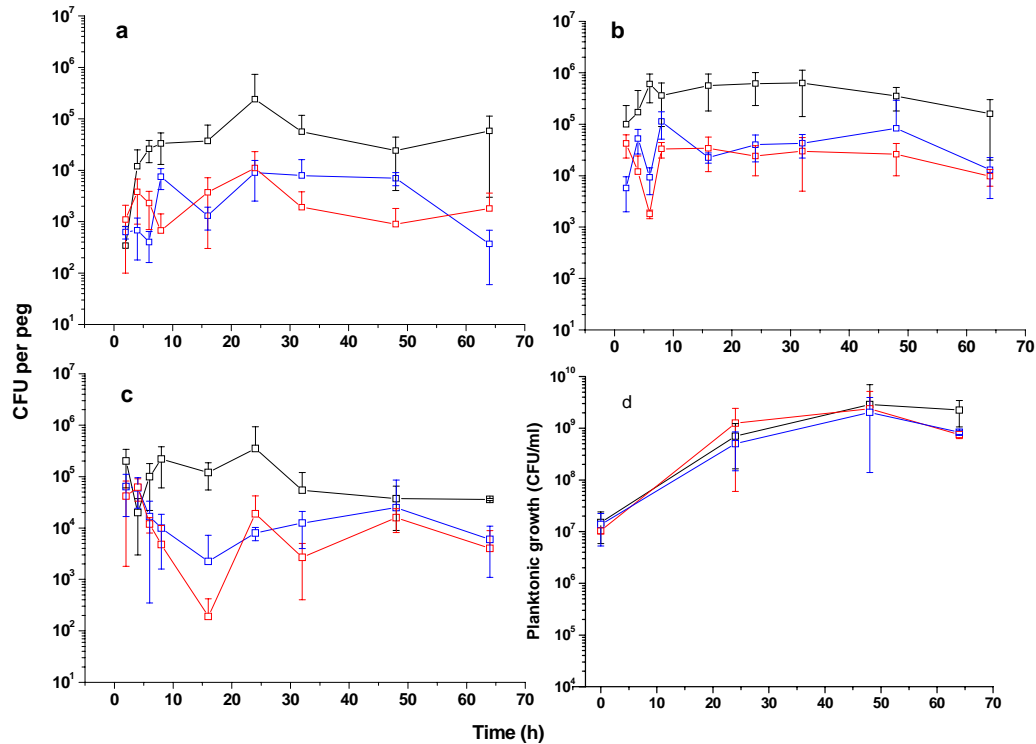


Figure 1.7. Growth curves of biofilms in LB (a), SA (b) and MSD (c) media. Viable cell counts were carried out to determine CFU per peg during biofilm development. The curves show the CFU per peg as a function of time for the KF707 wild type strain (black lines), the *cheA::Tn5* mutant (red lines) and the *cheA::Km* mutant (blue lines). The values presented and standard deviations are the means of at least four independent experiments, each performed in quadruplicate. Growth curves of planktonic cells in LB medium are reported as a control (panel d).

The *cheA::Tn5* mutant was found to be capable of early attachment to the abiotic surface but impaired in the development of a fully structured biofilm, as only small and dispersed cell aggregates were visible under confocal laser scanning microscopy (Figure 1.8). A peculiar feature of the mutant biofilm growth was a dramatic decrease in biofilm cell density after initial cell attachment, along with wide error bars during the first 16 h of growth in LB.

These observations suggested that mutant biofilms might be intrinsically unstable, formed by fragile cell clusters, or unable to develop into resilient mature biofilms.

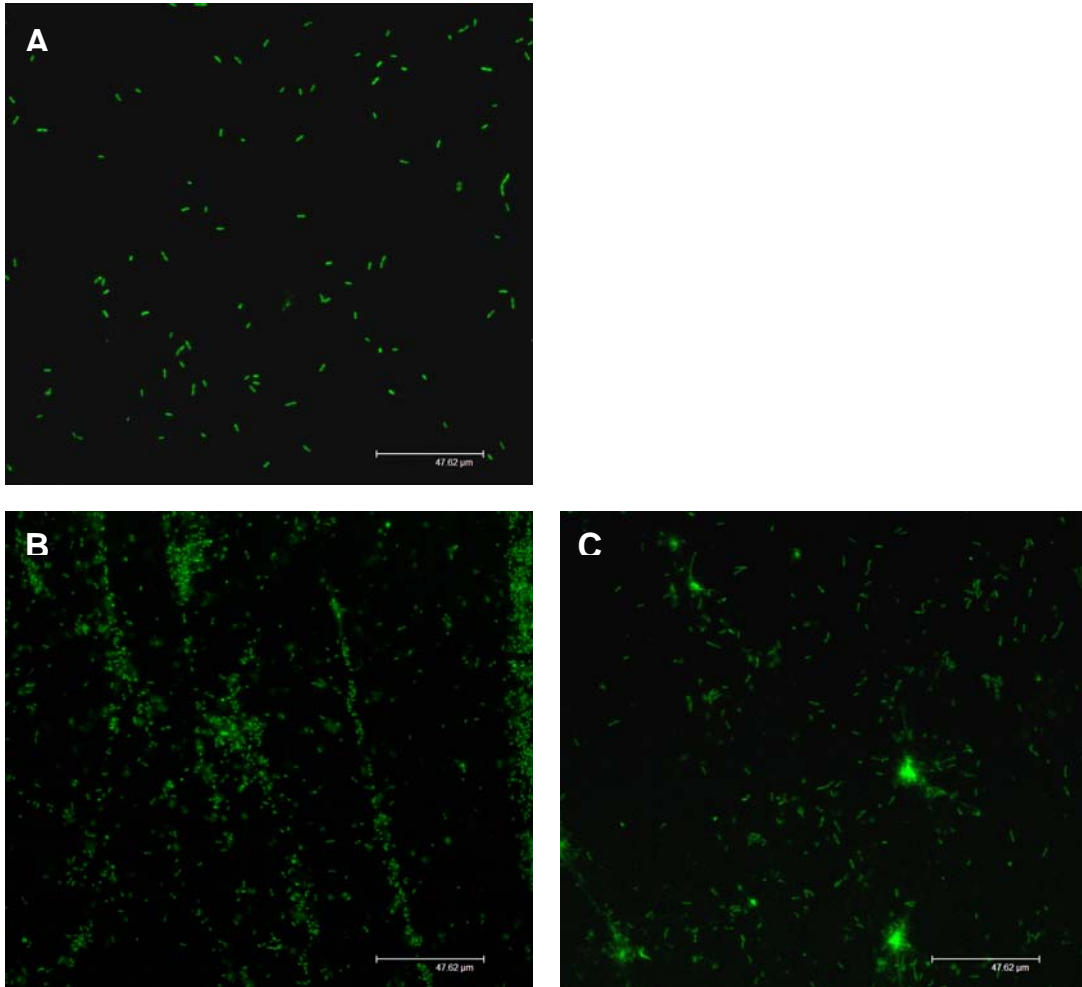


Figure 1.8. Representative images of *cheA* mutant biofilms grown for 24 h in LB (A), SA (B) or MSD (C) media. Cell aggregates are visible in biofilms grown in minimal media (panels B and C) but the cell density is greatly reduced in comparison to the wild type biofilms grown in the same media for the same period of time and presented in Figure 1.3 (panels C and D respectively).

Remarkably, the mutant strain was unable to form biofilms with a parental structure under any of the growth conditions tested and it did not show a delayed biofilm phenotype, since wild-type biofilms did not form even under prolonged incubation (up to 64 h). Planktonic growth was also monitored along with biofilm formation and the mutant strain exhibited growth rates that were comparable to

the wild type (Figure 1.7 d, red line), indicating that the impaired biofilm formation phenotype did not depend on a general growth defect.

Assessing the role of cheA in biofilm formation

Targeted gene disruption was carried out to assess whether the insertion of the Tn5 transposon in the *cheA* gene caused the observed defect in biofilm formation. The kanamycin resistance cassette derived from the Tn5 transposon was inserted close to the 5' end of the *cheA* gene, in a position that is approximately 150 bp upstream of the Tn5 insertion site. The biofilm phenotype of the *cheA::Km* and *cheA::Tn5* mutants was found to be indistinguishable. The number of cells attached to the CBD after 24 h of growth in both rich and minimal media was found to be decreased by 95 % in both mutant strains when compared to the parental organism. The growth curves of both mutants showed early dispersal events following the initial attachment to the plastic surface (Figure 1.7, red and blue lines), thus strengthening the hypothesis that the mutant cell aggregates are unstable. Planktonic growth of the *cheA::Km* mutant was monitored and the measured growth rates were found to be comparable to both the wild-type and the mutant *cheA::Tn5* strains (Figure 1.7 d). Although complementation assays are at present lacking, the genetic data and the similarity of the biofilm phenotype displayed by the two *cheA* mutants, suggest that the *cheA* gene plays a role in the development of structured biofilms in *Ps. pseudoalcaligenes* KF707.

The cheA mutants are impaired in chemotaxis

The ability of *Ps. pseudoalcaligenes* KF707 cells to swim towards a strong chemoattractant, such as tryptone, was investigated via the agarose plug assay (Yu and Alam 1997). In this assay, diffusion of tryptone from the agarose plug into the surrounding liquid results in the development of a concentration gradient. A chemotactic response was observed to occur within 15 minutes, in the form of a chemotactic ring produced by wild-type cells accumulating in a circle surrounding the tryptone-containing agarose plug. As expected, no ring formation was observed when either the *cheA::Tn5* or *cheA::Km* cells were tested in this assay (Figure 1.9).

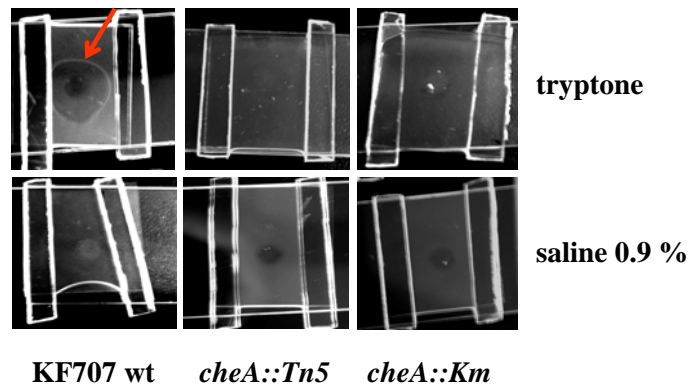


Figure 1.9. Agarose plug assay of *Ps. pseudoalcaligenes* KF707 wild type and *cheA* mutants for chemotactic behaviour towards tryptone (upper panels). The chemotactic ring formed by wild-type cells is indicated by a red arrow. No ring is formed in the mutant plug assays. Control plugs contained no attractant (lower panels).

Motile behaviour in KF707 wild type and mutant strains

Swimming. When KF707 cells are cultivated on agar plates containing a low percentage of agar, swimming zones form as a result of flagellum-driven motility. Figure 1.10 A shows the swimming motile behaviour of the wild type and mutant cells on tryptone semi-liquid medium (0.3 % agar). As expected, dispersion of the mutant cells from the point of inoculation did not occur, suggesting that the two *cheA* mutant strains are completely defective in swimming motility (Figure 1.10 A).

Swarming. In the presence of higher concentrations of agar, (0.5 %, semi-solid medium) *Pseudomonas* cells have been shown to propagate in a coordinated manner by swarming motility (Köhler *et al.* 2000, Rashid *et al.* 2000). Swarming motility is distinguishable from swimming because of the irregular branching that appears at the periphery of the colony and develops in a dendritic pattern all over the agar surface (Köhler *et al.* 2000). This swarming phenotype was not displayed by *Ps. pseudoalcaligenes* KF707 wild type and mutant cells under the condition tested (Figure 1.10 B).

Twitching. Twitching motility is a form of translocation on solid surfaces which is dependent on pili-assisted motility (Henrichsen 1972, Henrichsen 1983). When cells are inoculated through a thin 1 % agar layer to the bottom of a Petri dish, colony expansion occurs at the interstitial surface between the agar and the polystyrene. The twitch zones formed by the *cheA* mutants were indistinguishable from the wild type zones and no dispersion of the attached cells was observed when the agar layer was removed and the Petri dishes were washed with water. As shown by the diameter of the twitch zones in Figure 1.10 C, the *cheA* mutants displayed a parental phenotype as regards to twitching motility.

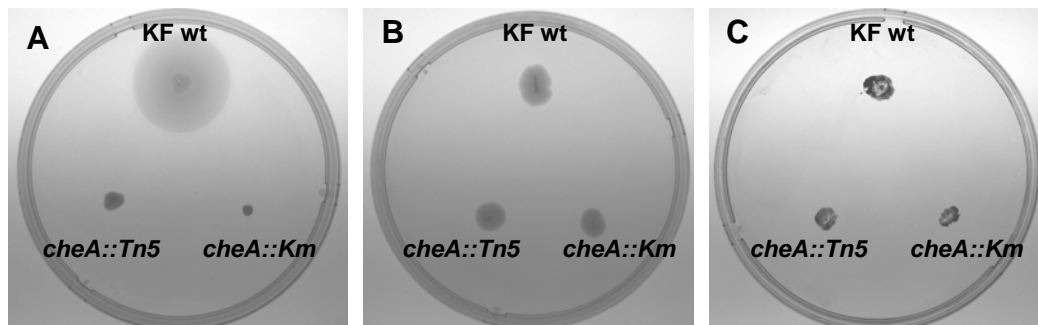


Figure 1.10. Differences in the motility phenotype of *Ps. pseudoalcaligenes* KF707 wild-type and mutant strains. (A) Swimming motility on a tryptone swim plate (0.3 % agar, semi-liquid medium). (B) Swarming motility on a swarm plate containing 0.5 % agar (semisolid medium). (C) Twitching motility on a thin (3 mm) LB 1 % agar plate. The image displays the twitching zones that remained attached to the polystyrene surface after removing the agar layer and washing with water. The attached cells were stained with crystal violet (1 %).

Tn5 transposon and Km insertions in the cheA gene do not affect flagellum number, position or structure

In *Pseudomonas aeruginosa*, *cheA* is part of a large operon coding for genes involved in flagellum positioning and number determination (Pandza *et al.* 2000). In order to ensure that the impaired biofilm phenotype displayed by the *cheA* mutants results solely from the disruption of the *cheA* gene and not from a non-parental flagellum number and placement, transmission electron microscopy visualization of wild-type and mutant cells was carried out. Figure 1.11 shows electron micrographs of KF707 wild type (A), *cheA::Tn5* (B) and *cheA::Km* (C) cells grown in liquid LB to the exponential phase ($OD_{660} \sim 0.7$). The mutant strains, as well as the wild type, had a single flagellum placed at the pole of the cell body. These observations show that the transposon and kanamycin cassette insertions in the *cheA* gene do not affect flagellum placement and number and that the observed biofilm phenotype is a consequence of the lack of a functional CheA protein.

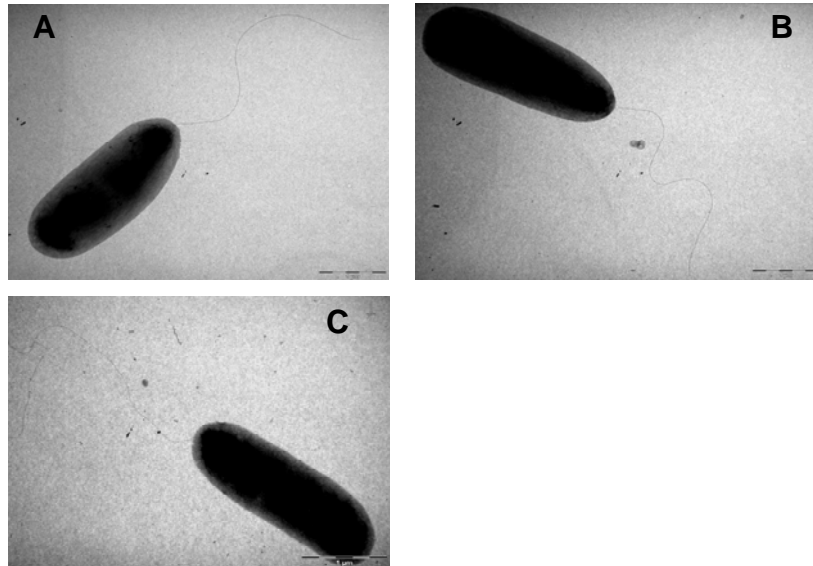


Figure 1.11. Electron micrographs of *Pseudomonas pseudoalcaligenes* KF707 wild type (A), *cheA::Tn5* (B) and *cheA::Km* (C) stained with 1 % uranyl acetate. A single flagellum placed at the pole of the parental as well as the mutant cells. The bar represent 1 μm ; the magnification was 19000X.

Proteome analysis of planktonic protein profiles of Pseudomonas pseudoalcaligenes KF707 wild type and cheA mutants

Soluble protein extracts from planktonic cultures of KF707 wild-type, *cheA::Tn5* and *cheA::Km* mutants were analysed by two-dimensional electrophoresis. Representative examples of 2D-gels are shown in Figure 1.12. 2D-gels were independently repeated two times to confirm the consistency of protein patterns of wild-type and *cheA* mutant planktonic cells. Protein patterns obtained from the wild-type and mutant strains displayed differential expression of protein functions focused in the 3-6.5 pH range. Globally, a small proteome difference was observed between *cheA* mutant and wild-type exponentially growing cells. However, three proteins were consistently expressed in the mutants but not in the wild-type strain (encircled in red in Figure 1.12). Protein spots were excised from the gel and subjected to LC/MS/MS analysis. Database searches in the NCBI database allowed the identification of the three differentially expressed proteins as periplasmic binding proteins. Spot A was identified with a score of 136 and 10 % sequence coverage with the PotF1 periplasmic putrescine-binding proteins of *Ps. fluorescens* (accession number AAK15487), *Ps. syringae* DC3000 (accession number NP_795038) and *Ps. entomophila* L48 (accession number YP_610699). PotF1 proteins have a mass (M_r) of approximately 40000 Da, a value that is concordant with the mass of spot A that can be estimated from 2D-gels. Spot B was identified with a score of 316 and 19 % sequence coverage with the putative periplasmic iron-binding protein of *Ps. putida* KT2440 (accession number NP_747297), *Ps. aeruginosa* PAO1 (accession number NP_253904) and *Ps. entomophila* L48 (accession number YP_610714). These periplasmic iron-binding proteins have a mass (M_r) of approximately 36000 Da, a value that is concordant with the mass of spot B that can be estimated from 2D-gels. Finally, spot C was identified with another putative periplasmic binding protein of *Ps. aeruginosa* PA7 (accession number ZP_01296605) which has a mass of 33000 Da. This periplasmic protein is highly homologous to amino acid-binding proteins of other *Pseudomonas* species, such as *Ps. entomophila* L48 glutamate/aspartate-binding protein and lysine/arginine,/ornithine (LAO)-binding protein. The protein in spot C was identified with a score of 157 and 16 % sequence coverage.

Periplasmic binding proteins are known to be involved in both transmembrane transport in association with ATP-binding cassette (ABC) transporters and in chemoreception processes via interaction with methyl-accepting chemotaxis receptors (MCPs) (Gilson *et al.* 1988, Higgins *et al.* 1990, Stock *et al.* 1991). Recently, periplasmic binding proteins have been shown to play a role in the initiation of sensory transduction pathways. As an example, the norspermidine-binding protein NspS has been shown to diminish the ability of the transducer membrane protein MbaA to inhibit biofilm formation in *V. cholerae*. The interaction of NspS with MbaA transducer seems to affect the rate of cyclic-di-GMP synthesis by MbaA protein (Kataran *et al.* 2005). In other studies, periplasmic binding proteins associated to ABC transporters have been shown to be involved in the colonization of root-tips by *Ps. fluorescens* WCS365. In particular, increased uptake of putrescine was observed to inhibit competitive root colonization (Kuiper *et al.* 2001). Consistent with this study is the observation that numerous membrane ABC transporters and the associated periplasmic binding proteins were found to be differentially expressed in planktonic and biofilm cells of *Ps. putida* during the initial stages of biofilm development (Sauer and Kamper 2001). In *Ps. putida*, PotB protein was observed to be up-regulated while PotF1 was down-regulated in biofilm cells as compared to planktonic cells (Sauer and Kamper 2001). These results suggest that the switch between planktonic and biofilm mode of growth requires the coordinated expression of membrane and periplasmic proteins, that may be involved in signalling pathways necessary for the development of a mature structure.

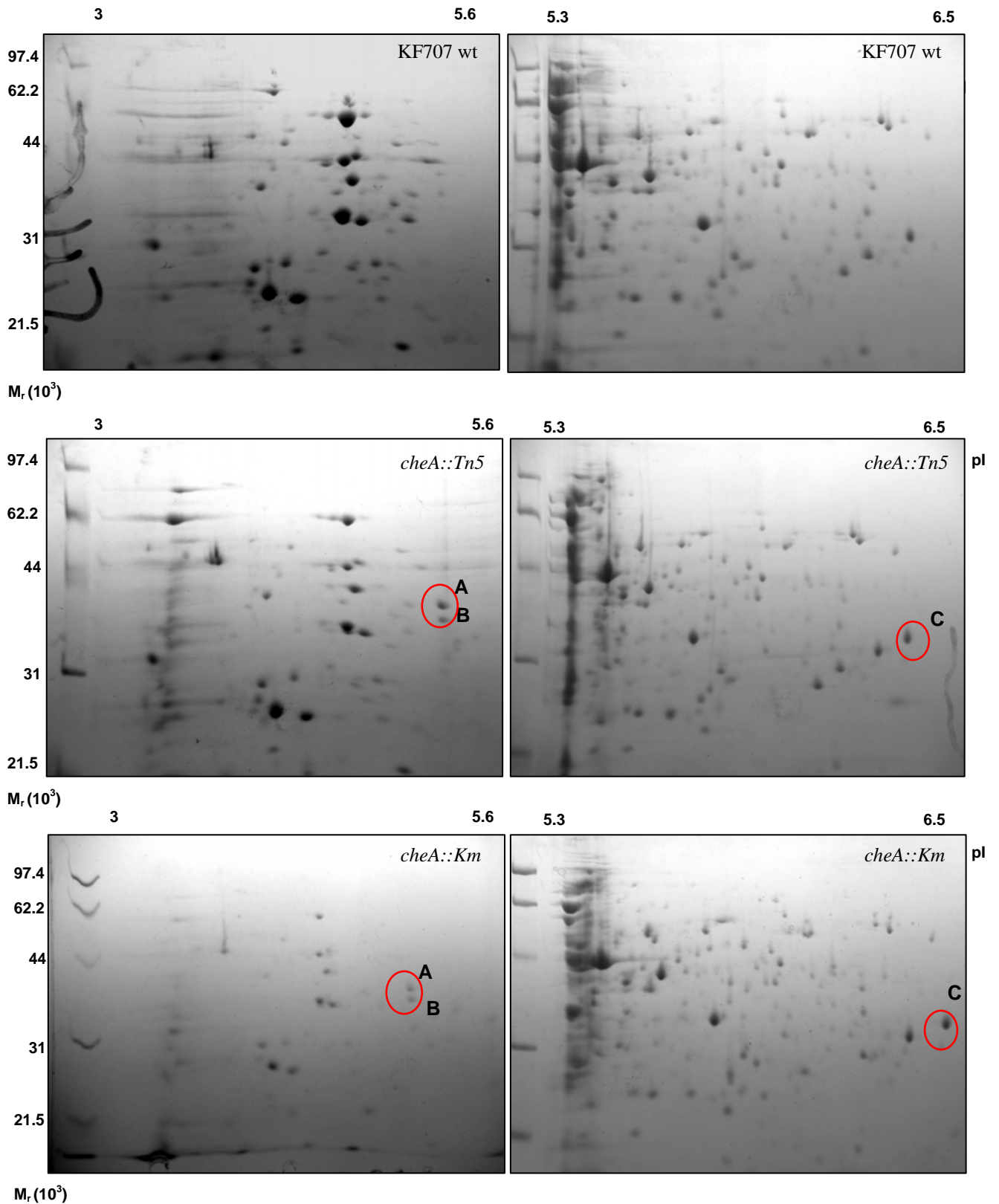


Figure 1.12. Comparative 2D-gel electrophoresis analysis of soluble proteins extracted from KF707 wild-type, *cheA::Tn5* and *cheA::Km* planktonic cells. Proteins differentially expressed are indicated by a red circle. Molecular weights are shown on the left while the pI range is indicated on the top of each panel.

Discussion

The data presented here provide a basic analysis of the process of biofilm development in *Pseudomonas pseudoalcaligenes* KF707. The study of biofilm formation is particularly relevant to the understanding of the physiology of this soil microorganism. The ability of *Pseudomonas pseudoalcaligenes* KF707 to form biofilms on the plastic surface of the Calgary biofilm device was investigated in both rich and minimal media. The microscopic analyses of KF707 biofilm development showed that bacterial cells attach to the plastic substratum first via the cell pole and then through the long axis of the cell body. At later incubation times, microcolonies are formed, which further evolve into a mature biofilm structure enclosed by an esopolysaccharide matrix (Figure 1.2). The observed process of KF707 biofilm formation follows the general four-step model proposed for biofilm development (O'Toole *et al.* (2000b) and is reminiscent of biofilm progression described for other bacteria, such as *Ps. aeruginosa* (Sauer *et al.* 2002, Tolker-Nielsen *et al.* 2000) and *E. coli* (Reisner *et al.* 2003).

Nutritional cues significantly affect biofilm formation and structure (Bollinger *et al.* 2001, Pratt and Kolter 1999, Kirisits and Parsek 2006). According to the nutritional environment *Ps. aeruginosa* forms two different types of biofilm, defined as flat or structured (Klausen *et al.* 2003, Kirisits and Parsek 2006). *Ps. pseudoalcaligenes* KF707 biofilms grown in different media were found to reach different cell densities (Figure 1.7, black lines) and display different structures (Figures 1.3-1.6). At 24 h of growth, KF707 cells formed flat, dense biofilms characterized by a confluent and almost uniform mat of cells covering the plastic surface when grown in minimal media (Figure 1.5) and structured, low density biofilms in LB rich medium (Figure 1.2 D). When biofilms were grown on other rich media, only small aggregates were produced (Figure 1.4 A, B). Biofilm structure was shifted to a thick biofilm when salt was added (Figure 1.4 C). The evolution of the biofilm architecture after prolonged times of growth results in few sparse cells remaining attached to the plastic surface or in the formation of a complex structure in rich LB medium and SA minimal medium respectively (Figure 1.6). These data suggest that biofilm

development in *Ps. pseudoalcaligenes* KF707 is metabolically controlled and that poor nutrient conditions and higher salinity result in a more robust biofilm for this soil bacterium. In this context, it has been proposed that in *E. coli* increased osmolarity could stimulate stable cell-surface interaction through the EnvZ/OmpR signalling pathway (Pratt and Silhavy 19995, Prigent-Combaret *et al.* 2001). The response of KF707 to different media compositions and high osmolarity may reflect the natural habitat to which this species is adapted. We can speculate that KF707 biofilm formation in rich media might not provide a growth advantage for the bacterial cells, because the free-swimming planktonic state would provide a greater surface area for nutrient acquisition than the biofilm surface-associated mode of growth. This consideration could also explain the phenotype of biofilms growing in LB for prolonged periods of time, which tend to disaggregate as opposed to biofilms growing in SA minimal medium, that rearrange their architecture and are less subjected to dispersal (Figure 1.6).

Members of the genus *Pseudomonas* inhabit soil and groundwater environments which are typically nutrient poor (Ghiorse and Wilson 1988, Henis 1987). A complex network of signals, often regulated by two-component systems, operate in bacteria to produce a physiological response suited to the specific environment (Hoch 2000). Chemotaxis is one of such networks, used by bacteria to respond to nutritional signals and to colonize niches that are optimum for their growth (Wadhams and Armitage 2004). In natural environments, surfaces preferentially accumulate proteins, polysaccharides and other molecules, forming a nutritionally rich zone that is metabolically favourable for bacterial cells (Lengeler *et al.* 1999). The ability to direct the movement against the flow and towards these surfaces via chemotaxis could be required for the successful colonization. Chemotaxis has been shown to be important during colonization and biofilm formation in both the human host and the environment (de Weert *et al.* 2002, Foynes *et al.* 2000, Kirov *et al.* 2004, Stelmach *et al.* 1999), although it is not considered to be a general requirement for biofilm formation (Pratt and Kolter 1998). In this study we have investigated a potential role for CheA, the sensor histidine kinase protein of the chemotaxis signalling pathway, in *Pseudomonas pseudoalcaligenes* KF707 biofilm formation. We show that *cheA* mutants are

defective in biofilm formation, as they form biofilms that have a 95 % decrease in the number of cells attached to the plastic surface. The observation that the flagellum number, placement and structure are indistinguishable from the parental ones (Figure 1.11), together with the ability of the mutant cells to initiate surface colonization to the same extent as the wild-type strain (Figure 1.7), suggest that the *cheA* mutant biofilms are blocked in the development of a structured wild type architecture, although *cheA* mutant cells are capable of performing early attachment to the plastic surface. It has been suggested that in *Pseudomonas aeruginosa* swarming motility may play a role in biofilm structure determination, with actively swarming cells forming flat biofilms and cells with reduced swarming motility forming structured biofilms (Shrout *et al.* 2006). Twitching motility on the other hand, may be required during microcolony formation for mediating cell-to-cell contacts as well as for movement along the surface (Thormann *et al.* 2004, Klausen *et al.* 2003, O'Toole and Kolter 1998). *Ps. pseudoalcaligenes* KF707 was found to be unable to swarm (Figure 1.10 B) but both the wild-type and the mutant strains were capable of performing twitching motility on plastic surfaces (Figure 1.10 C). This result indicates that the defect in biofilm formation does not rely on the impairment of flagellum-mediated attachment to the plastic surface or in surface translocation by pili-mediated motility. Accordingly, the microscopic analysis revealed the presence of small microcolonies on the surfaces colonized by the mutant cells but a parental biofilm structure never formed, under any growth condition tested (Figure 1.8). It is possible that the cell aggregates formed by mutant cells are unstable, formed by fragile clusters that disaggregate when a critical cell concentration is reached (Figure 1.7). Therefore, the data presented suggest that the signal transduction pathway regulated by the histidine kinase protein CheA is required for the progression of biofilm development in *Ps. pseudoalcaligenes* KF707. Chemotaxis could be necessary not only for swimming towards the plastic surface but also for coordinating the aggregation of microcolonies, that results in the production of the mature biofilm structure.

The comparison of the proteomic profiles demonstrated that some periplasmic binding proteins are differently expressed in the wild-type and mutant

cells, suggesting that the ChaA kinase may have a role in the regulation of the expression of these factors. The hypothesis of a cross-talk between two-component systems was first discussed late in the '80s (Ninfa *et al.* 1988, Stock *et al.* 1989). Since then, examples of cross-talk *in vitro* (Fisher *et al.* 1995, Igo *et al.* 1989, Ninfa *et al.* 1988, Yaku *et al.* 1997) and *in vivo* (Kim *et al.* 1996, Matsubara and Mizuno 1999, Wanner 1992) have been reported. However, evidence has also been given that two-component systems are highly specific and that cross-phosphorylation of non-cognate response regulators is likely to occur *in vivo* at a measurable rate when cells have been mutated in the cognate kinase (Verhamme *et al.* 2002). In this study, the possible role of the CheA histidine kinase in cross-regulated signal transduction pathways has not been investigated. Therefore, the genetic basis of the differential expression of the periplasmic binding proteins in *cheA* mutants is at the moment unknown. The role of the CheA histidine kinase in the regulation of the expression of such protein functions will be addressed in future studies.

The expression of periplasmic binding proteins associated to ABC transporters has been shown to be regulated during the switch from the planktonic to the sessile growth (Sauer and Kamper 2001). Moreover, a periplasmic binding protein was found to initiate a signalling pathway culminating in improved biofilm formation in *V. cholerae* (Karatan *et al.* 2005). The impaired biofilm phenotype showed by the *cheA* mutants of *Ps. pseudoalcaligenes* KF707 could be a consequence of the inability to optimally regulate the expression of periplasmic proteins and transporters required for the response to environmental signals that trigger biofilm formation. Otherwise, *cheA* mutant cells could be unable to reorganize protein expression after adhesion to the surface and the differential expression of periplasmic proteins in the *cheA* mutants may reflect a physiological state that is not suitable for biofilm development. Therefore, future studies will be aimed at understanding the role of periplasmic proteins in the development of a mature biofilm structure in *P. pseudoalcaligenes* KF707.

Although a general four step model of biofilm development (O'Toole *et al.* 2000b) can be applied to biofilms of different bacterial species as well as to *Ps. pseudoalcaligenes* KF707, this work adds evidence to the observation that the

molecular requirements for biofilm formation are different and differentially regulated in a species-specific manner (Stanley and Lazazzera 2004), even in closely related pseudomonads. These requirements are likely to be specifically adapted for the environment favoured by the bacterial species (i.e. low vs. high osmolarity or minimal vs. rich medium) according to the bacterial physiology. Chemotaxis has proven to be a selective advantage for the environmental fitness of degradative bacteria (reviewed in Pandey and Jain, 2002). Knowledge of the bacterial chemosensory behaviour towards naturally occurring chemicals and xenobiotics and of the coordinated regulation of biofilm development can be exploited for bioremediation of contaminated sites and will be useful for future research

Chapter 2

Tolerance of Pseudomonas pseudoalcaligenes KF707 biofilm and planktonic cells to metals

Introduction

Numerous physiological studies and recent global genome analyses have revealed that bacteria possess a copious number of specific resistance determinants that enable them to cope with metal toxicity. As an example, genome analysis showed that *Pseudomonas putida* KT2440, a model organism to which *Ps. pseudoalcaligenes* is evolutionarily closely related (Palleroni 1984), is equipped with 61 gene functions that are likely to be involved in metal homeostasis and/or tolerance, plus 7 systems coding for resistance mechanisms to heavy metals such as arsenic (*arsRBCH*), chromate (*chrA*), cadmium, zinc and cobalt (*czcCBA*) (Cánovas *et al.* 2003). In addition, *Ralstonia metallidurans* CH34, a type strain for metal resistance studies isolated from sites which are highly polluted with heavy metals (Diels *et al.* 1989, Diels and Mergeay 1990), was found to possess a remarkable set of ion efflux systems that can be specifically induced by metal ions (reviewed in Nies 2000). Increased efflux of metals is a widespread mechanism for metal resistance but is only one of the strategies that microbial cells have developed to survive metal toxicity: reduced uptake, reduction to elemental state, chemical modification via alchilation (mostly methylation), sequestration and chelation are a few more examples (Silver and Phung 1996 and Nies 1999).

Although fundamental, the existing knowledge of the mechanisms of metal toxicity and microbial responses is incomplete, as it mostly derives from the characterization of free-suspended (planktonic) microbial communities. Indeed, little is known about the mechanisms used by biofilms to counteract metal

toxicity, albeit biofilm is widely considered as the bacterial default mode of growth in natural environments (Costerton *et al.* 1994, Costerton *et al.* 1995).

Biofilms are inherently more tolerant to biocides and above all to antibiotics, in which case a 10-1000 times increase in tolerance has been observed in comparison to planktonic cultures (Costerton *et al.* 1999). Therefore, a large number of studies have focused on the mechanisms that cause the increased tolerance of biofilm to antibiotics and many reports can be found in the literature describing the multifactorial bases of this phenomenon (Lewis 2001, Mah and O'Toole 2001, Fux *et al.* 2005). Less information is available regarding biofilm tolerance to metals. Recent studies suggest that biofilm tolerance to metals is time-dependent (reviewed by Harrison *et al.* 2005c). In *Ps. aeruginosa*, short exposure times, such as 2-5 hours, result in high biofilm tolerance to metals, up to 600 times higher with respect to planktonic cells (Harrison *et al.* 2005b, Teitzel and Parsek 2003). On the other hand, longer exposure times (i.e. 24 hours) generally allow metals to kill 100 % of biofilm cells in both *E. coli* and *Ps. aeruginosa*, at concentrations that are often comparable to those required for killing planktonic populations (Harrison *et al.* 2005b, Harrison *et al.* 2005d). The information collected by Harrison and colleagues have shown that biofilm tolerance to metals, similarly to biofilm tolerance to antibiotics, is multifactorial (Harrison *et al.* 2005c). This means that several factors may contribute to the ability of biofilms to withstand biocide toxicity, namely: i) sequestering of biocides in the EPS matrix and slow diffusion across biofilm structure; ii) metabolic heterogeneity of populations; iii) distinct physiology of biofilm cells; iv) presence of specialized survivor cells, called 'persisters' (reviewed in Harrison *et al.* 2005c). It has been shown that EPS components are able to bind antimicrobial agents: a slow diffusion rate was observed for positively charged aminoglycoside antibiotics (Walters *et al.* 2003). Also, binding of heavy metals such as Pb^{2+} (Beyenal and Lewandowski 2004) and Zn^{2+} (Labrenz and Banfield 2004) was registered and EPS production was observed to be induced in sulfate-reducing bacteria and *Ps. aeruginosa* exposed to Cu^{2+} (White and Gadd 2000, Kazy *et al.* 2002). On the other hand, antibiotics such as rifampicin and fluoroquinolones were observed to efficiently penetrate biofilm structures and

diffuse freely (Dunne *et al.* 1993). Given that biofilms are also more tolerant to these antibiotics, it was apparent that binding and/or retardation of diffusion could not be the only factor involved in biofilm tolerance. Another factor that was suggested to contribute to biofilm tolerance is the physiological heterogeneity registered in biofilm populations. Physiological heterogeneity derives from the presence of oxygen and nutrient gradients that cause a decrease in metabolic activity and growth rate along the depth of biofilm structures (de Beer *et al.* 1994, Huang *et al.* 1995 and Wentland *et al.* 1996). Most antibiotics strictly target rapidly growing metabolically active cells (Tuomanen *et al.* 1986) and, accordingly, slow-growing bacteria nearest to surfaces in the biofilm structures have been documented to be tolerant to antibiotic killing (Borriello *et al.* 2004, Walters *et al.* 2003). The same structure-dependent metabolic heterogeneity has also been proposed to partly explain bacterial biofilm tolerance to metals (Harrison *et al.* 2005c). The observation that antimicrobial tolerance occurs in biofilms that are too thin to represent a relevant diffusion barrier for both biocides and metabolic substrates (Cochran *et al.* 2000, Das *et al.* 1998) and that freely-diffusing biocides able to kill non-growing cells are not effective against biofilms (Gilbert *et al.* 1997), suggested that other factors besides EPS matrix and metabolic dormancy are involved. It was proposed that a genetic control of a biofilm-specific phenotype exists and it has been recognised that a temporal protein expression pattern is realized during bacterial cell growth as a biofilm (Sauer *et al.* 2002, Schembri *et al.* 2003, Southey-Pilling *et al.* 2005). The expression of genes induced in planktonic cultures during starvation/stationary phase and general stress responses is shared amongst numerous biofilm systems, although a specific expression-pattern, common to all bacterial species studied so far, could not be delineated (for a review see Beloin and Ghigo 2005). Nonetheless, these genes may be relevant factors promoting the establishment of distinct physiological traits in biofilms, that enhance tolerance to antimicrobials. The observation that genes involved in heat shock, oxidative and envelope stress responses are generally induced within biofilms is important in the understanding of biofilm tolerance to metals (Ren *et al.* 2004, Beloin *et al.* 2004, Tremoulet *et al.* 2002, Sauer *et al.* 2002). Pure cultures of a bacterial species naturally produce

sub-populations of specialized survivor cells (persisters), that exhibit multidrug tolerance and neither grow nor die in the presence of antimicrobials (Bigger 1944, Lewis 2001, Spoering and Lewis 2001, Keren *et al.* 2004b). It has been suggested that persisters are present in biofilms at high levels and that they contribute to the high biofilm tolerance to biocides (Lewis 2001, Spoering and Lewis 2001). A genetic basis for persistence has been found in the expression of toxin-antitoxin modules and other genes that can block potential antibiotic targets (such as translation), thus preventing antibiotics from irreversibly damaging essential cellular functions (Keren *et al.* 2004a). Evidence has been given that persister cells may also mediate biofilm tolerance to metals (Harrison *et al.* 2005b, Harrison *et al.* 2005d). Ultimately, the tolerance of biofilms to both antibiotics and metals is likely to have a multifactorial foundation and clearly derives from the specificity of the biofilm mode of growth.

In the field of bioremediation, most of the studies on biofilm interactions with metals have focused on their sorption ability. Biofilms can act as adsorbents for heavy metals and for this reason biofilm-based bioreactors are commonly used for treating large volumes of dilute aqueous solutions such as industrial and municipal wastewaters (von Canstein *et al.* 1999, White and Gadd 1998). Biofilm-mediated bioremediation strategies are also effective in organic pollutant clean-up since the beneficial physical and physiological interactions among cells in high density biofilms, accelerate the use of xenobiotics (for a review see Singh *et al.* 2006). However, bacteria-based bioremediation requires that microorganisms are active in the presence of the target contaminant, as well as other contaminants. The remediation of co-contaminated sites, i.e. sites contaminated with both organic xenobiotics and heavy metals, is a major concern because they correspond to a high percentage of the hazardous waste sites on national priority lists for remediation, such as 40 % in the National Priority List of the U.S. Environmental Protection Agency (U.S. EPA) (Sandrin *et al.* 2000). Heavy metals are known to influence organic matter decomposition by the natural bacterial flora (Babich and Stotzky 1983) as well as biological remediation processes in both aerobic and anaerobic conditions (reviewed in Sandrin and Maier 2003). It has been reported for example, that the growth of a number of bacterial strains specialized in the

degradation of haloaromatic xenobiotics was totally inhibited at low heavy metal concentrations (Springael *et al.* 1993). To improve biodegradation in co-contaminated sites, the use of metal-resistant bacteria has been proposed as they are able to reduce the bioavailability of metals (i.e. by immobilization Valls *et al.* 2000) and/or protect indigenous bacterial communities from the noxious effects of heavy metals (Stephen *et al.* 1999). Therefore, understanding metal toxicity to strains with degradative abilities is particularly interesting and is crucial for the implementation of successful bioremediation strategies. To this end, the analysis of the tolerance of both biofilms and planktonic populations should be assessed in order to precisely predict bacterial behaviour in natural environments.

In this study, the effects of metal toxicity on biofilm and planktonic populations of the PCB-degrader microorganism *Ps. pseudoalcaligenes* KF707 were investigated under different growth conditions (i.e. rich medium and minimal medium). The toxicity of frequent contaminants of soil and groundwater, the metalloids oxyanions SeO_3^{2-} , TeO_3^{2-} and AsO_2^- and the metal cations Cd^{2+} , Ni^{2+} and Al^{3+} , was assessed. Arsenic, cadmium and nickel are all particularly common co-contaminants in sites polluted by organic compounds (Sandrin and Maier 2003) and are also some of the metals most frequently found in polluted sites (see U.S. EPA Superfund sites and ATSDR CERCLA priority list of hazardous substances). Antibiotic resistance is a hallmark of biofilms. Hence, the potential inherent tolerance of KF707 biofilms to biocides was also addressed. Both planktonic and biofilm cells were found to be particularly tolerant to the metalloids oxyanions selenite, arsenite and tellurite. Growth in minimal medium provided better conditions for the establishment of both antibiotic and metal-tolerant biofilm phenotypes.

Materials and methods

Bacterial strains and growth conditions

Ps. pseudoalcaligenes KF707 wild type was used in this study. The bacterial strain was grown on either LB rich medium or SA minimal medium. The composition of the media is described in the general material and methods chapter.

Stock solutions of antibiotics and metals

All metals [K_2TeO_3 , Na_2SeO_3 , $NaAsO_2$, $CdCl_2$, $Al_2(SO_4)_3$, $NiSO_4$] and antibiotics (amikacin, rifampicin) were purchased from Sigma Chemicals and Co. Stock solutions of metals were prepared in double-distilled water at 5 times (5×) the highest concentration used in the challenge plate, syringe-filtered and stored at room temperature. Antibiotic solutions were prepared in the same way as metal stock solutions but were frozen and stored at $-70\text{ }^\circ\text{C}$.

Stock solution of neutralizer

As recommended by the manufacturer and reported in Harrison *et al.* (2005a), the use of a neutralizing solution in metal susceptibility testing is required to reduce the carry-over of bioavailable metals from the challenge media to the recovery media, thus allowing for the discrimination of the bactericidal and the bacteriostatic effects of the substances tested. The recommended universal neutralizer (1.0 g/l L-histidine, 1.0 g/l L-cysteine, 2.0 g/l reduced glutathione) was used in this study, prepared as a 50 times concentrated solution (50×) in double-distilled water, syringe-filtered and stored at $-20\text{ }^\circ\text{C}$. Glutathione is used by microorganisms to counter toxicity of metals, such as cadmium and metalloids (i.e. arsenite, selenite and tellurite) and can thus be used as a neutralizing agent in this assay (Harrison *et al.* 2005a). Moreover, metal toxicity is commonly ascribed to the binding of metal ions to sulfhydryl ($-SH$) groups (Nies 1999). Therefore, L-cysteine is added to prevent the binding of metal ions to cellular proteins after the exposure to metals and as a result of the carry-over in recovery media. Finally, L-histidine is used because of its affinity for transition metal ions such as Zn^{2+} , Co^{2+} , Ni^{2+} and Cu^{2+} .

Biofilm cultivation and metal susceptibility testing

Biofilm cultivation. Biofilms were cultivated using the Calgary Biofilm Device (CBD), as described in Chapter 1 (Material and methods and Figure 1.1 A to C). An overview of biofilm cultivation procedure in the CBD is also reported in Figure 2.1 (panels 1 to 4). KF707 biofilms were grown in LB and SA minimal medium for a period of time of 4 h and 24 h.

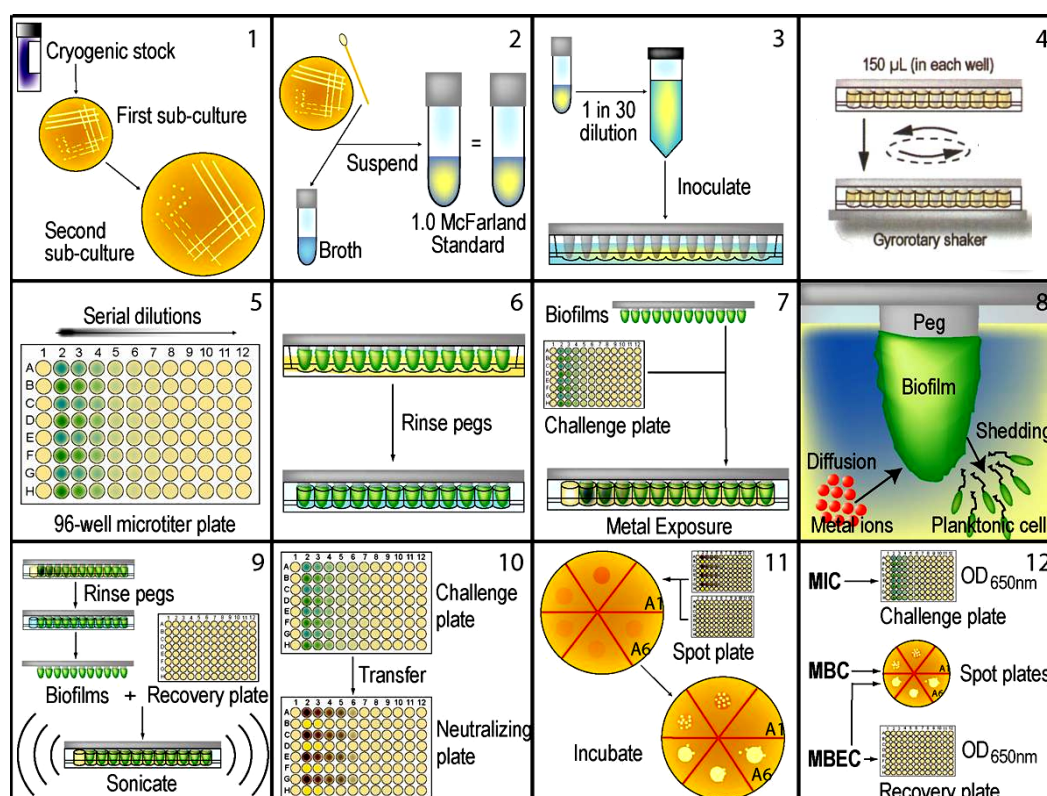


Figure 2.1. Biofilm cultivation on the CBD (panels 1 to 4) and high-throughput assay for biocide susceptibility testing (panels 5 to 12). MIC, minimum inhibitory concentration; MBC, minimum bactericidal concentration; MBEC, minimum biofilm eradication concentration. Adapted from Harrison *et al.* 2005a.

Metal susceptibility testing. Antibiotic and metal susceptibility assays were performed using the MBECTM-HTP assay according to the procedure described by Ceri *et al.* (1999) and Harrison *et al.* (2004a, 2005a). This assay for metal susceptibility testing is a high throughput method that allows for a rapid and efficient screening of biofilm and planktonic cell susceptibility to biocides. In each assay, ten concentrations of two different biocides were tested against the biofilms grown on the 96 pegs of the CBD. Each concentration of each biocide was tested in quadruplicate. An overview of the experimental protocol is given in Figure 2.1 (panels 5 to 12). Challenge media (media containing the metal or antibiotic to be tested) were prepared by diluting the metal or antibiotic stock solution 5 times in the LB or SA growth media. Challenge media were prepared just prior to use, to avoid metal precipitation. Serial two-fold dilution gradients of the challenge media were prepared along the rows of a 96 microtitre plate, to create the so-called challenge plate (Figure 2.1, panel 5). The first and the last well of the plate contained fresh medium in the absence of biocide and served as a sterility control and a growth control respectively. After 4 h or 24 h of growth, the biofilms formed on the CBD were rinsed once in 0.9 % saline to remove loosely adherent planktonic cells (Figure 2.1, panel 6) and then exposed to metals or antibiotics by inserting the peg lid into the challenge plate (Figure 2.1, panel 7). Metal exposure was carried out in the same medium used for biofilm growth (i.e. biofilms grown for 4 or 24 h in LB were exposed to LB challenge media and SA grown biofilms were exposed to SA challenge media). Both biofilm and planktonic growth were monitored before the exposure by collecting four sample pegs and four aliquots of planktonic cultures for the determination of the CFU per peg and CFU/ml respectively, as described in Chapter 1 (Materials and methods, § *Biofilm and planktonic growth curves*). The exposure was carried out at 30 °C and 95 % relative humidity in a gyrorotary shaker at 100 rpm for 24 h. During the exposure, planktonic cultures are inoculated with the cells shed from the biofilm, in a way that reflects the duality of the bacterial life cycle, where biofilm cells that survive biocide exposure serve as a source of free-swimming cells that can repopulate the surrounding environment (Figure 2.1, panel 8). After exposure, biofilms were rinsed twice in 0.9 % saline solution and then transferred into a new

microtitre plate (recovery plate) containing the recovery medium (LB broth, 0.1 % Tween-20, universal neutralizer diluted 1:50 from the stock solution). The biofilm cells were disrupted and collected in the recovery medium by sonication using an Aquasonic 250HT ultrasonic cleaner (VWR International, Mississauga, ON, Canada) set at 60 Hz for 5 minutes (Figure 2.1, panel 9). The planktonic cultures grown in the challenge plate were also neutralized. In this case, 10 μ l of neutralizing stock solution diluted 1:10 in 0.9 % saline was added to 40 μ l of planktonic cultures in the neutralizing plate (Figure 2.1, panel 10), so that the neutralizer solution was finally diluted 1:50. Aliquots of both the neutralized biofilm and planktonic cultures were spot plated onto LB agar plates, that were incubated for 36 h at 30 °C (Figure 2.1, panel 11). MBCs (minimum bactericidal concentrations) and MBECs (minimum biofilm eradication concentrations) were determined by scoring the spot plates for bacterial growth (Figure 2.1, panel 12) while MICs (minimum inhibitory concentrations) were determined by reading the optical density at 650 nm (OD_{650}) of challenge plates after 48 h at 30 °C using a THERMOmax microplate reader with SOFTMAX PRO data analysis software (Molecular Devices, Sunnyvale, CA).

Results

Biofilm formation

The susceptibility of *Pseudomonas pseudoalcaligenes* KF707 to metals and antibiotics was assayed on biofilms grown in LB rich medium and SA minimal medium for 4 h or 24 h. As shown in Chapter 1, KF707 biofilm formation follows the proposed four-step model for biofilm development, consisting in reversible attachment, irreversible attachment, maturation and dispersion (O'Toole *et al.* 2000b). At 4 h, KF707 cells are involved in the establishment of the irreversible attachment to the surface (Chapter 1, Figure 1.2 A). After 24 h, biofilms reach the maximum cell density and display a mature architecture, that can be defined as structured or flat in LB and SA media respectively (Chapter 1, Figure 1.2 D and Figure 1.4 A). Viable cell counts were carried out in order to determine the number of viable cells forming KF707 biofilms after 4 and 24 h of growth in both media. The mean values and standard deviations were calculated for the pooled data obtained from the growth controls performed during each susceptibility assay (at least 16 replicates for each data set) and are reported in Table 2.1. After 4 h of growth, approximately 10^4 CFU per peg were irreversibly attached on the pegs of the CBD in both LB and SA media, while after 24 h the cell density of SA grown biofilm was found to be higher than the cell density of biofilms grown in LB for the same period of time (i.e $\sim 10^5$ in LB vs. $\sim 10^6$ in SA, Table 2.1). The number of cells in 4 h LB or SA grown biofilms were not found to be statistically different according to the student-t test.

Table 2.1. Cell density of *Ps. pseudoalcaligenes* KF707 biofilms grown in LB rich medium or SA minimal medium for either 4 or 24 h. Means and standard deviations are in CFU per peg.

Time of growth (h)	Growth medium	
	LB	SA
4 h	$(4.3 \pm 1.9) \times 10^4$	$(3.1 \pm 1.9) \times 10^4$
24 h	$(2.4 \pm 2.0) \times 10^5$	$(1.5 \pm 0.3) \times 10^6$

Definition of MIC, MBC and MBEC values for biocide susceptibility assays

Planktonic cell susceptibility to antimicrobials is described by two different measurements, the MIC (minimum inhibitory concentration) and the MBC (minimum bactericidal concentration). According to standard definitions, the MIC is the lowest concentration required to prevent planktonic growth, while the MBC is the lowest concentration required to kill 3 log₁₀ of the initial number of cells, i.e. 99.9 % of the planktonic culture (MBC_{99.9}). The MIC reflects the ability of a bacterial population to grow in the presence of a antimicrobial agent, hence it is a measure of planktonic resistance to a biocide. In contrast, the MBC reflects the ability of a bacterial population to survive the exposure and therefore it is a measure of planktonic tolerance to a certain antimicrobial. The MBC_{99.9} definition is often inadequate to describe the tolerance of bacterial communities to biocides because 99.9 % of a population is killed rapidly (i.e. MBC_{99.9} is usually low) and the fraction of surviving cells is not negligible because of the multidrug tolerance commonly exhibited by these cells (persister cells, reviewed in Lewis 2005). Therefore, the MBC₁₀₀ definition has been adopted in this study, that is the lowest concentration required to kill 100 % of the planktonic population. In the same way, the tolerance of biofilms has been described by the MBEC₁₀₀ (minimum biofilm eradication concentration), that is the lowest concentration required to kill 100 % of the bacterial cells in a biofilm. MCB₁₀₀ and MBEC₁₀₀ are appropriate parameters for the description of planktonic and biofilm tolerance to antimicrobials because they include the killing of persister cells. This is of particular importance for an accurate definition of biofilm susceptibility to

antimicrobials given that persister cells are considered responsible for the recalcitrance of bacterial infections associated with biofilms, despite the fact that they correspond to only a small fraction of bacterial populations (Lewis 2001).

Susceptibility of *Ps. pseudoalcaligenes* KF707 biofilm and planktonic cells to antibiotics and metal compounds

It has been suggested that biofilm structure affects tolerance to biocides, with flat biofilms being more susceptible to antimicrobials than the structured counterparts (Landry *et al.* 2006). In this study the requirement of a structured architecture for the development of biofilm tolerance to antibiotics and metals was addressed by using different biofilm systems produced by *Ps. pseudoalcaligenes* KF707 on the CBD (i.e. 4 h LB or SA grown biofilms and 24 h LB or SA grown biofilms). Biofilms grown for 4 h consisted of just attached cells in both LB and SA media, while 24 h mature biofilms displayed a structured architecture in LB and a flat architecture in SA (see Chapter 1). The susceptibility of biofilm and planktonic cultures to antibiotics and metals was assayed by measuring the MIC, MBC and MBEC values after a 24 h exposure time. Metal and antibiotic exposures were carried out in the same medium used for biofilm growth. MIC, MBC and MBEC values and standard deviations are reported in Table 2.2 – 2.5. The fold tolerance value was used to describe biofilm vs. planktonic tolerance and was defined as the $MBEC_{100}/MBC_{100}$ ratio on a \log_2 sensitivity scale, that is due to the two-fold dilution gradients of antimicrobials realized in the challenge plate (see Material and methods for further details).

Table 2.2. Metal and antibiotic susceptibility of *Ps. pseudoalcaligenes* KF707 biofilm and planktonic cells grown for 4 h in LB and exposed for 24 h in the same medium. MIC, MBC and MBEC values are in mM and $\mu\text{g ml}^{-1}$ for metals and antibiotics respectively. The fold tolerance is used to describe biofilm vs. planktonic tolerance and is defined as the MBEC:MBC ratio on a \log_2 sensitivity scale.

Compound	MIC	MBC	MBEC	Fold Tolerance
K_2TeO_3 (mM)	0.098 ± 0	0.196 ± 0	0.24 ± 0.08	1.2
Na_2SeO_3	28.8 ± 0	115 ± 0	115 ± 0	1
NaAsO_2	1.92 ± 0	38.5 ± 13.3	53.9 ± 13.3	1.4
$\text{Al}_2(\text{SO}_4)_3$	0.73 ± 0	5.9 ± 0	1.5 ± 0	0.25
CdCl_2	0.39 ± 0	0.98 ± 0.34	0.78 ± 0	0.8
NiSO_4	3.2 ± 0	3.2 ± 0	3.2 ± 0	1
Amikacin ($\mu\text{g ml}^{-1}$)	2.5 ± 0.9	4 ± 0	4 ± 0	1
Rifampicin	2 ± 0	4 ± 0	4 ± 0	1

Table 2.3. Metal and antibiotic susceptibility of *Ps. pseudoalcaligenes* KF707 biofilm and planktonic cells grown for 24 h in LB and exposed for 24 h in the same medium. MIC, MBC and MBEC values are in mM and $\mu\text{g ml}^{-1}$ for metals and antibiotics respectively. The fold tolerance is used to describe biofilm vs. planktonic tolerance and is defined as the MBEC:MBC ratio on a \log_2 sensitivity scale.

Compound	MIC	MBC	MBEC	Fold Tolerance
K_2TeO_3 (mM)	0.098 ± 0	0.49 ± 0	0.098 ± 0	0.20
Na_2SeO_3	36.7 ± 10.5	115 ± 0	115 ± 0	1
NaAsO_2	1.92 ± 0	30.8 ± 0	30.8 ± 0	1
$\text{Al}_2(\text{SO}_4)_3$	0.73 ± 0	3.6 ± 1.5	0.73 ± 0	0.2
CdCl_2	0.8 ± 0	0.98 ± 0.39	0.78 ± 0	0.8
NiSO_4	3.2 ± 0	6.5 ± 0	4.8 ± 1.9	0.75
Amikacin ($\mu\text{g ml}^{-1}$)	2 ± 0	4 ± 0	21.3 ± 7.5	5.3
Rifampicin	3.5 ± 0.9	4 ± 0	96 ± 45	24

Table 2.4. Metal and antibiotic susceptibility of *Ps. pseudoalcaligenes* KF707 biofilm and planktonic cells grown for 4 h in SA and exposed for 24 h in the same medium. MIC, MBC and MBEC values are in mM and $\mu\text{g ml}^{-1}$ for metals and antibiotics respectively. The fold tolerance is used to describe biofilm vs. planktonic tolerance and is defined as the MBEC:MBC ratio on a \log_2 sensitivity scale.

Compound	MIC	MBC	MBEC	Fold Tolerance
K_2TeO_3 (mM)	0.05 ± 0	0.05 ± 0	0.05 ± 0	1
Na_2SeO_3	14.4 ± 0	28.8 ± 0	21.6 ± 7.2	0.75
NaAsO_2	1.92 ± 0	30.8 ± 0	19.2 ± 6.7	0.5
$\text{Al}_2(\text{SO}_4)_3$	-	0.73 ± 0	0.73 ± 0	1
CdCl_2	-	< 0.39	0.98 ± 0.34	> 2
NiSO_4	1.6 ± 0	2 ± 0.7	2.4 ± 0.8	1.2
Amikacin ($\mu\text{g ml}^{-1}$)	1 ± 0	2 ± 1	128 ± 0	64
Rifampicin	4 ± 0	4 ± 0	208 ± 83	52

Table 2.5. Metal and antibiotic susceptibility of *Ps. pseudoalcaligenes* KF707 biofilm and planktonic cells grown for 24 h in SA and exposed for 24 h in the same medium. MIC, MBC and MBEC values are in mM and $\mu\text{g ml}^{-1}$ for metals and antibiotics respectively. The fold tolerance is used to describe biofilm vs. planktonic tolerance and is defined as the MBEC:MBC ratio on a \log_2 sensitivity scale.

Compound	MIC	MBC	MBEC	Fold Tolerance
K_2TeO_3 (mM)	0.05 ± 0	0.1 ± 0.02	0.20 ± 0	2
Na_2SeO_3	10.8 ± 3.6	115 ± 0	115 ± 0	1
NaAsO_2	1.92 ± 0	30.8 ± 0	61.6 ± 0	2
$\text{Al}_2(\text{SO}_4)_3$	-	2.9 ± 0	5.9 ± 0	2
CdCl_2	-	6.3 ± 0	7.8 ± 2.7	1.2
NiSO_4	6.5 ± 0	19.4 ± 6.5	22.6 ± 5.6	1.2
Amikacin ($\mu\text{g ml}^{-1}$)	1 ± 0	2 ± 1	192 ± 64	96
Rifampicin	4 ± 0	4 ± 0	208 ± 83	52

Susceptibility to antibiotics. A hallmark trait of biofilms is their high inherent tolerance to antibiotics (Prosser *et al.* 1987, Nickel *et al.* 1985, Gristina, *et al.* 1987, Evans and Holmes 1987, Costerton *et al.* 1999, Hogan and Kolter 2002). *Ps. pseudoalcaligenes* KF707 susceptibility to antibiotics was assayed by measuring MIC, MBC and MBEC values resulting from a 24 h exposure to the antibiotics amikacin and rifampicin. Rifampicin exerts its toxic effects on bacterial cells by inhibiting the microbial DNA-dependent RNA polymerase while amikacin is an aminoglycoside, whose toxicity relies on its ability to block the initiation of translation by specifically binding to microbial ribosomes. In the susceptibility assays performed in this study, KF707 planktonic growth was inhibited at concentrations of antibiotics as low as 2 $\mu\text{g ml}^{-1}$ and killing of the free-swimming cells occurred using 4 $\mu\text{g ml}^{-1}$ of both antibiotics (Table 2.2-2.5). Biofilms were found to be from 5 to 96 times more tolerant than the corresponding planktonic cultures, although tolerance varied according to growth conditions. In LB medium, 4 h biofilms were efficiently eradicated at concentrations of antibiotics as low as 4 $\mu\text{g ml}^{-1}$ and did not display increased tolerance in comparison to the planktonic cells (Figure 2.2 A, B). On the other hand, 24 h LB biofilms showed increased tolerance to antibiotics, with a fold tolerance of 5 and 24 for amikacin and rifampicin respectively (Figure 2.2 B). The results were different for biofilms grown in SA minimal medium. In this case, 4 h and 24 h biofilms were eradicated at much higher concentrations than LB biofilms grown for the same period of time (Figure 2.2 A) and were more tolerant than the corresponding planktonic cultures. Interestingly, the increase in tolerance occurred immediately after attachment to the plastic surface, in 4 h SA grown biofilms (Figure 2.2 B).

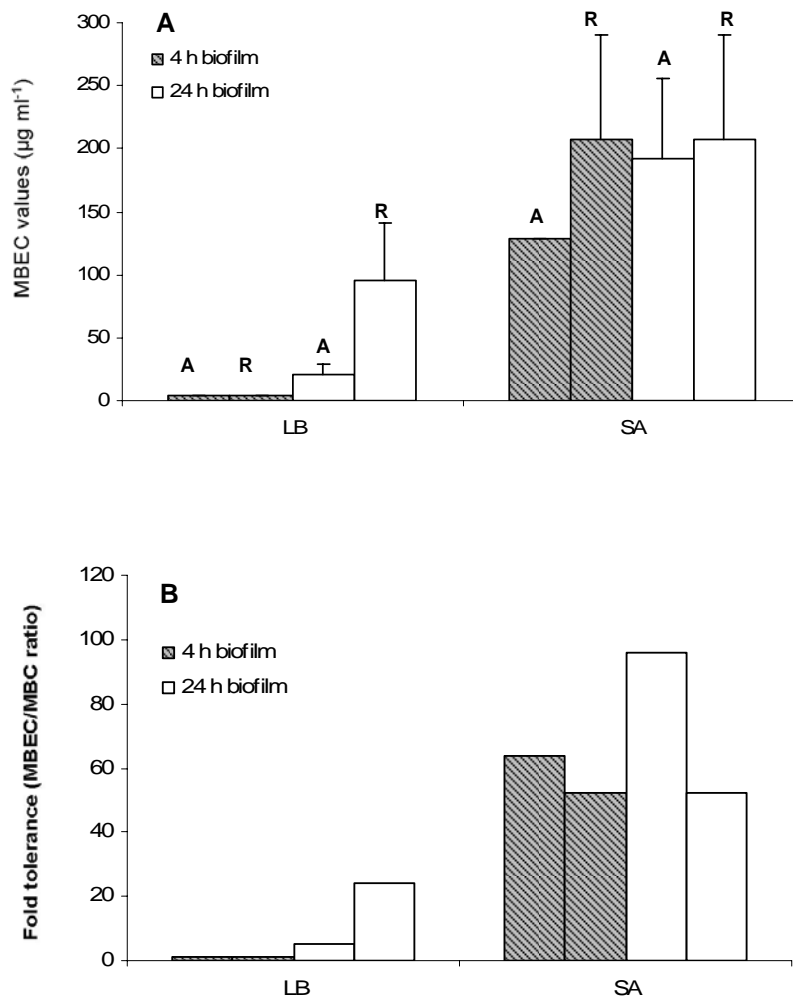


Figure 2.2. Eradication of *Ps. pseudoalcaligenes* KF707 biofilms by antibiotics. Grey bars represent (A) MBEC values (minimum biofilm eradication concentration) and (B) fold tolerance of 4 h grown biofilms. White bars represent (A) MBEC values and (B) fold tolerance for 24 h grown biofilms. Age and structure of biofilms are relevant factors for biofilm tolerance in LB medium only. SA grown biofilms are highly tolerant to antibiotics and the increase of tolerance occurs as soon as planktonic cells become attached to the substratum (i.e. 4 h of growth). LB grown biofilms are eradicated more easily than SA grown biofilms and, in LB medium, attachment to the plastic surface does not provide the cells with increased tolerance to antibiotics (i.e. fold tolerance is equal to 1 in 4 h LB biofilms). The fold tolerance value is a measure of biofilm increased tolerance and is defined as the MBEC/MBC ratio. A fold tolerance higher than 1 indicates increased biofilm tolerance in relationship to planktonic cultures. A, amikacin; R, rifampicin.

As expected, the data described here show that mature biofilms display decreased susceptibility to antibiotics compared to the corresponding planktonic cells in both LB and SA media. However, KF707 flat biofilms grown in SA medium are more tolerant than structured biofilms grown in LB for the same period of time, suggesting that a structured architecture is not required for increased biofilm tolerance. Accordingly, a tolerant phenotype was displayed by 4 h SA biofilms, formed by just sparse cells, lacking any kind of structure. Hence, in *Ps. pseudoalcaligenes* KF707 tolerance to antibiotics was mainly dependent on growth conditions and only slightly on biofilm density or structure.

Susceptibility to metals. The susceptibility of the PCB-degrader KF707 strain to SeO_3^{2-} , TeO_3^{2-} and AsO_2^- oxyanions and Cd^{2+} , Ni^{2+} and Al^{3+} cations was assayed in this study. As for the antibiotic susceptibility testing, sensitivity of KF707 to metals was assayed by measuring MIC, MBC and MBEC values of biofilms and planktonic cells grown in LB or SA media for 4 h and 24 h and then exposed to metal ions for 24 h. MIC, MBC and MBEC values and corresponding standard deviations are summarized in Table 2.2 – 2.5. In the case of exposure to tellurite (TeO_3^{2-}) and selenite (SeO_3^{2-}), MIC values were found to be higher for planktonic cells grown in rich medium (LB) than in SA minimal medium, while MIC values for arsenite (AsO_2^-) and nickel (Ni^{2+}) were comparable in both media. MIC values for aluminium (Al^{3+}) and cadmium (Cd^{2+}) in SA medium could not be determined because of metal precipitation. The concentrations of metals that inhibit KF707 growth are higher than concentrations inhibitory to the gram-negative model organisms *E. coli* (Nies 1999). As an example, MIC values for *E. coli* grown in TRIS-buffered minimal salt medium at pH 7 is 1.0 mM for Ni^{2+} (Nies 1999) while *Ps. pseudoalcaligenes* KF707 is able to grow in the presence of nickel concentrations as high as 6.5 mM (Figure 2.3 A). This value is comparable to the MIC of *R. metallidurans* CH34, a well known heavy metal resistant strain (Mergeay *et al.* 1985, Nies 2000). KF707 planktonic cultures were found to be particularly resistant to selenite toxicity (MIC ranging in 11-37 mM depending on growth conditions, Figure 2.3 A).

The killing of planktonic cultures generally occurred at concentrations of metals higher than those required for growth inhibition (i.e. $MBC > MIC$). Planktonic cultures deriving from low density biofilms were killed at higher concentrations of metals when cells were seeded in LB medium in comparison to SA medium (Figure 2.3 B). This result could be due to the presence of metal-binding components in LB medium that can reduce solution-phase metal concentrations (i.e. yeast extract, Sandrin and Maier 2003). MBC values of planktonic cultures inoculated by 24 h grown biofilms were generally comparable, with the exception of Cd^{2+} and Ni^{2+} cations, i.e. higher MBC values were measured in SA medium (Figure 2.3 B). This could be due to the basification of the pH during growth in SA (up to 7.5 after a 24 h period of growth leading to $OD_{660} \sim 0.8$) and the presence of 3 mM PO_4^{2-} in the medium. Indeed, these conditions can cause a decrease in the solubility of metal cations such as cadmium (Sandrin and Maier 2003). Killing of planktonic cultures seeded by low density biofilms occurred at lower concentrations of metals. It is possible that in this case a lower number of cells is released from biofilms into the wells of the microtitre plate containing the metal solutions and therefore the culture is more easily eradicated. Overall, KF707 planktonic cultures were particularly tolerant to killing mediated by selenite and arsenite metalloids oxyanions (MBC \sim 115 mM and 30 mM respectively, Figure 2.3 B).

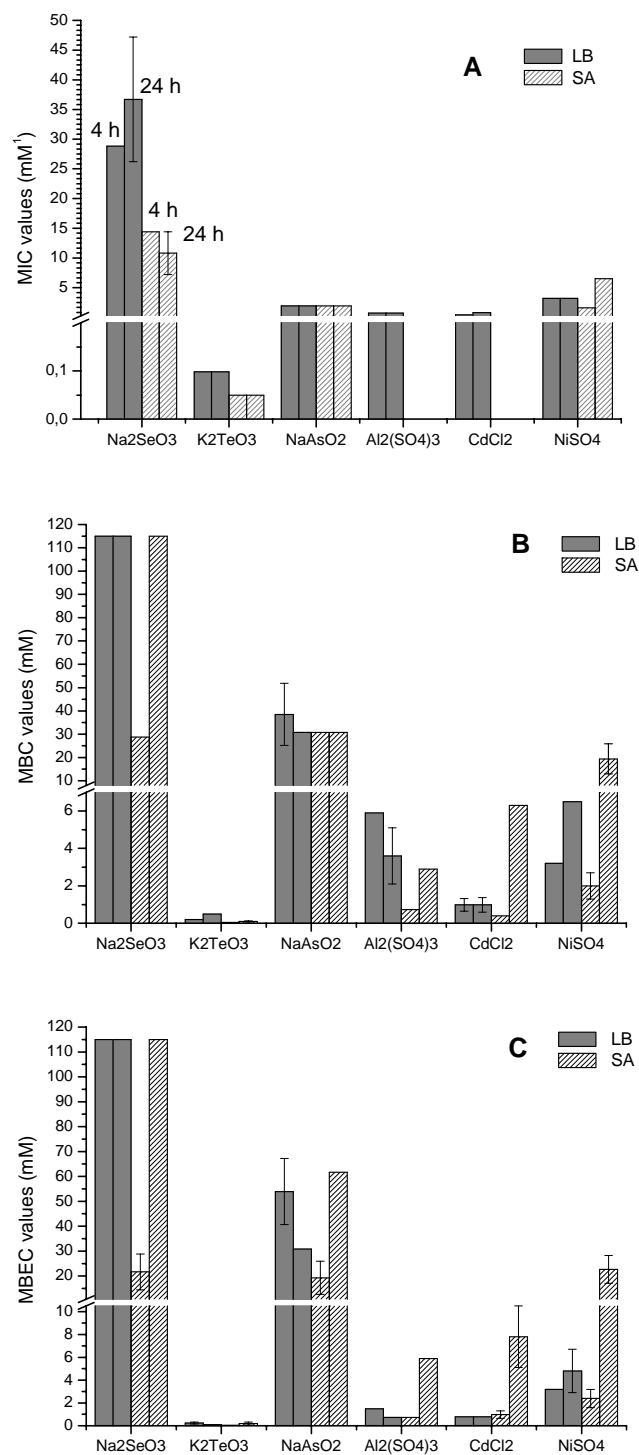


Figure 2.3. Susceptibility of *P. pseudoalcaligenes* KF707 to metals. Planktonic cultures were inoculated by biofilms grown for 4 h or 24 h in LB or SA media on the pegs of the CBD, as illustrated in Figure 2.1. A) Minimal inhibitory concentrations (MIC) of planktonic cells grown in LB and SA media. B) Minimal bactericidal concentrations (MBC) able to kill 100 % of the planktonic populations in LB and SA media. C) Minimal biofilm eradication concentrations (MBEC) killing 100 % of biofilm cells. All values and standard deviations are in mM.

The tolerance of KF707 biofilms to metal toxicity was found to vary as a function of the metal species (oxyanion vs. cation), the biofilm density (4 h low density vs. 24 h high density biofilms) and the growth medium (LB vs. SA). Biofilms grown for 4 h in LB medium were found to be more tolerant to oxyanions than those grown in SA for the same period of time (Figure 2.3 C). Again, this result could be explained considering the presence of metal-binding components in rich media which are able to complex oxyanions and reduce the bioavailable concentrations of those compounds. As regards to metal cations, KF707 4 h grown biofilms were equally susceptible in both media (Figure 2.3 C). In general, low density biofilms did not display increased tolerance to metal killing in comparison to the corresponding planktonic cells (fold tolerance ~ 1 , Figure 2.4 A). A fold tolerance ranging from 0.5 to 1.5 cannot be considered significant because it corresponds to a two-fold decrease or increase in biofilm susceptibility respectively, that means it is equal to the sensitivity of the assay. For cadmium, the fold tolerance of biofilms grown in SA for 4 h was found to be ~ 2.5 because of the low MBC of the planktonic cells, that are killed at the threshold of the minimum concentration of Cd^{2+} used in the susceptibility assay. From these results, it is apparent that cell attachment to the plastic surface does not provide increased tolerance to metal toxicity. Therefore, KF707 tolerance to antibiotics and metals is likely to originate from different mechanisms, given that an increase in tolerance to metals does not occur immediately upon attachment to the plastic surface, as is the case for antibiotics. Mature biofilms grown for 24 h in SA medium were found to be more tolerant to both oxyanions and cations than LB grown biofilms (i.e. $\text{MBEC}_{\text{SA}} > \text{MBEC}_{\text{LB}}$, Figure 2.3 C). In most cases, SA 24 h biofilms displayed increased tolerance in comparison to the corresponding planktonic cultures (fold tolerance = 2, Figure 2.4 B) while biofilms grown in LB for 24 h were equally or more susceptible to metal toxicity than planktonic cells (Figure 2.4 B).

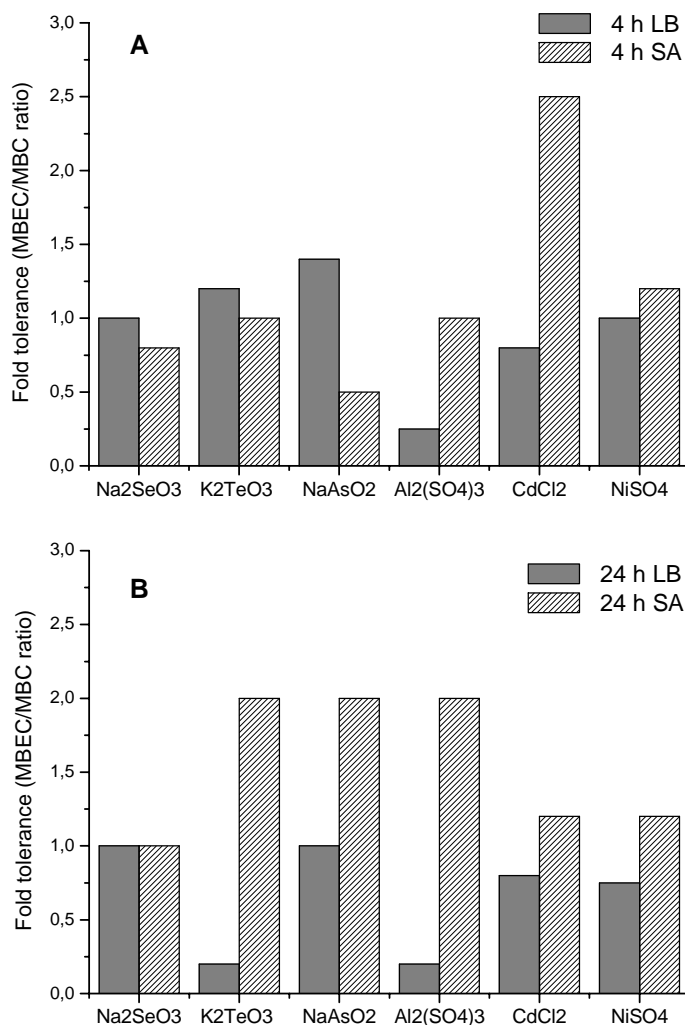


Figure 2.4. Susceptibility of 4 h (A) and 24 h (B) grown biofilms in comparison to the corresponding planktonic cells. The fold tolerance value is a measure of biofilm increased tolerance to metal toxicity and is defined as the MBEC/MBC ratio. A fold tolerance higher than 1 indicates increased biofilm tolerance in relationship to planktonic cultures.

Concordant with the high tolerance of SA grown biofilms to antibiotics, the observed tolerance to metals suggests that growth in this medium could provide KF707 with a physiological state that makes KF707 cells less vulnerable to environmental stresses. Tolerance to metals as well as tolerance to antibiotics does not seem to depend on the structured architecture of biofilms as much as on the physiological and metabolic conditions of KF707 cells, with the flat biofilms formed during growth in SA minimal medium being less susceptible to both kind of stresses than structured LB grown biofilms.

Selenite and tellurite transformation in *Ps. pseudoalcaligenes* KF707 biofilm and planktonic cells

Ps. pseudoalcaligenes KF707 is able to grow in the presence of high concentrations of tellurite (Di Tomaso *et al.* 2002) as well as selenite (shown in this study). Growth in the presence of tellurite and selenite is often characterized by the reduction of the oxyanions to their elemental forms selenium (Se^0) and tellurium (Te^0), that confer a distinctive black or orange colour respectively to microbial cultures. Reduction of selenite and tellurite has been described as a resistance mechanism to tellurite toxicity, although growth without reduction has also been shown to occur (mechanisms of tellurite resistance are reviewed in Turner 2001). Planktonic cultures of KF707 were observed to reduce tellurite and selenite to their black and orange end-products. However, the corresponding biofilm populations did not show a visible reduction of the metalloids oxyanions. Loss of reduction did not correspond to an increase in biofilm susceptibility to either selenite or tellurite. As an example, fold tolerance to selenite was ~ 1 , meaning that planktonic and biofilm population were equally susceptible to selenite killing (Figure 2.3 A, B) even though biofilms did not reduce the oxyanion. In the case of tellurite, a fold tolerance higher than 1 was observed for biofilm growing cells, and again no reduction was clearly visible. No evidence was given that reduction of selenite and tellurite by KF707 cells is accomplished as a resistance strategy to counter selenite and tellurite toxicity (Di Tomaso *et al.* 2002, this study). Nevertheless, loss of selenite and tellurite reduction ability during growth as a biofilm suggests that biofilms correspond to a different physiological and/or metabolic condition than the planktonic state. Accordingly, it has been observed that biofilms formed by other bacterial species process metalloids oxyanions in different ways to planktonic cultures (Harrison *et al.* 2004b).

Discussion

The study of the mechanisms of microbial adaptation and resistance to metal toxicity has provided the tools to carry out bioremediation of polluted sites (de Lorenzo 1994, Keasling and Bang 1998). Extending this knowledge to the mechanism of biofilm tolerance to metals can surely provide new potential solutions for bioremediation of contaminated areas. Of particular interest is the understanding of tolerance to metal toxicity to degradative and environmentally robust bacterial strains such as *Ps. pseudoalcaligenes* KF707.

In this study the ability of *Ps. pseudoalcaligenes* KF707 to withstand metal toxicity in both liquid and biofilm cultures was tested. We assayed the toxicity of the metalloids oxyanions SeO_3^{2-} , TeO_3^{2-} and AsO_2^- and the metal cations Cd^{2+} , Ni^{2+} and Al^{3+} by means of a high-throughput technique, the MBECTM-HTP assay (Figure 2.1). Given that the nature of media formulations affect bacterial susceptibility to metals, KF707 sensitivity was studied in both rich and minimal medium, LB and SA respectively. These media were chosen because: i) they provide good growth conditions to KF707 both in liquid and as a biofilm (see Chapter 1) and ii) their use in testing metal toxicity in bacteria have been reported in previous studies (for the use of LB see Harrison *et al.* 2004, Harrison *et al.* 2005a-b). In particular, asparagine-based media such as SA (sucrose-asparagine), described as an ideal growth medium for *Ps. aeruginosa* (Highsmith and Abshire 1975), have a relatively simple composition, low metal-binding capacity and have been used for the assessment of metal tolerance in environmental bacteria (Hassen *et al.* 1998). A key feature of the MBECTM-HTP assay is that it reproduces *in vitro* a natural environmental system in which a biofilm is a source of cells that can populate the surrounding milieu. In this study we used concentrations of heavy metals that are comparable and in most cases exceed the total metal concentrations in contaminated sites [see NABIR Field Research Centre (FRC)]. It is known that the activity of a free metal ion, which is considered to be the toxic metal species that determines the microbial response, correlates with the bioavailable fraction (Morrison *et al.* 1989). This fraction rarely approaches the total metal concentration added to media (Angle and Chaney 1989) because of

metal precipitation and/or chelation by media components (i.e. tryptone and yeast extract present in rich media can bind metal ions, while the presence of phosphates at neutral pH can cause metal precipitation in minimal media Sandrin and Maier 2003). However, in spite of this limit, MIC, MBC and MBEC values determined in this study can be a valid tool to estimate the action of heavy metals on the microbial activity and environmental fitness of a degrader strain such as *Ps. pseudoalcaligenes* KF707 at polluted sites. In order to obtain an extensive understanding of KF707 biofilm tolerance to biocides, tolerance to the antibiotics amikacin and rifampicin was also assessed. Susceptibility assays were performed on 4 h-grown low density biofilms as well as on mature 24 h-grown biofilms with the purpose of addressing the role of mature biofilm formation on the biofilm tolerant phenotype. The toxicity of metals and antibiotics to ‘structured’ and ‘flat’ biofilms was compared in order to verify the hypothesis that a flat architecture may confer a more susceptible phenotype to microbial biofilms compared to a structured one (Allesen-Holm *et al.* 2006, Landry *et al.* 2006).

The analysis of susceptibility to antibiotics showed that mature KF707 biofilms display increased tolerance to amikacin and rifampicin in comparison to planktonic cells. These data confirm previous observations indicating that both structured and flat biofilms, such as KF707 biofilms grown in LB and SA media respectively, show enhanced tolerance to antimicrobials relative to free-swimming cells (Hentzer *et al.* 2001, Teitzel and Parsek 2003). However, we observed that biofilms grown in SA for 24 h and presenting a typical flat architecture, were more tolerant than structured LB biofilms in terms of both minimum eradication biofilm concentration (MBEC) and increase of tolerance relative to planktonic cells (Figure 2.2). Interestingly, a significant increase in biofilm tolerance occurred immediately after cell attachment to the plastic surfaces in 4 h SA-grown biofilms (Figure 2.2 B) and the sparse attached cells were almost as tolerant to antibiotics as the corresponding mature biofilms. This phenotype has been observed also for other microbial biofilm systems, in which attached cells were found to be highly tolerant to numerous biocides (Das *et al.* 1998). In contrast to SA biofilms grown for 4 h, low density biofilms formed in LB did not display increased tolerance upon surface attachment. We may argue that, somehow,

growth in LB results in the uncoupling of the attachment to a surface with the development of antimicrobial tolerance. The data presented here strongly suggest that cellular metabolism plays a key role in the development of KF707 biofilm tolerance to antibiotics. Biofilm structure may be a contributing factor that raises the killing concentrations of low diffusible biocides. In fact, we observed that the development of a mature architecture produced an increase of biofilm tolerance to a low diffusible biocide such as amikacin but not against a free diffusible antimicrobial such as rifampicin (Figure 2.2). It has been known for some time that cells undergo physiological and metabolic changes upon attachment to a surface (Davies and McFeters 1988, McFeters *et al.* 1990, Griffith and Fletcher 1991, Davies *et al.* 1993, Vandevivere and Kirchman 1993, Ascon-Cabrera *et al.* 1995, Wentland *et al.* 1996). Now, it would be interesting to understand to what extent these changes are encoded by the genome, are dependent on signalling circuits that affect protein activities or if they are associated to a specific metabolic state.

Analysis of the MIC, MBC and MBEC data reveals that *Ps. pseudoalcaligenes* KF707 is tolerant to metals, both oxyanions and cations. In fact, the oxyanions tested here completely inhibit the growth of sensitive strains such as *E. coli* at concentrations between 5 μM (TeO_3^{2-}) (Taylor 1999) and 6 mM (SeO_3^{2-}) (Turner *et al.* 1998) while KF707 growth is inhibited at concentrations that are 20 and 6 times higher respectively (Table 2.2-2.5). As for metal cations, the use of 1-2.5 mM Ni^{2+} has been reported for the discrimination of metal sensitive and metal resistant strains of *A. eutrophus* (now *Ralstonia* spp.) (Mergeay *et al.* 1985, Springael *et al.* 1994). These concentrations did not inhibit KF707 growth in the conditions tested here. Minimal inhibitory concentrations (MIC) were determined on solid agar medium for *E. coli* and *A. eutrophus* (Taylor 1999, Mergeay *et al.* 1985, Springael *et al.* 1994) while in liquid medium for KF707, by means of the MBECTM-HTP (this study). In order to compare the MIC values reported above, one should take into account the fact that toxicological assays in liquid media are sensitive at lower concentrations than those obtained in solid media (10 to 100 times difference, as reported in Hassen *et al.* 1998).

The concentration of metal required to kill planktonic cells (MBC values) was higher than the concentration required to inhibit growth (MIC values). Planktonic cultures were killed at millimolar concentrations of metals with the exception of tellurite that was toxic at micromolar concentrations (Figure 2.3 B). Overall, considering both MIC and MBC values, metal toxicity to planktonic cells increased in the order $\text{Se} < \text{As} < \text{Ni} < \text{Al} \sim \text{Cd} < \text{Te}$. Therefore, KF707 proved to be particularly tolerant to selenite and arsenite oxyanions. These data also confirm previous observations showing that tellurite is a highly toxic oxyanion (reviewed in Taylor 1999, Turner 2001), exerting its effects at lower concentrations than other hazardous metal ions. However, planktonic KF707 is tolerant to high concentrations of this metalloid in comparison to sensitive strains.

After a 24 h exposure to metals, susceptibility of KF707 biofilms increased as follows: $\text{Se} < \text{As} < \text{Ni} < \text{Cd} < \text{Al} < \text{Te}$. Therefore, tellurite is the most toxic metal compound to KF707 cells in both planktonic and biofilm mode of growth and high tolerance is observed to the other metalloid oxyanions selenite and arsenite. Overall, metal cations were toxic to biofilm populations at lower molar concentrations than metalloid oxyanions. When compared to planktonic cultures, biofilms were observed to be up to 2 times more tolerant to metals and the increase in tolerance to metal killing occurred in mature biofilms grown in SA medium but not in those grown in LB (Figure 2.3 C). This observation is concordant with the increased tolerance of SA-grown biofilms to antibiotics in comparison to LB biofilms. Given that flat biofilms formed during growth in SA medium were less susceptible than structured LB-grown biofilms to both antibiotic and metal stresses, it can be concluded that KF707 tolerance to metals does not depend on the structured architecture of biofilms. However, it was observed that low density biofilms were killed at lower concentrations of metal than mature biofilms. Also, MBC values for planktonic cultures inoculated by mature biofilms were found to increase. These results indicate that the formation of a mature biofilm in SA medium might be beneficial to both biofilms and planktonic populations for two possible reasons: 1) the mature biofilm can inoculate the surrounding environment with a greater bacterial load or 2) the EPS matrix of mature biofilms may adsorb metal ions. In this way, the EPS matrix may

reduce the bioavailable concentration of the metals in solution, providing a more favourable environment for planktonic growth. However, KF707 biofilm tolerance to metals can not be explained by considering biofilm cell density and EPS adsorbing ability as the only factors involved in the development of a tolerant phenotype. In fact, when biofilms were grown in LB medium, the toxicity of metals to both planktonic and biofilm cultures did not decrease with the age of biofilms, that is to say that MBEC values were comparable for 4 h-grown and 24 h-grown biofilms. Interestingly, young LB biofilms, characterized by a low number of cells (Table 2.1) and lacking EPS matrix and ultrastructure (see Chapter 1), were killed at higher concentrations of TeO_3^{2-} , AsO_2^- and Al^{3+} than LB mature biofilms (Fig 2.3 C). At the moment we do not know which are the bases for the different phenotype observed for LB biofilms and it is not clear whether the decreased tolerance displayed by LB mature biofilms in comparison to SA biofilms is dependent on a different genetic, physiologic or metabolic state. However, on the basis of the multifactorial model of biofilm tolerance to metals, we may speculate that growth in SA medium may provide KF707 with a physiological state that makes bacterial cells less vulnerable to environmental stresses or perhaps produce persister cells at increased rates in the population.

In contrast to what has been observed for tolerance of KF707 biofilms to antibiotics, cell attachment to the plastic surface did not provide increased tolerance to metal toxicity. Moreover, KF707 biofilms were found to be up to 2 times more tolerant than planktonic cells (vs. 5-96 times increase in tolerance to antibiotics). At prolonged exposure times, other bacteria biofilm systems (i.e. *E. coli* and *Ps. aeruginosa*) have also been shown to display a modest 2-fold increase in tolerance to heavy metals respective to planktonic cultures (Harrison et al. 2005b, Harrison et al. 2005d). These data indicate that biofilm tolerance to antibiotics and to metals is likely to originate from different mechanisms. In fact, in contrast to antibiotics, metals are toxic to microbial cells at high concentration and act non-specifically. As an example, metal toxicity is commonly ascribed to the binding of ions to sulfhydryl (-SH) groups of proteins and cellular thiols, thus causing general disulfide and oxidative stresses (reviewed in Nies 1999). Harrison and colleagues have shown important similarities but also differences between

biofilm killing mediated by metals and antibiotics. Both metals and antibiotics kill biofilms in a biphasic manner. Therefore, the majority of the population is rapidly killed by both metals and antibiotics while the small fraction of surviving cells (persister cells, 0.1 % or less) is killed at a slower rate. This characteristic is a distinguishing feature of bacterial persistence (Keren *et al.* 2004). However, metals and antibiotics have different long-term activities against bacterial biofilms: bacterial killing mediated by antibiotics reaches a plateau and the persister cells surviving the exposure cannot be killed by either prolonged exposure or increased antibiotic concentration. On the other hand, given a long exposure time (i.e. 24 h), metals can completely eradicate also the persistent sub-population (Harrison *et al.* 2005b, Harrison *et al.* 2005d). Therefore, one may argue that a susceptible bacterial population may be negatively selected in heavy metal polluted environments even when growing as a biofilm. In this way, metals can affect both the physiology and the ecology and can reduce the diversity of environmental bacterial communities.

Pseudomonads are ubiquitous bacteria that engage in important metabolic activities in the environment and have considerable potential for biotechnological applications in the area of bioremediation (Dejonghe *et al.*, 2001). The metabolic pathway for biphenyl catabolism and PBC degradation by *Pseudomonas pseudoalcaligenes* KF707 are among the best known degradative pathways studied in bacteria (Furukawa and Kimura, 1995). Despite the detailed biochemical and genetic analyses of this metabolic property, other aspects of KF707 physiology and tolerance to environmental stresses of this organism have not been addressed. In this study we analyzed the ability of this soil organism to tolerate toxic heavy metals during growth as suspended cells as well as biofilms. Not only did we observe that low nutrient availability does not limit the ability of KF707 to form a biofilm (Chapter 1) but we also showed that this condition provides KF707 biofilms with a tolerant phenotype to environmental stresses. From the data obtained in this study we may expect KF707 to be able to maintain a high metabolic potential in polluted sites. In particular, the fact that KF707 shows tolerance to selenite and arsenite oxyanions illustrates its potential for use in sites containing high concentrations of these compounds. The

potential beneficial effects of the use of this metal-tolerant strain in the remediation of areas polluted by both PCB and heavy metals will be the object of further experimental work.

Chapter 3

Evidence for the generation of reactive oxygen species and absence of a tellurite-mediated adaptive response to oxidative stress in cells of *Pseudomonas pseudoalcaligenes* KF707*

*based on:

Valentina Tremaroli¹, Stefano Fedi¹, and Davide Zannoni¹ (2007) *Arch Microbiol* 156: 807-813

¹Department of Biology, General Microbiology Unit, University of Bologna, 40126 Bologna, Italy

Introduction

The metalloid tellurite (TeO_3^{2-}) is a rare-earth oxyanion which is highly toxic to most bacteria at concentrations as low as $1 \mu\text{g ml}^{-1}$ (Taylor 1999). As a consequence of the increasing number of applications that tellurite has in the electronic industry of photoreceptors, thermocouples and batteries, but also in industrial glasses, the accumulation of this oxyanion near sites of waste discharge and manufacturing have drastically increased in the last decade (Taylor 1999). Tellurite toxicity in *Escherichia coli* is several orders of magnitude higher than the toxicity of heavy metals, such as cobalt, zinc and chromium, which are a subject of major environmental and public health concern (Nies 1999). Hence, the demand in understanding the mechanism of both tellurite toxicity and bacterial resistance to it is compelling.

Studies on tellurite metabolism and toxicity in *E. coli* have shown that tellurite interacts with cellular reduced thiols (RSH) and that glutathione (GSH) is the initial target of tellurite reactivity (Turner *et al.* 2001). Based on the similarity between selenium (Se) and tellurium (Te) chemistry, both elements belonging to

the same group of the periodic table, it has been postulated that glutathione can reduce tellurite to elemental tellurium (Te^0) (Turner *et al.* 2001); furthermore, superoxide oxyanions (O_2^-) are likely to be generated during the reduction of tellurite, as has been shown for selenite oxyanions (SeO_3^{2-}) (Bébién *et al.* 2002, Kessi and Hanselmann 2004).

Despite tellurite toxicity, an increasing number of natural tolerant bacteria is being isolated from both clinical (Bradley 1985, Taylor 1999) and environmental settings (Tantaleán *et al.* 2003, Turner 2001). Notably, the molecular bases of tellurite resistance appears to be diverse both at the genetic and biochemical levels (Turner 2001). Most microorganisms counteract tellurite toxicity by chemically modifying it through methylation or reduction to the less toxic elemental tellurium (Te^0) (Turner 2001) and this last strategy is phenotypically characterized by cell darkening (Taylor 1999).

Pseudomonas pseudoalcaligenes KF707 has been described for its ability to co-metabolize polychlorinated biphenyls (PCBs) under aerobic conditions (Taira *et al.* 1992). We have shown that this soil bacterium can grow in media containing up to $150 \mu\text{g ml}^{-1}$ of potassium tellurite (Di Tomaso *et al.* 2002) so that sub-inhibitory tellurite was used as a marker to detect and quantify the release of KF707 cells in soil microcosms contaminated with PCBs (Zanaroli *et al.* 2002). It has been shown that organochlorine compounds, including PCBs, induce oxidative stress in bacteria able to metabolize these xenobiotics (Schilderman *et al.* 2000, Chavez *et al.* 2004). Therefore, one can presume that the aerobe *Ps. pseudoalcaligenes* KF707 can withstand high levels of reactive oxygen species (ROS).

Bacteria have evolved several mechanisms to protect themselves against environmental stresses and, in general, the exposure to low levels of a stress or chemical often induce increased resistance to a subsequent exposure to the same (adaptive response) or an unrelated agent (a cross-protective response) (Mongkolsuk *et al.* 1997). Adaptive and cross-protective responses have been shown to play an important role in bacterial adaptation to oxidative stress (Mongkolsuk *et al.* 1997) as well as to metal toxicity. In the soil bacterium *Xanthomonas campestris* low concentrations of cadmium induced cross-

protection against peroxide killing (Banjerdkij *et al.* 2005) while in *E. coli* sub-lethal concentrations of selenite triggered an adaptive response which increased the tolerance towards SeO_3^{2-} and induced cross-protection against the ROS generator paraquat (Bébién *et al.* 2002).

Although emerging data indicate that tellurite toxicity may arise from oxidative stress (Borsetti *et al.* 2005, Tantaleán *et al.* 2003), *in vivo* evidence for a tellurite-mediated generation of ROS is lacking and no indication of the presence of a tellurite-induced adaptation mechanism has been reported. To provide insights into the mechanisms of tellurite toxicity and cellular protection against this toxic oxyanion, the effects of tellurite on cell adaptation and oxidative stress responses in *Ps. pseudoalcaligenes* KF707 were investigated. Our results show for the first time that tellurite triggered an increase in ROS production *in vivo* but neither adaptation nor protection against oxidant agents such as paraquat, diamide, tBH and H_2O_2 were induced. Conversely, the cytosolic superoxide generator paraquat and the thiol reactive molecule diamide strongly increased the tolerance of KF707 cells to tellurite; furthermore, SOD enzyme activity was far more stimulated by addition of these oxidants than it was by tellurite addition. We conclude that the activation of the cellular response against superoxide oxyanion is a key factor in *Pseudomonas pseudoalcaligenes* KF707 tolerance to tellurite and that the absence of SOD stimulation, most probably due to the slow kinetics of both tellurite uptake and ROS release, can account for the lack of KF707 cell adaptation to the toxic metalloid.

Materials and methods

Bacterial strains and growth conditions

Ps. pseudoalcaligenes KF707 was grown aerobically at 30 °C on LB medium. Overnight cultures were used as a source of 1.5 % inoculum to obtain exponentially growing cultures ($A_{660} \sim 0.7$).

Determination of basal resistance levels to tellurite and oxidants

Analyses of the effects of tellurite and oxidants on *Ps. pseudoalcaligenes* KF707 cells were performed by exposing exponential phase cultures to increasing concentrations of paraquat, diamide, tBH and H₂O₂. Samples were taken after 0, 40, 80 and 120 minutes, washed and serially diluted in saline solution (NaCl 8,5 g/l). Appropriate dilutions were plated onto LB agar plates and colonies were counted after 24 h of incubation at 30 °C. Each experiment was performed in triplicate.

Adaptation and cross-protection experiments

Exponential phase cultures were exposed for 1.5 h to sub-lethal doses of the oxidants (tellurite 2.5 µg/ml, PQ²⁺ 2 mM, diamide 2.5 mM, tBH 0.1 mM and H₂O₂ 0.1 mM) and subsequently to lethal doses of tellurite (50 µg/ml) or other oxidants (PQ²⁺ 25 mM, diamide 25 mM, tBH 2.5mM, H₂O₂ 1 mM). Samples were taken after 0, 40, 80 and 120 minutes, washed and serially diluted in saline solution. Appropriate dilutions were plated onto LB agar plates and colonies were counted after 24 h of incubation at 30 °C. Each experiment was performed in triplicate. In similar viability assays, exponentially growing cells were treated for 3 h with 50 mM buthionine sulfoximine (BSO), a specific inhibitor of the enzyme γ -glutamylcysteine synthetase which catalyses the first reaction of glutathione biosynthesis, before treatment with lethal concentrations of tellurite (50 µg/ml). Viable cell counts were performed as described for oxidants and tellurite pre-treated cultures.

In vivo detection of ROS

Overproduction of ROS was assayed by using the oxidative stress-sensitive probe 2',7'-dichlorodihydrofluorescein diacetate (DCFH-DA) (Crow 1997). When DCFH-DA is taken up by living cells, the acetyl group is removed by membrane esterases and 2',7'-dichlorodihydrofluorescein (DCFH) is formed. DCFH is then oxidized by ROS to the fluorescent compound 2',7'-dichlorofluorescein (Ischiropoulos *et al.* 1999). Exponentially growing cultures were exposed for 1 h to different concentrations of tellurite (2.5, 5, 10, 25 and 50 $\mu\text{g/ml}$) or to PQ^{2+} 2 mM, diamide 2.5 mM, tBH 0.1 mM and H_2O_2 0.1 mM. Cells were harvested and suspended in saline solution in the presence of 5 μM DCFH-DA added from a 2 mM stock solution in dimethylsulfoxide (DMSO). Fluorescence was measured with a spectrofluorimeter (Wallac Victor 1420 Multilabel Counter, Perkin-Elmer) after 1 h incubation in DCFH-DA under agitation at 70 rpm in the dark at room temperature. All experiments were performed in triplicate and repeated independently at least four times. Kinetics measurements of ROS production were performed as follows: exponentially growing cells were harvested, washed and suspended in saline solution in the presence of DCFH-DA as described above. ROS production was measured at 0, 30, 60 and 90 minutes after the addition of the oxidants (tellurite 25 $\mu\text{g/ml}$, PQ^{2+} 2 mM and diamide 2.5 mM) with a FP-770 Jasco Spectrofluorimeter.

Determination of reduced thiol (RSH) content

To investigate the effects on RSH cell content, exponentially growing cultures were exposed to either tellurite (25 $\mu\text{g/ml}$ and 50 $\mu\text{g/ml}$) or diamide (2.5 mM). Samples of 500 μl were taken at 0, 15, 30, 45, 60 and 90 minutes and the assay was performed as previously described (Turner *et al.* 1999). Additional samples were removed at 0, 30, 60 and 90 minutes for the determination of protein content by the method of Lowry (Lowry *et al.* 1951) using bovine serum albumine (BSA) as a standard. Each experiment was performed in duplicate and repeated at least four times.

Detection of tellurite uptake

The quantitative determination of potassium tellurite in liquid media was performed with the diethyldithiocarbamate (DDTC) reagent (Sigma) as described by Turner *et al.* (Turner *et al.* 1992a).

Preparation of cell lysates

Ps. pseudoalcaligenes KF707 cells were grown aerobically to $A_{660} \sim 0.7$ and then exposed for 1.5 h to sub-lethal doses of oxidants (tellurite 2.5 $\mu\text{g/ml}$, PQ^{2+} 2 mM, diamide 2.5 mM). The cells were harvested, washed once in phosphate buffered saline pH 7.4 (PBS) and suspended in potassium phosphate buffer 50 mM pH 7.8 in the presence of 1 mM phenylmethyl-sulfonyl fluoride (PMSF). Cells were disrupted by ultrasonication (MSE Soniprep150) at 4°C (ten bursts of 45 s each, 15 s off, 4 power, 10 μm of amplitude, titanium exponential probe of 3 mm end diameter) and the lysates were centrifuged at 7000 rpm for 15 minutes at 4°C. The supernatants were cleared by ultracentrifugation (32500 rpm, 1 h, 4 °C) and the amount of total soluble protein content was estimated by the method of Lowry (Lowry *et al.* 1951).

Characterization of SOD activity by gel staining

For the identification of the isoform of the SOD enzyme expressed by *Ps. pseudoalcaligenes* KF707, 40 μg of cleared lysates were loaded in non-denaturing 8% polyacrylamide gels. The gels were incubated 30 minutes in potassium phosphate buffer 50 mM pH 7.8 in the presence of either KCN 2 mM or H_2O_2 5 mM, differential inhibitors of Cu,ZnSOD and FeSOD respectively; MnSOD is resistant to these inhibitors (Langford *et al.* 2002). Gel assays for the characterization of SOD activity were performed by gel staining (Donahue *et al.* 1997, Tseng *et al.* 2001).

Quantification of SOD activity by xanthine/xanthine oxidase-cytochrome *c* assay

The assay was performed by essentially following the method described by McCord and Fridovich (McCord and Fridovich 1969) except that 20 μM horse-heart cytochrome *c*, 500 μM xanthine and 6.6 mU/ml of xanthine oxidase from buttermilk were used in the presence of 35 μg of protein extracts. Reduction of cytochrome *c* was determined by monitoring the increase in absorbance at 550 nm (Jasco UV/VIS Spectrophotometer 7800) in the presence of 0.1 mM KCN, which was added to inhibit the cytochrome *c* oxidase activity.

Results

Effect of oxidants on ROS production

It has been proposed that tellurite toxicity results from the ability of this oxyanion to generate free radicals as byproducts of tellurite reduction (Turner *et al.* 2001, Tantaleán *et al.* 2003). To test this proposal, we determined the levels of ROS production in cells of *Ps. pseudoalcaligenes* KF707 exposed to tellurite and other oxidants by means of the ROS-sensitive probe DCFH-DA (Crow 1997). Cells incubated with 25 $\mu\text{g/ml}$ tellurite showed a strong increase in fluorescence, which was comparable to the signal detected in cells incubated with either PQ^{2+} or H_2O_2 . Diamide caused the highest increase in ROS production (Figure 3.1).

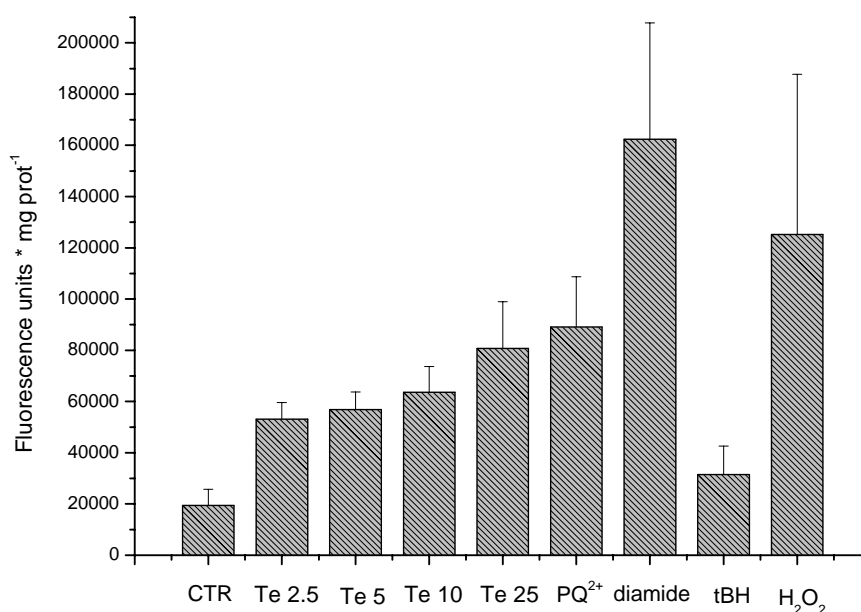


Figure 3.1. Levels of ROS production in *Ps. pseudoalcaligenes* KF707 cells exposed to different oxidants and various tellurite (Te) concentrations ($\mu\text{g/ml}$). Exponentially growing cells ($\text{OD}_{660} \sim 0.7$) were exposed to tellurite, PQ^{2+} , diamide, tBH and H_2O_2 for 1 h and then washed and suspended in saline solution in the presence of 5 μM DCFH-DA (see Materials and Methods for further details). The values presented and standard deviations are the means of four independent experiments, each performed in triplicate.

The kinetics of ROS production during the first 90 minutes of exposure to the oxidants is presented in Figure 3.2. High amounts of ROS were produced in the presence of both diamide and PQ^{2+} ($t_{1/2} < 10$ min) whereas ROS production following tellurite exposure was much slower ($t_{1/2} \gg 30$ min) and differed significantly from control cells after 30 min of incubation.

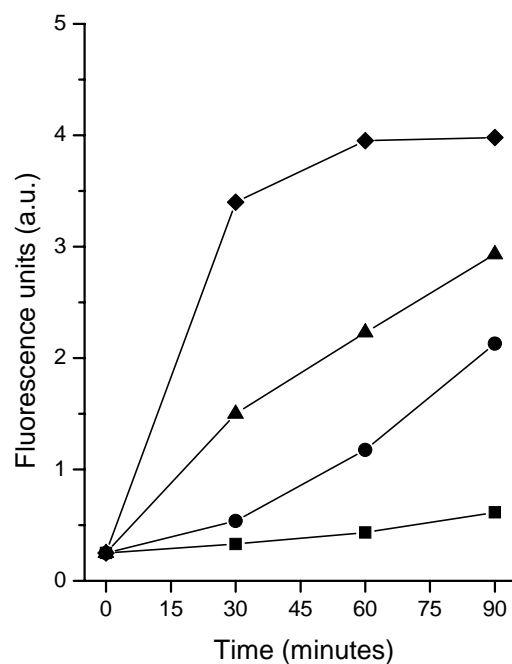


Figure 3.2. Time course of ROS production. Exponentially growing cells were washed, suspended in saline solution in the presence of DCFH-DA and exposed to tellurite (*filled circle*), PQ^{2+} (*filled triangle*) and diamide (*filled diamond*). Samples were taken after 0, 30, 60 and 90 min after exposure. ROS production during aerobic metabolism of KF707 cells is reported as a control (*filled square*). The trend of a representative experiment is reported.

Adaptive and cross-protective responses against oxidative stress-induced killing

To determine the basal levels of resistance to oxidants of *Ps. pseudoalcaligenes* KF707, cell survival experiments were performed in the presence of variable amounts of tellurite, paraquat, diamide, tBH and H₂O₂. These control experiments (shown in Figure 3.3) indicated that 2.5 µg/ml of K₂TeO₃, 2.5 mM of PQ²⁺ and diamide, 0.1 mM of tBH and 0.1 mM H₂O₂ did not cause loss of cells viability.

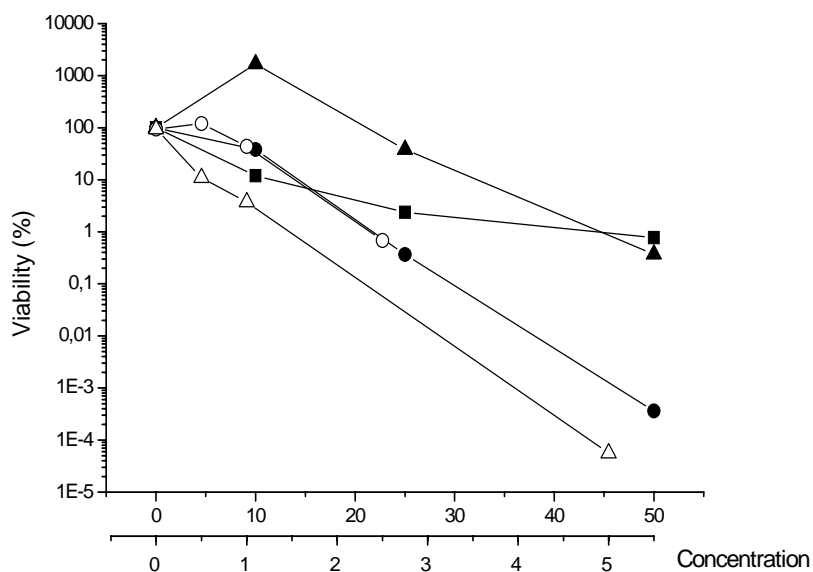


Figure 3.3. Basal levels of resistance of *Pseudomonas pseudoalcaligenes* KF707 to tellurite (filled square), diamide (filled circle), paraquat (filled triangle), tBH (open circle) and H₂O₂ (open triangle). The curves indicate the viability of exponential phase cultures incubated for 1.5 h at increasing concentrations of tellurite, PQ²⁺, diamide, tBH and H₂O₂. Solid symbols are plotted against the upper abscissa scale (0–50 µg/ml tellurite, 0–50 mM paraquat and diamide). Open symbols are plotted against the lower abscissa scale (0 – 5 mM tBH and H₂O₂). Values are the means of three replicates (standard deviation between 5-10 %).

The effects of cell exposure to low amounts of tellurite on the physiological response to tellurite itself (adaptive response) and to superoxide, peroxide and disulfide induced stresses (cross-protective responses) were also tested. Figure 3.4 shows that tellurite induced neither adaptive response (Figure 3.4, panel a) nor cross-protection against the superoxide generator PQ²⁺, the peroxide generators tBH and H₂O₂ and also the disulfide stress inducer diamide

(Figure 3.4, panels b to e). Conversely, tellurite exerted a synergistic effect on the toxicity of all the oxidants tested.

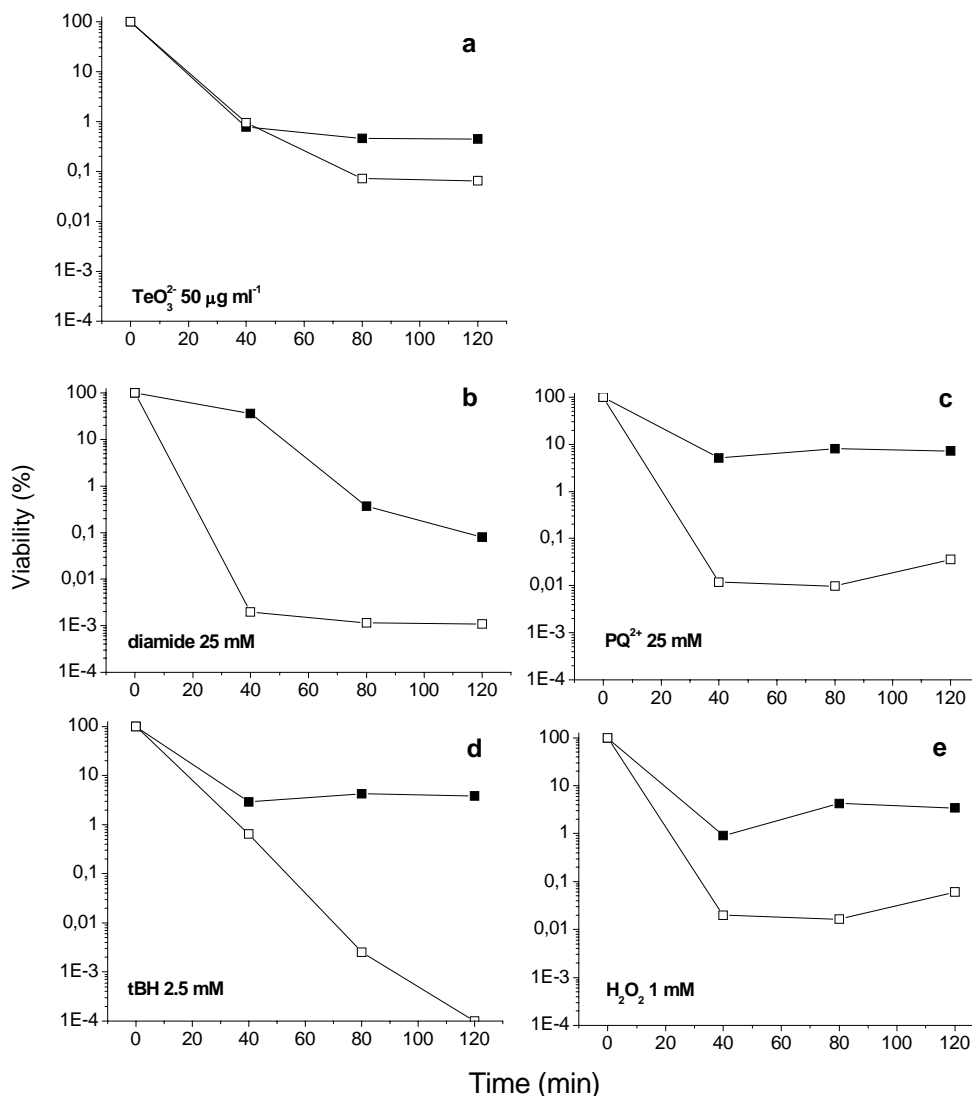


Figure 3.4. Panel a. Analysis of the adaptive response of *Pseudomonas pseudoalcaligenes* KF707 to tellurite. LB exponentially growing cells were pre-incubated for 1.5 h at low tellurite concentrations (2.5 µg/ml) before being exposed to a lethal concentration of the oxyanion (50 µg/ml) (*open square*). The viability of non pre-incubated cultures is reported as a control (*filled square*). Panels b to e. Analysis of tellurite-mediated cross-protective response against superoxide (PQ²⁺), peroxide (tBH, H₂O₂) and disulfide (diamide) stress generators. For this experiment, cultures pre-incubated for 1.5 h at low tellurite concentrations (2.5 µg/ml) were subsequently exposed to lethal doses of diamide (25 mM), PQ²⁺ (25 mM), tBH (1 mM) and H₂O₂ (1 mM) (*open squares* in panels b, c, d, e). The viability of cultures non pre-incubated in low tellurite is reported as a control (*filled squares* in panels b, c, d, e). Values presented are the means of three replicates (standard deviation between 5-10 %).

In additional experiments, exponentially grown cultures were exposed to sub-lethal concentration of PQ^{2+} , diamide, tBH and H_2O_2 before treatment with lethal doses of tellurite. The results presented in Figure 3.5 indicate that both PQ^{2+} and diamide, well known SOD activity inducers, strongly increased the tolerance to tellurite.

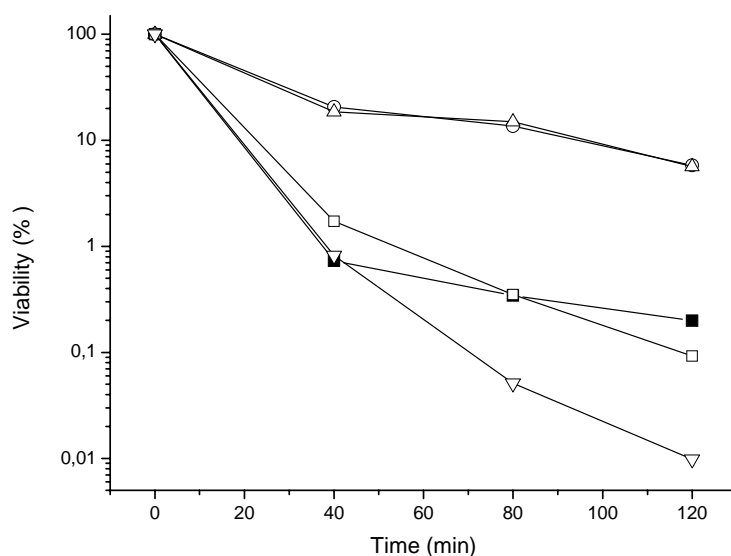


Figure 3.5. Oxidant induced cross-protective responses against tellurite toxicity. For this experiment cultures were pre-incubated for 1.5 h at low concentrations of diamide (*open triangle*), PQ^{2+} (*open circle*), tBH (*open inverted triangle*) and H_2O_2 (*open square*) and subsequently exposed to lethal doses of tellurite. The viability of non pre-incubated cultures is reported as a control (*filled square*). Values presented are the means of three replicates (standard deviation between 5-10 %).

Effect of tellurite and diamide on RSH content

It has been shown that tellurite causes a rapid loss of cellular RSH content (Turner *et al.* 1999) and that glutathione is a major target of tellurite reactivity (Turner *et al.* 2001). Diamide is a specific oxidant for thiols, reacting with free thiols to produce a disulfide bond and a hydrazine derivative (Kosower and Kosower 1995). It has been reported that diamide can induce SOD activity (Privalle *et al.* 1993) and this compound has been used in a recent study to induce both disulfide and oxidative stress responses in the soil gram positive bacterium *Bacillus subtilis* (Leichert *et al.* 2003). The effects of both tellurite and diamide on cellular reduced thiols as a function of time are shown in Figure 3.6.

Exponentially grown cells, exposed to either tellurite (25, 50 $\mu\text{g}/\text{ml}$) or diamide (2.5 mM) underwent a similar loss in RSH content, while significant loss of viability occurred in the presence of tellurite only. Conversely, the viability of KF707 cells treated with low concentrations of diamide before exposure to tellurite 50 $\mu\text{g}/\text{ml}$ increased (Figure 3.5) although the same level of RSH oxidation was seen (Figure 3.6, dotted line).

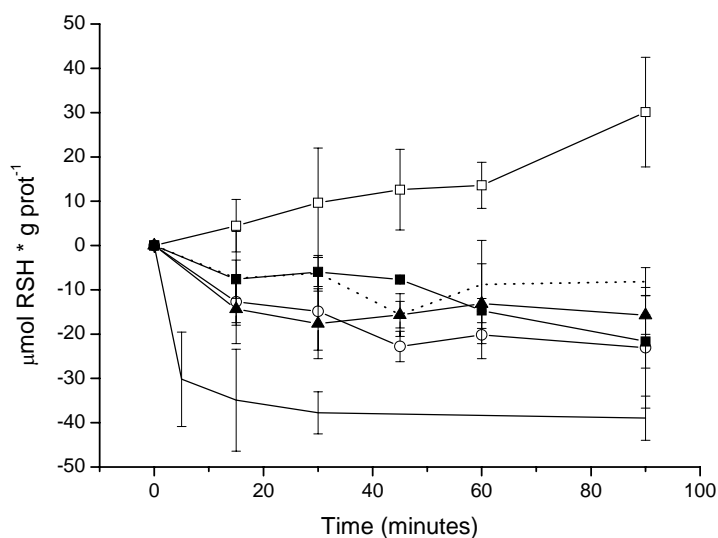


Figure 3.6. Effects of tellurite (25 $\mu\text{g}/\text{ml}$ filled square, 50 $\mu\text{g}/\text{ml}$ filled triangle), diamide (open circle) and Hg^{2+} (solid line) reactivity towards cellular reduced thiols (RSH). Oxidants were added at time zero. RSH loss in cell cultures treated with low diamide before exposure to 50 $\mu\text{g}/\text{ml}$ tellurite is also reported (dotted line). RSH content of non-incubated KF707 cells is reported as a control (open square). Values presented are the means and standard deviations of four independent experiments each performed in duplicate.

Figure 3.6 also shows the levels of RSH oxidation caused by cell exposure to 100 μM HgCl_2 . In the latter case the cell viability was comparable to the viability of cultures treated with 50 $\mu\text{g}/\text{ml}$ tellurite, even though the metal cation Hg^{2+} oxidized RSH at a higher rate. These results demonstrate that the loss of RSH cellular content is not due to cells death but it results from oxidation of thiols by tellurite.

Effects of glutathione synthesis on tellurite toxicity

We sought to assess the role of glutathione in tellurite-mediated toxicity and cellular response. As glutathione is supposed to be the major target of tellurite

reactivity (Turner *et al.* 2001), we analyzed KF707 response to TeO_3^{2-} in cultures treated with buthionine sulfoximine (BSO), a specific inhibitor of the enzyme γ -glutamylcysteine synthetase (Griffith and Meister 1979) that catalyses the first reaction of the glutathione biosynthesis pathway (Meister 1974). Cells treated with 50 mM BSO in LB rich medium for 3 h (approximately 3 generation times) where subsequently exposed to lethal concentrations of tellurite (50 $\mu\text{g}/\text{ml}$) and the viability of cultures was assessed by means of viable cell counts (Figure 3.7).

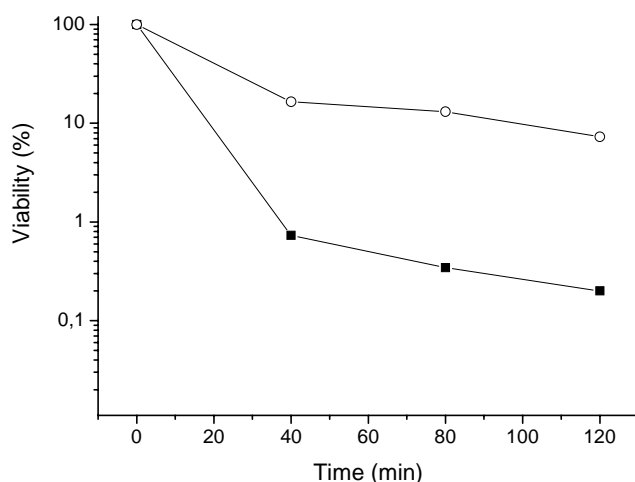


Figure 3.7. Effects of glutathione synthesis on tellurite toxicity. For this experiment cultures were pre-incubated for 3 h in 50 mM BSO and then exposed to a lethal dose of tellurite (*open circle*). The viability of non pre-incubated cultures is reported as a control (*filled square*). Values presented are the means of three replicates (standard deviation between 5-10 %).

Figure 3.7 shows that the inhibition of glutathione synthesis results in increased tolerance to potassium tellurite. The viability of KF707 cells was increased approximately 30 times in comparison to control cells not treated with BSO. This increase in tolerance is comparable to the increase observed for cultures pre-incubated with paraquat and diamide (Figure 3.5).

Effect of oxidants on SOD activity

The data presented above suggest that the activation of the cellular response against superoxide stress, but not to peroxide, can increase the tolerance to tellurite. Superoxide dismutases (SODs) are ubiquitous enzymes catalyzing the detoxification of the superoxide anion to hydrogen peroxide and molecular

oxygen (Fridovich 1995, Kho *et al.* 2004, Storz *et al.* 1990, Tabares *et al.* 2003). An increase in SOD activity might therefore justify a parallel increase in cell tolerance to tellurite. Clarified lysates from *Ps. pseudoalcaligenes* KF707 cells treated with sub-lethal doses of tellurite, PQ^{2+} , diamide, and H_2O_2 were assayed for SOD activity by nondenaturing PAGE. In order to characterize the SOD enzyme isoform(s) present in KF707, the gels were treated with either KCN or H_2O_2 , specific inhibitors of Cu,ZnSOD and FeSOD (coded by the *sodB* gene) respectively. A third isoform of SOD enzyme exists in bacteria, that is not inhibited by either KCN or H_2O_2 and is a MnSOD, coded by the *sodA* gene. After staining, SOD activity was detected in gels pretreated with KCN only, while in gels treated with H_2O_2 no SOD activity was seen. This result suggests that in *Ps. pseudoalcaigenes* KF707 a FeSOD is present. The presence of this SOD isoform in KF707 was also confirmed by PCR amplification of a 440 bp *sodB* fragment with primers designed on the sequence of *Ps. aeruginosa* PAO1 *sodB* gene. The same cell lysates were tested for *in vitro* cytochrome *c* reduction by superoxide anions generated by X/Xox (McCord and Fridovich 1969). This assay allows the indirect measurement of the endogenous SOD activity which competes with cytochrome *c* for superoxide oxyanions. The results presented in Table 3.1 indicate that SOD activity is enhanced by PQ^{2+} and diamide so that an inhibition of cytochrome *c* reduction by 21 % and 28 % respectively was detected in comparison to control experiments. In lysates from tellurite treated cells the inhibition of cytochrome *c* reduction was 10 %. This result suggests that the oxyanion fails in fully activating the cellular SOD activity, even though exposure to tellurite caused an increase in ROS production.

Table 3.1. Ferricytochrome *c* reduction assay in lysates from *Ps. pseudoalcaligenes* KF707 incubated for 1.5 h in the presence of tellurite (TeO_3^{2-}), paraquat (PQ^{2+}), diamide and H_2O_2 . Values and standard deviations are the means of three independent measurements in cell lysates obtained from different cell cultures. Assays were performed using 35 μg of proteins.

		Activity (nmol cyt <i>c</i> reduced mg prot ⁻¹ min ⁻¹)	% inhibition
Control		47.8 ± 2.2	0
+ TeO_3^{2-}	25 $\mu\text{g ml}^{-1}$	43.1 ± 3.8	10
+ PQ^{2+}	2 mM	37.6 ± 3.9	21
+ diamide	2.5 mM	34.4 ± 8.9	28
+ H_2O_2	0.1 mM	46.6 ± 3.9	2.5

Discussion

In contrast to an early interpretation of tellurite toxicity, arguing that tellurite (TeO_3^{2-}) would act as a general oxidant (Summers and Jacoby 1977), emerging evidence tends to show that TeO_3^{2-} is a thiol-specific reactant and that glutathione is the major initial target of its reactivity (Turner *et al.* 2001, Turner *et al.* 1999). On the basis of the similarity between the chemistry of tellurite and selenite (SeO_3^{2-}), tellurite interaction with reduced thiols (RSH) is expected to follow a Painter-like mechanism, in which reactive oxygen species are produced as byproducts of the reaction (Turner *et al.* 2001, Turner 2001). In line with this hypothesis, a study by Kessi and Hanselmann (2004) has shown that superoxide oxyanions (O_2^-) are generated during the first step of the abiotic selenite (SeO_3^{2-}) dissimilatory reduction with glutathione (GSH). For the first time, the present study brings to light experimental evidence which illustrates a tellurite-induced generation of ROS *in vivo* and of the involvement of superoxide-mediated oxidative stress in the toxicity mechanism of the metalloid oxyanion.

Upon incubation with tellurite, an increase in ROS production takes place (Figure 3.1) and the content of reduced thiols (RSH) diminishes (Figure 3.6), indicating that tellurite affects the cytosolic thiol status and causes oxidative stress. Due to the slow rate of tellurite uptake in *Ps. pseudoalcaligenes* KF707 cells (0.1-0.3 nmol mg prot⁻¹ min⁻¹, additional data), which is about 100 times lower than that reported in cells of the facultative phototroph *Rhodobacter capsulatus* (Borsetti *et al.* 2003), tellurite reduction by reduced thiols is likely to occur at high RSH:TeO₃²⁻ ratios, the cytosolic concentration of glutathione (GSH) being in the order of 1-10 mM in Gram-negative bacteria (Gérard-Monnier and Chaudière 1996, Newton and Fahey 1989, Apontoweil and Berends 1975). Under such conditions (i.e. high RSH:TeO₃²⁻ ratio), the interaction of selenite with cellular thiols has been shown to prevalently cause a release of superoxide ions (Kramer and Ames 1988). Therefore, assuming that a similar mechanism is involved in tellurite reduction, O₂⁻ production is favoured in KF707 cells exposed to tellurite. Indeed, the observation that tolerance to tellurite is increased by the activation of the cellular response to O₂⁻-generators but not to H₂O₂ provides indirect evidence that *in vivo* production of superoxide and not hydrogen peroxide is responsible for tellurite toxicity.

The data presented in this study show that the effects of diamide and tellurite on RSH oxidation and ROS generation is fundamentally different. In the case of cell exposure to the thiol specific oxidant diamide, RSH oxidation and ROS release are characterized by similar kinetics, both reaching a plateau within 45 minutes from exposure. When cells are exposed to tellurite, RSH oxidation reaches a steady-state level within 45 minutes after the addition of tellurite (Figure 3.6). The release of ROS occurs at slower rates, as it starts being significantly different from the release of ROS caused by aerobic metabolism 30 minutes after the exposure (Figure 3.2). The latter result indicates that the rates of RSH oxidation and ROS generation during tellurite metabolism in KF707 cells are not the same. In this respect it is worth mentioning very recent data obtained from cells of the facultative phototroph *Rhodospirillum rubrum*, showing that selenite reduction is not strictly correlated with the decrease of cytosolic glutathione (Kessi 2006). The latter results, along with those of the present study, tend to

suggest that generation of superoxide oxyanions (O_2^-) is not totally coupled to dissimilatory reduction of metalloids by reduced thiols as *vice versa* proposed for the abiotic reduction of selenite (SeO_3^{2-}) with glutathione (Kessi and Halselmann 2004). Apparently, the biochemical mechanisms connecting ROS production to RSH oxidation during the dissimilatory reduction of metalloids are not fully understood at the moment. However, the observation that the inhibition of glutathione synthesis relieves tellurite toxicity to a level comparable to the activation of the cellular response to O_2^- suggests that glutathione may be directly involved in the production of superoxide, although other and presently unknown cellular targets may also be involved. This result is concordant with the observation that both *E. coli* and *Salmonella* serovar Typhimurium devoid of glutathione ($\Delta gshA$) display increased tolerance to sodium selenite (Bébién *et al.* 2002, Kramer and Ames 1988).

Sub-inhibitory amounts of tellurite did not induce adaptation to subsequent exposure to high concentrations of the oxyanion itself (this work, Figure 3.4 panel a). Similarly, sublethal tellurite treatment did not increase tolerance to oxidants such as PQ^{2+} , diamide, H_2O_2 and tBH. *Vice versa*, tellurite exerted a synergistic effect on the toxicity of all the oxidants tested (Figure 3.4 panel b to e). These data indicate that a short exposure to potassium tellurite is not able to induce adaptation to the stress induced by the oxyanion and that the final response to metalloid-mediated toxicity may not be the activation of rescue and/or repair pathways but cell death. Accordingly, the quantification of total SOD activity of *Ps. pseudoalcaligenes* KF707 cultures exposed to non inhibitory concentrations of TeO_3^{2-} , PQ^{2+} and diamide indicated that tellurite is poorly effective at inducing the activation of the cellular response to superoxide oxyanions. These data suggest that in *P. pseudoalcaligenes* KF707, the activation of a cellular response against superoxides (O_2^-) is a key factor in establishing tolerance to tellurite. Furthermore, the lack of a tellurite-induced resistance to PQ^{2+} , diamide and TeO_3^{2-} itself is likely to derive from the inability of the metalloid to significantly stimulate SOD activity.

Cells exposed to either tellurite or PQ^{2+} show similar levels of oxidative stress (this work). The analysis of cell viability on the other hand, indicates that

the oxidative stress can be easily overcome by *Ps. pseudoalcaligenes* KF707 cells in the presence of PQ^{2+} but not after treatment with TeO_3^{2-} (shown in Figure 3.3). Under physiological aerobic growth conditions, ROS are detected and rapidly cleared away by the activities of enzymes such as SOD, catalase and/or glutathione (GSH) peroxidase. The main damage to cells resulting from ROS generation is the alteration of macromolecules such as, for example, polyunsaturated fatty acids, proteins, and DNA. Because of the low rate of ROS release by tellurite (shown in Figure 3.2) along with the limited activation of SOD activity (Table 3.1), one can presume that KF707 cells start to be affected by tellurite before the cellular response machinery against superoxide toxicity (Frazzon and Dean 2001; Tantaleán et al 2003) is fully operative. In this scenario, tellurite oxidation of RSH compounds and glutathione, whose role in microbial responses to oxidative stress is well documented (Carmel-Harel and Storz 2000), will add to the oxidative cellular damage. We conclude that in *Ps. pseudoalcaligenes* KF707, tellurite pro-oxidant activity would exceed the cellular antioxidant defences and/or the cellular repair systems thus leading to cell death. An aspect related to this, which deserves further investigation, concerns the role of the plasma membrane carriers and redox systems in tellurite toxicity. Indeed, as we have shown in the past that the amount of *c*-type hemes of KF707 drastically drops in membranes from cells grown in the presence of tellurite (Di Tomaso *et al.* 2002), here we report that KF707 cells grown in LB rich medium are unable to perform a consistent tellurite uptake. The reduction of tellurite by cells of *E. coli*, *Erwinia carotovora*, *Agrobacterium tumefaciens* and *Pseudomonas aeruginosa* has been related by Trutko *et al.* (2000) to the activity and polarity of the respiratory cytochrome *c* oxidases. Since preliminary evidences suggest that tellurite uptake depends on the conditions of cell growth, experiments aiming to elucidate the primary role of the plasma membrane redox complexes as possible targets for tellurite toxicity but also as ROS generators, are in progress.

Chapter 4

Global analysis of cellular factors and responses involved in Pseudomonas pseudoalcaligenes KF707 tolerance to tellurite

Introduction

The metalloid elements, such as As, Sb, Bi, Se and Te, are extensively produced and utilized in industry and agriculture. In particular, selenium and tellurium compounds have been used in the manufacture of ceramics and glass, in photoelectric cells, in semiconductors and as fungicides in agriculture and medicine. Lately, selenium and tellurium have found a new interesting application in molecular biology, with selenomethionine and telluromethionine being used as allosteric analogues to facilitate structural analysis of proteins by X-ray diffraction (Budisa *et al.* 1997, Budisa *et al.* 1998, Boles *et al.* 1991, Boles *et al.* 1995). Arsenic compounds have been used in the manufacture of bronze materials, fireworks, agricultural chemicals, laser materials, glass, semiconductors, wood preservatives, copper and lead alloys and insecticides. However, the use of arsenic is now minimal. Selenium is an essential trace element for living organisms (McKeehan *et al.* 1976, Shamberger 1983) while tellurium and arsenic have not been shown to play any defined biological function and are mainly associated with toxicity (Silver 1998, Westenberg and Guerinot 1997). The study of the mechanisms of bacterial resistance to Se, Te and As has led to the identification of genetic determinants for Te and As resistance while in the case of Se no specific resistance determinants have been found. Resistance to tellurite is conferred by at least five different determinants, most of which are membrane proteins of unknown function and also produce cross-resistance to colicins and bacteriophage infections (reviewed in Taylor 1999). Although the prooxidant ability of tellurite suggests that oxidative damage is at least one of the mechanisms of toxicity of Te compounds, tellurite resistance determinants do not confer protection to oxidants.

As for arsenic compounds, resistance to the oxyanions arsenate and arsenite is generally dependent on the presence of *ars* genes, which are highly conserved among both Gram-negative and Gram-positive bacteria (Silver and Phung 1996). Six different *ars* operons have been isolated and all of them code for at least three proteins, i.e. the transcriptional repressor protein ArsR, the chemiosmotic arsenite transport protein ArsB and the arsenate reductase ArsC. In some operons, ArsA protein function is also encoded, that energizes arsenite efflux by ATP hydrolysis (for a review see Silver and Phung 1996). Therefore, arsenic resistance is mainly an extrusion strategy, while the function of most of the isolated tellurium resistance determinants is still elusive. It is possible to hypothesize that resistance to Te oxyanions may be an additional activity of the proteins encoded by Te resistance determinants, so that the presence or expression of such proteins would perhaps constitute a general and indirect form of tellurite resistance.

In an attempt to improve the general understanding of how tellurite affects microbial physiology, we investigated the effects of metal stress induced by arsenite and selenite toxicity on *Ps. pseudoalcaligenes* KF707, with the aim of identifying possible common mechanisms of metalloid-mediated toxicity and overlap between the biochemistry of such elements in bacterial cells. In addition, we investigated the proteomic response of tellurite-adapted cells, with the intent of elucidating possible mechanisms of adaptation. The results of this study suggest that oxidative stress is not the only factor involved in tellurite toxicity and heat shock response or the expression of specific chaperon functions is likely to be required for resistance to metalloid oxyanions.

Materials and methods

Growth of Ps. pseudoalcaligenes KF707 in the presence of potassium tellurite

Ps. pseudoalcaligenes KF707 wild type was grown in LB medium in the presence of 25 µg/ml (100 µM) potassium tellurite. Growth was followed by measuring the OD₆₆₀ of cultures during a 48 h period of time. Cultures were assayed at different time points to determine the amount of residual tellurite remaining in the medium. The concentration of tellurite was quantified spectrophotometrically at 340 nm using the DDTC method as described by Turner *et al.* (1992a). Uninoculated LB containing 25 µg/ml of potassium tellurite served as the abiotic control. As a control of the effect of tellurite on growth, the growth of KF707 in LB unamended with tellurite was also monitored.

Protection experiments

Exponential phase cultures (OD₆₆₀ ~ 0.6) growing in LB medium were pre-incubated for 1.5 h with sub-lethal doses of the metalloid oxyanions SeO₃²⁻ and AsO₂⁻ (6.3 mM and 0.5 mM respectively). Subsequently, the same cultures were exposed to lethal doses of tellurite (50 µg/ml ~ 200 µM). Samples were taken after 0, 40, 80 and 120 minutes and treated with a neutralizing solution (as described in Chapter 2: § *Stock solution of neutralizer*, § *Biofilm cultivation and metal susceptibility testing*) to avoid metal carry-over to the subsequent serial ten-fold dilutions in 0.9 % saline solution. The induction of tolerance to tellurite after heat shock was assayed by exposing LB exponentially growing cells to 50 °C for 30 minutes and then to a lethal dose of tellurite. Samples were removed and processed as described above, except that no neutralization reaction was performed. Appropriate dilutions were plated onto LB agar plates and colonies were counted after 24 h of incubation at 30 °C. Each experiment was performed in triplicate.

In similar assays, KF707 cultures treated for 1.5 h with low amounts of selenite and arsenite were subsequently exposed to high doses of the same metal in order to test the occurrence of a metal-specific adaptation response.

Northern blot analysis of sodB gene expression

Exponentially growing cells were treated with 2.5 and 5 ug/ml (10-20 μ M) tellurite, 6.3 mM selenite and 2 mM paraquat and collected after 10 and 30 minutes. Total RNA preparation and blotting conditions are described in the General materials and methods chapter. The *sodB* probe was obtained by PCR with the *sodB* Forward and *sodB* Reverse primer (see Table 1, General materials and methods).

Sample preparation for two-dimensional gel electrophoresis (2-DE) and matrix assisted laser desorption ionization-time of flight mass spectrometry

KF707 cells were grown in LB to the late exponential phase ($OD_{660} \sim 1.8$) in the presence or absence of 100 μ M potassium tellurite (i.e. for 36 h and 18 h respectively). Preparation of soluble protein fractions, 2-DE and identification of proteins differentially expressed were carried out as described in the General materials and methods chapter.

Results

Effects of tellurite on growth

Relatively low concentrations of potassium tellurite (i.e. 10 $\mu\text{g/ml}$ \sim 40 μM) added to exponentially growing KF707 cells were sufficient to slow the growth (4.1 A). The effects of tellurite exposure under these conditions have been described in part in Chapter 3, where we suggested that the viability of tellurite-shocked cultures is highly reduced most probably because of tellurite-induced oxidative stress. However, it has been shown that KF707 is able to grow in the presence of high concentrations of tellurite (up to 150 $\mu\text{g/ml}$ \sim 600 μM in LB medium, Di Tomaso *et al.* 2002). Indeed, if tellurite is added to the growth medium upon inoculation, the initial lag phase increases as a function of tellurite concentration (Figure 4.1 B) but, from then on, growth resumes with a doubling time (1.3-1.5 h) that is similar to the generation time of control cells (\sim 1.3 h). Figure 4.1 B also shows the variation of tellurite concentration during growth of KF707 in LB in the presence of 25 $\mu\text{g/ml}$ (100 μM) tellurite. TeO_3^{2-} is not significantly removed from the medium until the middle of the exponential phase, when cellular uptake starts (Di Tomaso *et al.* 2002). The population of cells growing in the presence of tellurite was considered to be tellurite-adapted. Adapted cells were harvested for proteomic experiments at a time point marked by the removal of approximately 95 % of the added tellurite.

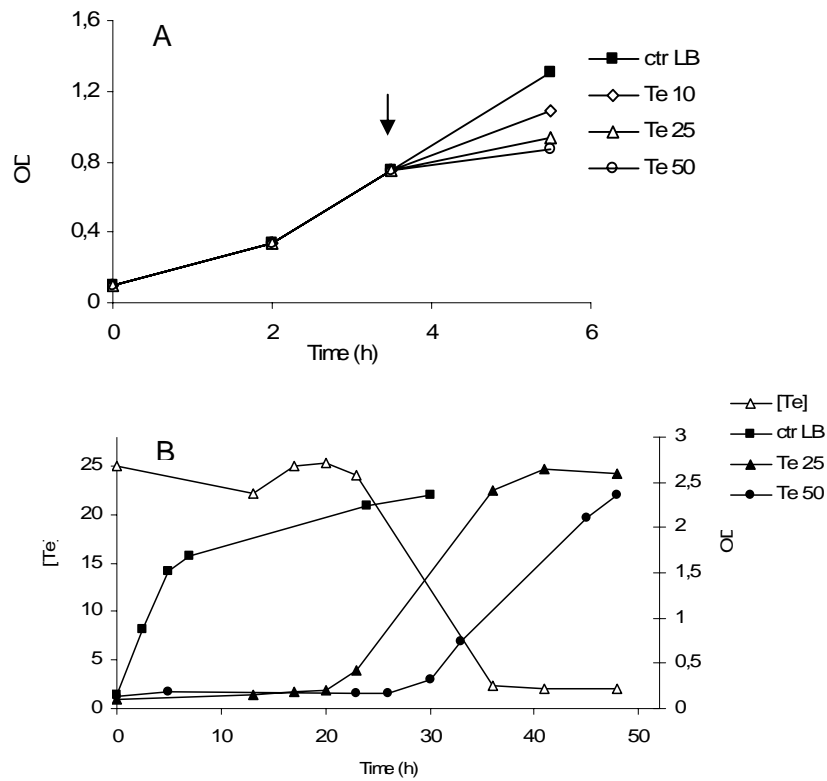


Figure 4.1. Growth curves of *Pseudomonas pseudoalcaligenes* KF707 cultures exposed to potassium tellurite. Panel A: Te-shocked cultures. Increasing concentrations of tellurite were added to LB exponentially growing cells at the point indicated by the black arrow. The OD_{660} was measured after a 2 h incubation period and a 3-7 fold increase in the generation time was observed for cells exposed to tellurite relative to LB growing control cells. Panel B: Te-adapted cultures. In this case, tellurite was added to LB medium upon inoculation of the cultures. The presence of tellurite in the growth medium resulted in a concentration-dependent increase of the lag phase. Residual amounts of TeO_3^{2-} in the medium are shown for cells growing in the presence of 25 $\mu\text{g/ml}$ of tellurite (*open triangles*).

Effects of selenite and arsenite on tellurite toxicity

In Chapter 3 we have tested the hypothesis of the involvement of oxidative stress in tellurite-mediated toxicity by assaying the ability of TeO_3^{2-} to induce adaptation to common oxidants as well as to the stress mediated by the oxyanion itself. In no instance were low concentrations of tellurite able to increase the viability of cultures exposed to high concentrations of tellurite or other stressors.

On the other hand, it has been shown that other toxic metals such as selenite and cadmium can induce adaptation to oxidants and to increased concentrations of the same metal (Bébién *et al.* 2002, Ferianc *et al.* 1998, Banjerdkij *et al.* 2005). Moreover, it has been shown that the induction of the *arsABC* operon in *E. coli* conferred increased tolerance to tellurite (Turner *et al.* 1992b). To date, no specific selenite resistance determinant has been isolated and, therefore, the increased tolerance to selenite toxicity has been prevalently linked to the activation of oxidative stress responses (Bébién *et al.* 2002). In this study we have assayed the ability of selenite and arsenite oxyanions to confer induced tolerance to potassium tellurite. Unexpectedly, arsenite, but not selenite was able to induce cross-protection to tellurite-mediated toxicity. Notably, pre-treatment with selenite resulted in synergism with tellurite toxicity (Figure 4.2 A). We also observed that low concentrations of arsenite were able to induce adaptation to subsequent exposures to high concentrations of the same metalloid (Figure 4.2 B). This would suggest that a survival strategy is activated in *Ps. pseudoalcaligenes* KF707 in response to arsenite, which is also able to mitigate tellurite toxicity. In the case of selenite, no adaptation was observed when KF707 cultures were pretreated with low selenite and then exposed to higher concentrations of the same metalloid (Figure 4.2 C). Finally, when KF707 cultures were exposed to sublethal concentrations of tellurite and then to high concentrations of AsO_2^- or SeO_3^{2-} , a synergistic effect of tellurite on selenite and arsenite toxicity was observed (Figure 4.3). Lethal and sublethal concentrations of metals were chosen based on the MBC (minimal bactericidal concentration) determinations obtained from the MBEC-HTP assay (Chapter 2). The MBC of selenite and arsenite is 115 and 31 mM respectively but the exposure of KF707 cells for 2 h to these concentrations of metalloid oxyanions did not result in a significant loss of cell viability (control curves in Figure 4.3 A, B). Therefore, the lethal concentrations of the metalloids were established as 3 times higher than the MBC values (345 and 93 mM for selenite and arsenite respectively). Overall, selenite was less effective at killing KF707 cultures than arsenite. Sublethal concentrations of selenite and arsenite were 50 and 200 times lower than the respective lethal concentrations (i.e. 6.3

mM for selenite and 0.5 mM for arsenite) and did not cause loss of cell viability (data not shown).

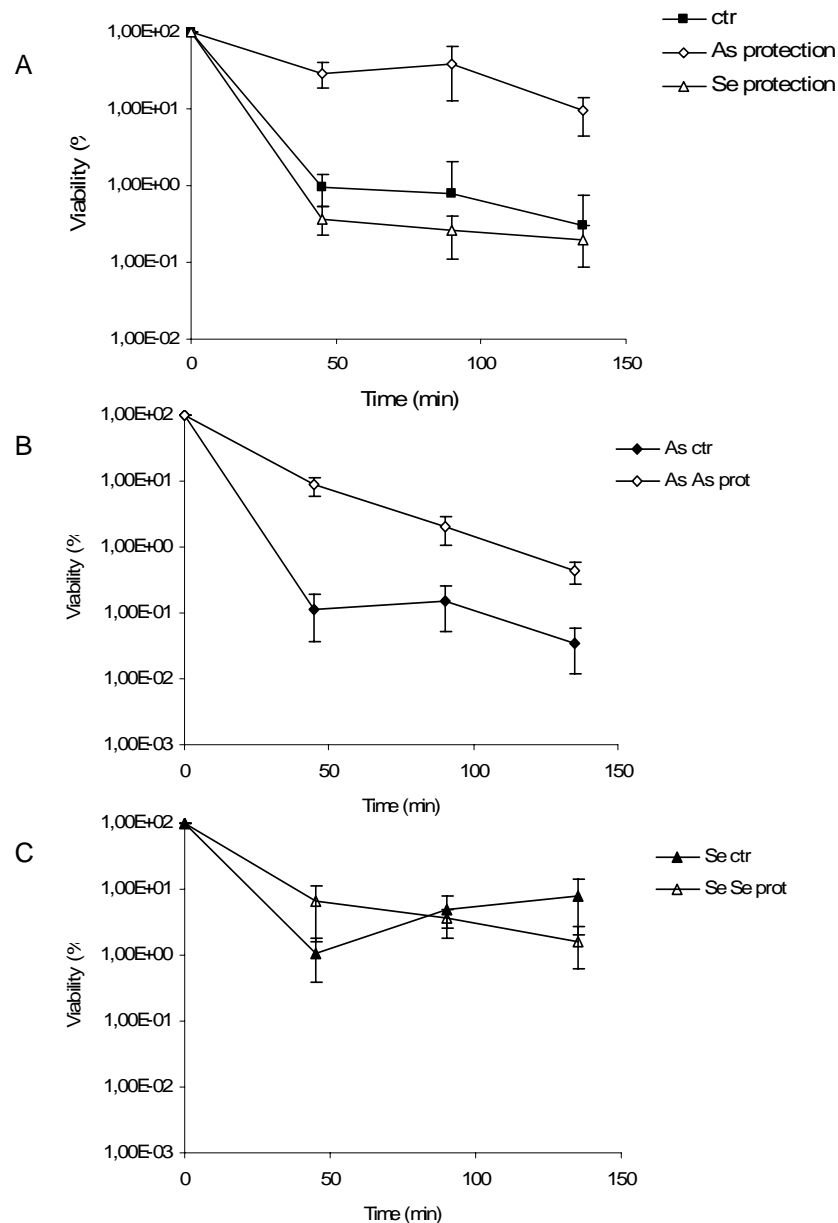


Figure 4.2. Effects of the exposure to low concentrations of arsenite and selenite on tellurite toxicity. Exponentially growing cells were pretreated with 0.5 mM arsenite and 6.3 mM selenite for 1.5 h and then exposed to a lethal dose of tellurite. Pretreatment with arsenite highly increased KF707 tolerance to tellurite, while selenite exerted a synergistic effect on tellurite toxicity (A). As a control of the activation of metal specific adaptive responses to arsenite and selenite, KF707 cells were pretreated with 0.5 mM arsenite and then exposed to 93 mM arsenite (B) or pretreated with 6.3 mM selenite and then exposed to 315 mM selenite (C). The induction of an adaptive response to arsenite but not to selenite was observed in *Ps. pseudoalcaligenes* KF707.

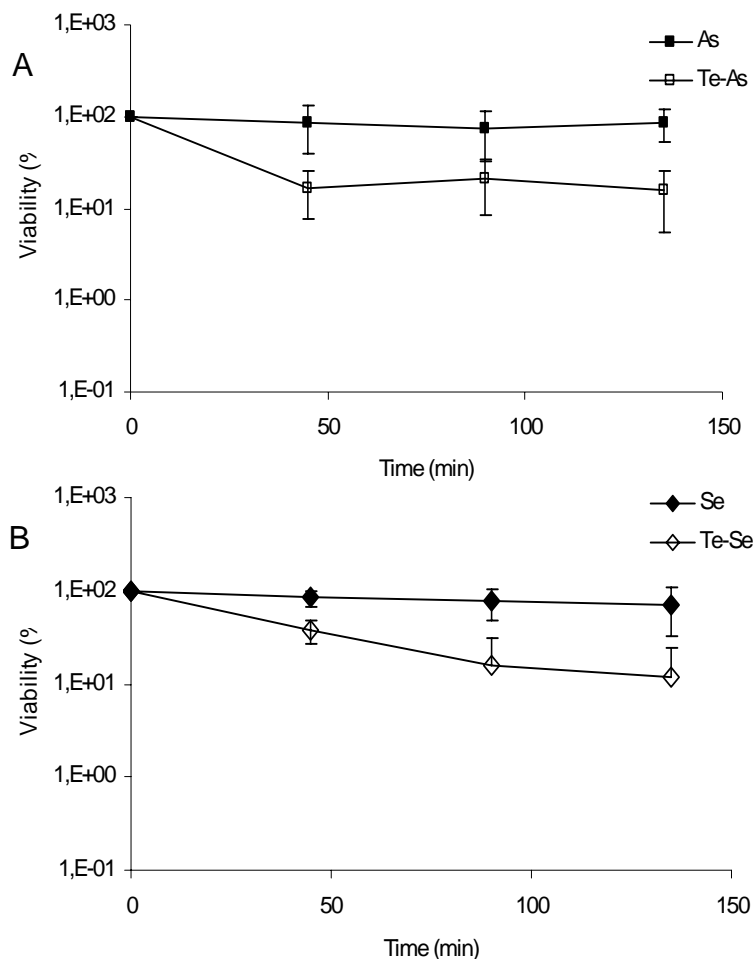


Figure 4.3. Effects of the exposure to low concentrations of tellurite on the toxicity of arsenite (A) and selenite (B). Exponentially growing cells were pretreated with 2.5 $\mu\text{g/ml}$ ($\sim 10 \mu\text{M}$) tellurite for 1.5 h and then exposed to 31 mM arsenite (A) and 120 mM selenite (B). Pretreatment with tellurite exerted a synergistic effect on the toxicity of the other metalloid oxyanions. Solid symbols indicate control viability assays for KF707 cultures exposed to MBC of arsenite (A, *solid square*) or MBC of selenite (B, *solid diamond*). Experiments were performed in triplicate.

Induction of sodB gene by tellurite and selenite

In *E. coli*, *sod* genes are transcriptionally induced in response to selenite (Bébién *et al.* 2002). In *Ps. aeruginosa*, total SOD activity was not observed to vary significantly between non-stressed cells and those exposed to arsenite (Parvatiyar *et al.* 2005). We analyzed the expression of the *sodB* gene in selenite- and tellurite-treated KF707 cells. The characterization of total SOD activity by non-denaturing PAGE (Chapter 3) showed that a *sodB* gene (coding for FeSOD) is present in KF707. This result was confirmed by the successful amplification of

a 440 bp fragment of KF707 *sodB* gene by PCR using primers designed on the basis of the *sodB* sequence of *Ps. aeruginosa* PAO1. In contrast, no evidence of the presence of either the MnSOD or Cu-ZnSOD isoforms in KF707 was obtained. For Northern blot analysis, cells were treated with sublethal concentrations of selenite, tellurite and paraquat and total mRNA was prepared from samples collected after 10 and 30 minutes. The *sodB* gene was strongly induced by both selenite and paraquat within 10 minutes after exposure (Figure 4.3). After 30 minutes of treatment, the induction of *sodB* was still manifest for selenite treatment, confirming the ability of this oxyanion to activate a defence response against $O_2^{\cdot-}$. In accordance with the observation that tellurite poorly increased total SOD activity in exposed cells (Chapter 3), we observed that *sodB* expression was only slightly induced after 30 minutes of tellurite treatment. This result is also in agreement with the slow kinetics of ROS release caused by tellurite interaction with cellular targets (Chapter 3).

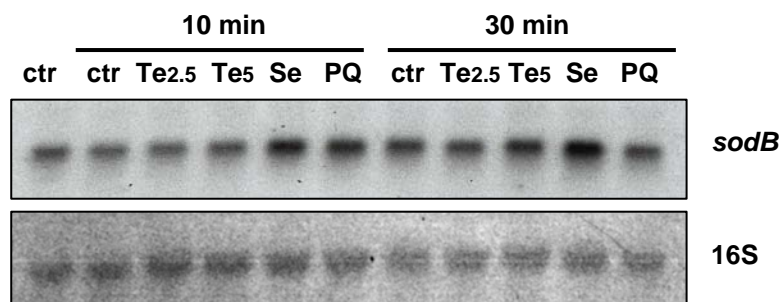


Figure 4.3. Transcriptional induction of the *sodB* gene in response to tellurite and selenite. Total RNA was isolated from cells treated with 2.5 and 5 $\mu\text{g/ml}$ TeO_3^{2-} (Te2.5, Te5), 6.3 mM SeO_3^{2-} (Se) and 2 mM paraquat (PQ) for 0, 10 and 30 minutes. The Northern blot was stripped with hot 0.1 % SDS and then hybridized with 16S radiolabelled probe for loading calibration.

Proteomic response to tellurite adaptation

Proteomic analysis was conducted to initiate a more global assessment of cellular physiology of tellurite-adapted *Ps. pseudoalcaligenes* KF707. Soluble-protein fractions of control and tellurite-adapted bacteria were separated by two-dimensional gel electrophoresis (2-DE). The soluble-protein profiles of KF707

cells showed that tellurite caused changes in the expression of numerous factors but the overall complexity of protein profiles did not vary (Figure 4.4 A-C). 13 proteins that were consistently observed to vary between control and tellurite-treated proteomes (Figure 4.4 A-C, spots are indicated by black arrows) were excised from 2D gels and subjected to MALDI-TOF analysis. Unfortunately, peptide fingerprint searches did not yield confident identification of the excised proteins. *Ps. pseudoalcaligenes* KF707 genome has not been sequenced and this lack of information is likely to hinder the effectiveness of global analysis approaches, such as proteomics, for the study of KF707 physiology. However, in order to identify some of the factors responsible for adaptation to tellurite, a few selected spots were subjected to LC/MS/MS and two proteins were confidently identified (circled in Figure 4.4 A). The identified proteins are GroEL, uniquely present in the 3-5.6 pI range of the control profile, and trigger factor which is uniquely present in the 3-5.6 pI range of adapted cells. GroEL was identified with a score of 699 and 27 % sequence coverage with the GroEL chaperonine of *Ps. aeruginosa* (accession number AAA53369). *Ps. aeruginosa* GroEL has a mass (M_r) of 57036 Da and a calculated pI value of 5.04, concordant with the mass and pI values that can be estimated from the 2D gel of control cells. On the other hand, trigger factor was identified with a score of 383 and 18 % sequence coverage with trigger factor of *Ps. mendocina* ymp (accession number ZP_01527887), having M_r of 48300 Da and pI 4.78. The nominal mass and pI values of the identified protein were concordant with the values estimated from the 2D gel also in this case. In order to assess the importance of the heat shock response in the protection against tellurite toxicity, a cross-protection assay was performed in which KF707 heat shocked cells exposed to a temperature of 50 °C for 30 minutes were subsequently treated with a lethal concentration of potassium tellurite. Tolerance to potassium tellurite was highly increased in cells subjected to heat shock treatment in comparison to non heat-shocked cells (Figure 4.5).

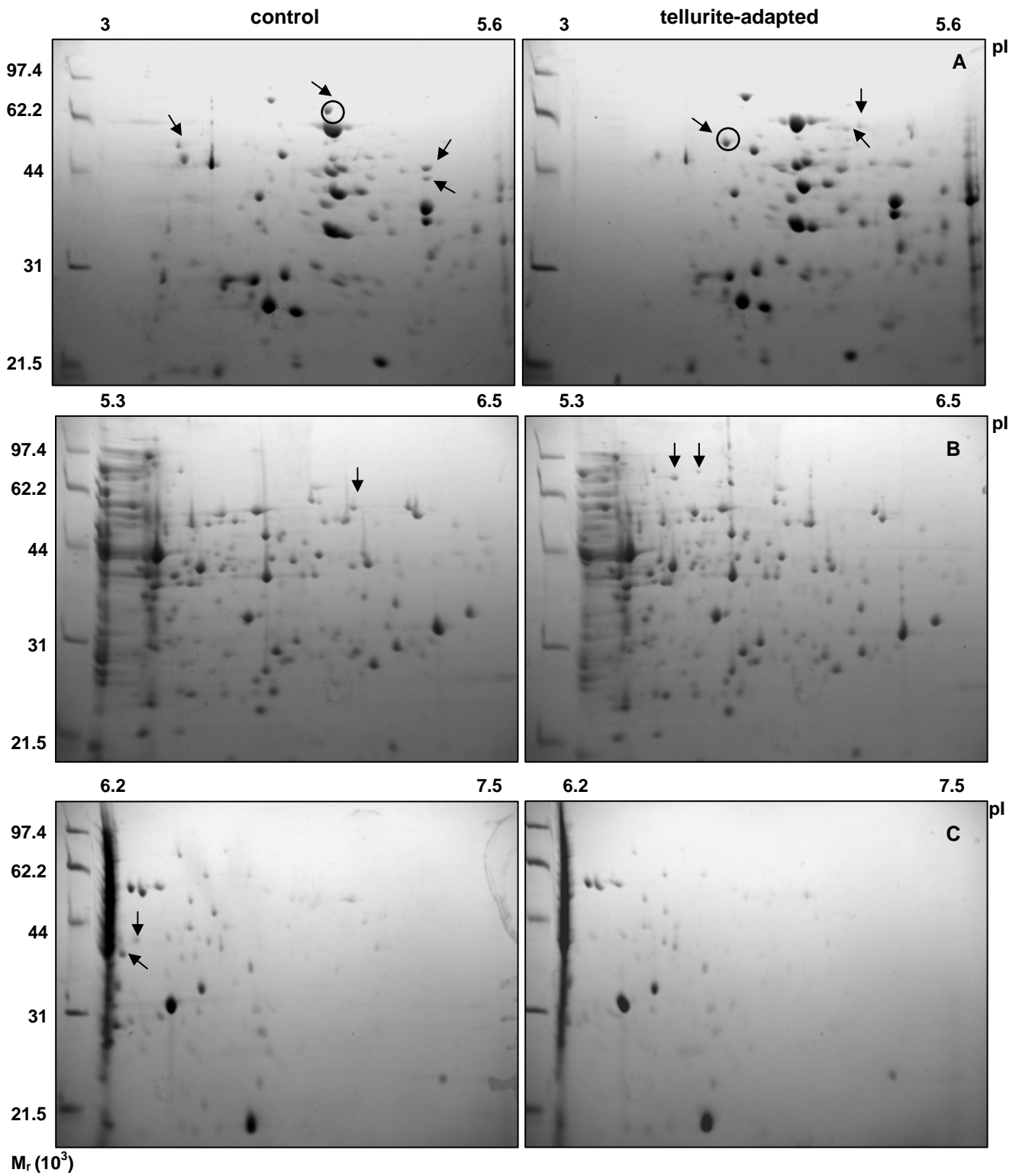


Figure 4.4. Comparative 2D gel electrophoresis analysis of the *Ps. pseudoalcaligenes* KF707 soluble proteins expressed in tellurite-adapted cells (on the right) in comparison to control cells (on the left). Proteins differentially expressed are indicated by a black arrow and proteins that have been identified are circled. Molecular weights are shown on the left while the pI range is indicated on the top of each panel (A, pI 3-5.6; B, pI 5.3-6.5; C, pI 6.2-7.5).

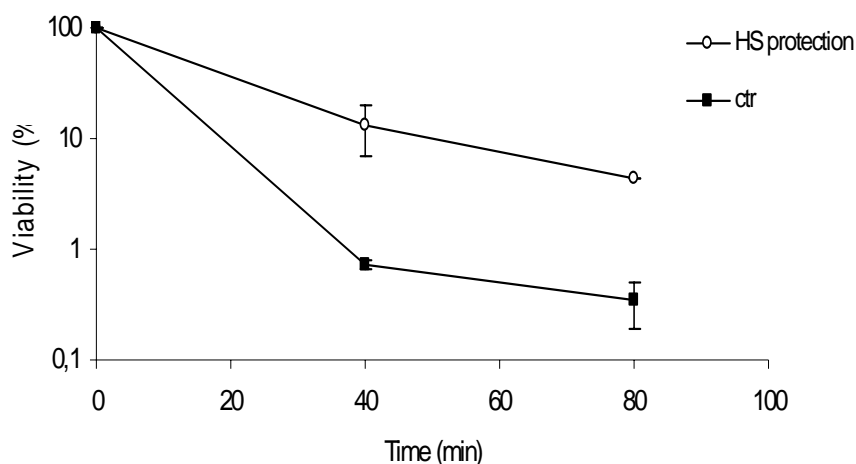


Figure 4.5. Effects of heat shock on tellurite toxicity. Exponentially growing cells were exposed to 50 °C for 30 minutes and subsequently exposed to 50 µg/ml tellurite. The activation of the heat shock response highly increased KF707 tolerance to tellurite.

Discussion

The goal of the present study was to establish a better understanding of the cellular responses involved in bacteria-tellurite interactions. To this end, we investigated the physiology of *Ps. pseudoalcaligenes* KF707 under two different conditions: i) exposure to a brief pulse of tellurite or other oxyanions (i.e. arsenite and selenite) (shock response) and ii) active growth in the presence of tellurite (adaptation response). The involvement of oxidative stress in the tellurite shock response was investigated in Chapter 3, where it was shown that exposure to tellurite results in the release of reactive oxygen species, most probably $O_2^{\cdot-}$, and depletion of anti-oxidant molecules (i.e. oxidation of reduced thiols and primarily glutathione). Chapter 3 also shows that adaptation to tellurite shock is not achieved during a short exposure time. Indeed, treatment with low concentrations of tellurite did not increase the viability of cultures subsequently exposed to high concentrations of this metalloid.

In this chapter we investigated the effects of the induction of a shock response to selenite and arsenite on tellurite toxicity, with the intent to identify possible overlapping mechanisms of stress response to metalloids in KF707. Selenite was able to induce the expression of the *sodB* gene, coding for the FeSOD isoform, at higher levels and for a longer duration than paraquat, a strong superoxide generator. We showed in Chapter 3 that the induction of SOD activity by paraquat was able to increase tolerance to tellurite in protection assays. Selenite on the other hand, did not induce cross-protection to tellurite. This result was quite unexpected, since selenite is far less toxic than tellurite and is able to induce a general oxidative stress response in *E. coli*, as shown by B ebien and colleagues (2002). Similarly to tellurite, selenite is able to react with sulfhydryl groups of thiol-containing molecules, a reaction leading to the final reduction and detoxification of Se(IV) compounds and eventually to the release of reactive oxygen species (Kessi and Hanselmann 2004, Kessi 2006). However, it has been shown that RSH content recovers over a short period of time (i.e. 90 minutes) during exposure to selenite but not to tellurite (Turner *et al.* 2001). This recover of RSH levels during selenite treatment was linked to the ability of glutathione reductase to process selenodiglutathione (GS-Se-SG), a key intermediate of the selenite reductive metabolic pathway (Turner *et al.* 1998). *Vice versa*, GS-Te-SG reduction was not observed *in vitro* and no recovery of RSH content occurred in either *E. coli* (Turner *et al.* 2001) or *Ps. pseudoalcaligenes* cells exposed to tellurite (this study). The different effects of selenite and tellurite oxyanions on cellular thiol status may help to explain the basis of the 1000-fold increased toxicity of tellurite in comparison to selenite oxyanion. It is worth mentioning here that *Ps. pseudoalcaligenes* KF707 harbours a *tpm* gene, encoding for a SAM-dependent thiopurine methyltransferase enzyme. This enzyme is considered to be involved in the methylation and detoxification of both selenite and tellurite oxyanions (Cournoyer *et al.* 1998, Ranjard *et al.* 2003). The isolation and characterization of *Ps. pseudoalcaligenes* KF707 *tpm* gene will be described in Chapter 5, but we will point out here the ability of this gene to increase *E. coli* DH5a resistance to tellurite. When KF707 *tpm* determinant is expressed in *E. coli*, the MIC increases from 1 $\mu\text{g/ml}$ to more than 25 $\mu\text{g/ml}$. Notably, the presence of

KF707 *tpm* determinant in *E. coli* DH5 α reduced the blackening of colonies growing in the presence of tellurite, suggesting that the volatilization of tellurite is a first line of defence that prevents the interaction of tellurite with its cellular targets and thus mitigates its toxicity. Therefore, we may speculate that one of the reasons that can account for the synergism of selenite to tellurite toxicity in KF707 is the saturation of TPM enzyme activity during selenite detoxification. In this case, when tellurite is added to cells previously exposed to selenite in protection assays, the TPM enzyme could be engaged in methylation of selenite so that the cytosolic tellurite would be free to interact with cellular targets and poison cell metabolism in a way that exceeds the antioxidant defences induced by selenite.

Unlike selenite, the metalloid oxyanion arsenite induced adaptation to increased concentrations of arsenite itself and also protection against tellurite toxicity. Therefore, the survival strategy that is activated in *Ps. pseudoalcaligenes* KF707 in response to arsenite is also able to mitigate tellurite toxicity. It has been previously shown that the arsenite resistance determinant *arsABC* of pR773 resistance plasmid increased resistance to tellurite and reduced the intracellular accumulation of TeO_3^{2-} in cells of *E. coli* (Turner *et al.* 1992b). The *ars* genes occur widely in both Gram-negative and Gram-positive bacteria and basically the same *ars* operon confers resistance to arsenate, arsenite and antimonite (Cervantes *et al.* 1994, Diorio *et al.* 1995). As an example, *Pseudomonas aeruginosa* harbours a chromosomal *arsRBCH* operon plus an additional *arsC* reductase at a different locus. It is possible to assume that a similar operon may be present in the KF707 genome, given that the MIC value of arsenite for these two closely related organisms is in the range of 2-3 mM [Parvatiyar *et al.* 2005, this study (Chapter 2)]. The induction of the expression of the *ars* operon during exposure to arsenite may mediate the observed increased tolerance to the following exposure to tellurite by reducing the amount of TeO_3^{2-} internalized. Indeed, we observed that cells previously exposed to arsenite were less subjected to darkening during treatment with tellurite (data not shown). A closer analysis of the presence of *ars* genes in KF707 and of the functions of the proteins encoded by this operon in mediating tolerance to tellurite is warranted.

Proteomic experiments were performed in order to extend the understanding of cellular factors involved in the response of KF707 to tellurite. In this case, we sought to identify protein functions required for cellular adaptation. KF707 cells were harvested while growing in the presence of tellurite at a time point of the late exponential phase, marked by the almost complete removal of tellurite from the medium (approximately 5 % of the added tellurite was remaining in the medium after 36 h of growth in the presence of 25 µg/ml tellurite, Figure 4.1 B). We observed the constant occurrence of both up- and down-regulated genes in the proteome profile of tellurite-adapted cells and we also observed some spots that were uniquely and consistently present in either control or tellurite-adapted populations. The lack of information regarding the KF707 genome sequence meant that MALDI-TOF analysis was inadequate for the identification of the differently expressed protein functions. Therefore, we subjected a few selected proteins to LC/MS/MS analysis, that allowed for the identification of two proteins, namely GroEL, which was specifically expressed in control conditions and trigger factor (TF), which was specifically expressed in the adapted cells. TF was also found to be up-regulated in *E. coli* cells exposed to cadmium (Ferianc *et al.* 1998) and in *E. coli* cells exposed to selenite (Bébién *et al.* 2002). Moreover, in *Streptococcus mutans* this chaperone was found to be involved in acid and oxidative stress responses (Wen *et al.* 2005). TF is a ribosome-associated chaperone with a peptidyl-prolyl *cis-trans* isomerase, widely conserved among bacteria (Hesterkamp and Bukau 1994). It has been proposed that GroEL and TF chaperones assist the folding of proteins of different sizes: proteins of 60 kDa or less are common substrates for GroEL (Ewalt *et al.* 1997, Houry *et al.* 1999) while large-sized proteins preferentially interact with TF (Deuerling *et al.* 2003, Mogk *et al.* 2001), thus suggesting a difference in substrate pools for these two chaperones. Recently, induced expression of the *ibpA* gene, which encodes for a small heat shock protein (sHsp) involved in resistance to heat and superoxide stresses (Kitagawa *et al.* 2000, Kitagawa *et al.* 2002), has been reported for *S. oneidensis* MR-1 adapted to chromate (Chourey *et al.* 2006), for *Pseudomonas aeruginosa* exposed to arsenite stress (Parvatiyar *et al.* 2005) and for *E. coli* cells subjected to tellurite exposure (Pérez *et al.* 2007). In

mammalian cells, it has been reported that sHsps homologous to the bacterial IbpA, work as regulators responding to the intracellular redox state to reduce the level of reactive oxygen species and also to maintain the intracellular levels of glutathione (Arrigo 1998). Chaperones induced during both acute and chronic stress responses to oxyanions may be required to mediate the correct folding of a fraction of *de novo* polypeptides and/or function in the reactivation or degradation of proteins damaged by metal-mediated stresses. The involvement of the heat shock response in KF707 tolerance to tellurite has been confirmed by the observation that a short exposure to 50 °C prior to tellurite treatment highly increased cell tolerance to the oxyanion. Therefore, both heat shock and oxidative stress responses are likely to be involved in the KF707 shock and adaptive responses to tellurite toxicity. Taken together, the data presented indicate that the observed increased tolerance to tellurite mediated by arsenite might be derived not only from the induced expression of *ars* genes that could reduce tellurite uptake, but also from the activation of a general stress response involving factors such as IbpA, as has been shown for *Ps. aeruginosa* (Parvatiyar *et al.* 2005). Ultimately, the high toxicity of tellurite in comparison to other oxyanions, and selenite in particular, may originate from the combination of the unbalance of the redox cellular status and the production of reactive oxygen species with the inability to induce an adequate cellular stress response. From the data described here it is apparent that metalloids exert their toxicity at various levels of bacterial metabolism and that a general stress response is required to counteract the pleiotropy of their noxious effects during both shock and adaptive responses.

Chapter 5

*Isolation and characterization of a tellurite-resistance genetic determinant from *Pseudomonas pseudoalcaligenes* KF707*

Introduction

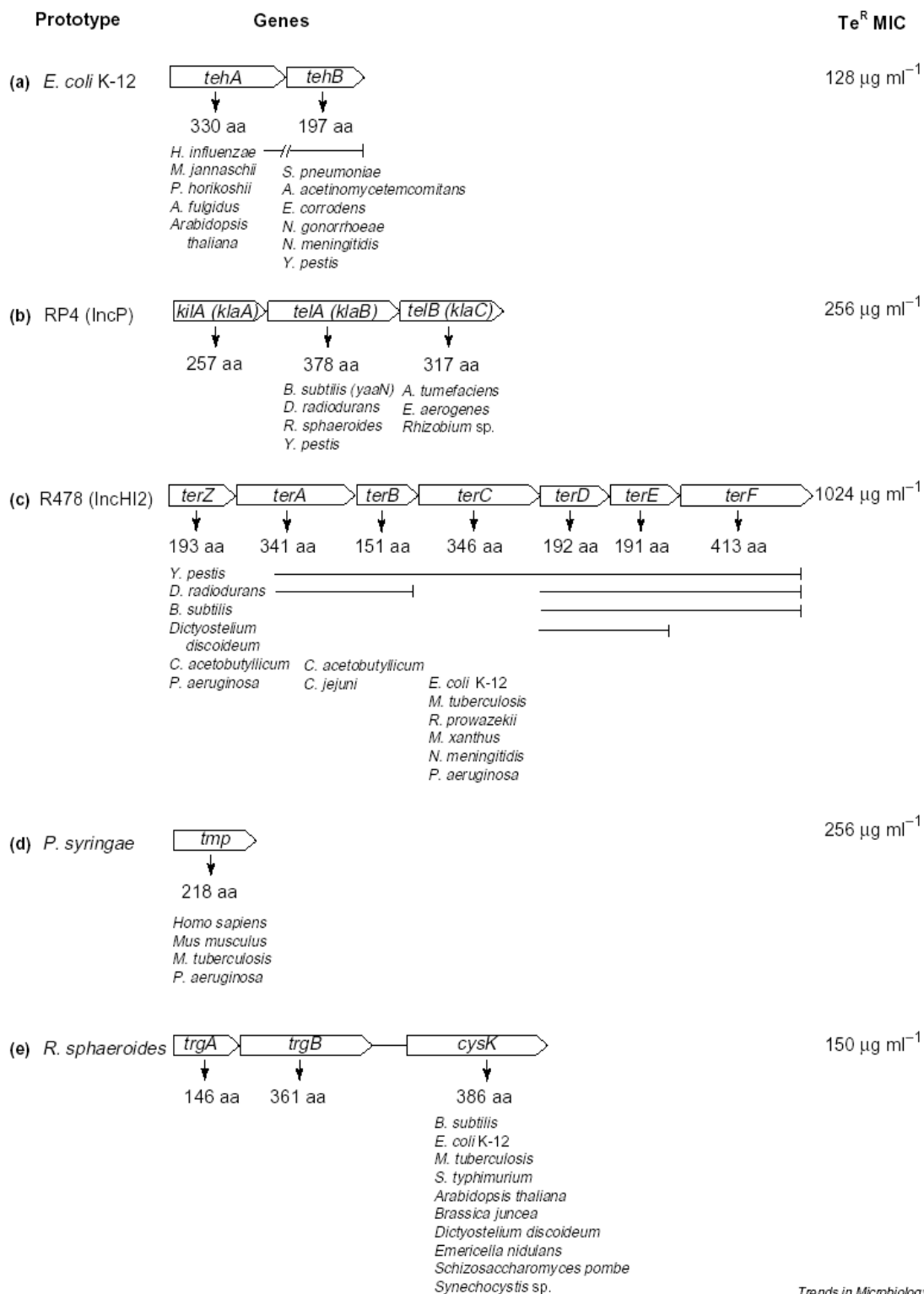
Genes responsible for tellurite resistance (Te^{R}) have been isolated from various organisms and were found to be encoded by at least five distinct genetic determinants (Taylor 1999, Turner 2001) (Figure 5.1). The Te^{R} determinants isolated so far encode for protein functions highly specific for TeO_3^{2-} and do not display cross-resistance to other oxyanions or oxidant agents (reviewed in Turner 2001). Although Te^{R} determinants do not show homologies with one another, they generally contain membrane associated proteins and often confer other phenotypes, such as resistance to colicins and bacteriophages (i.e. *terABCD* and *cysK*). The emergence of tellurite resistance determinants in many different bacterial species, including human pathogens, along with the observation that they also confer other phenotypes, suggests that these determinants may provide a selective advantage in natural environments, that may be unrelated to the phenotype of tellurite resistance. Notwithstanding the scientific effort aimed at elucidating the genetic bases of tellurite resistance, both the biochemical mechanisms and the possible physiological functions of Te^{R} determinants are still poorly understood. In general, reduced uptake and/or increased efflux are not involved in tellurite resistance (Turner *et al.* 1995). This evidence points out a fundamental difference in the mechanisms of tellurite detoxification as compared to other toxic metals, for which resistance determinants often encode efflux transporters (reviewed in Nies 1999). As an example, resistance to arsenite is commonly conferred by a conserved *ars* operon. The operon codes for a chemiosmotic arsenite transport protein ArsB (Bröer *et al.* 1993), a membrane-associated oxyanion-stimulated ATPase protein, ArsA, that can convert ArsB into

an ATPase efflux system (Dey and Rosen 1995) and a the soluble arsenite reductase ArsC, that converts As(V) to As(III) (Ji and Silver 1992). The *ars* system was found to mediate TeO_3^{2-} efflux from *E. coli* cells (Turner *et al.* 1992b). The *ter*, *kilA* and *teh* systems on the other hand, did not mediate a similar reduction of uptake and did not increase tellurite efflux (Turner *et al.* 1995). Another common mechanism of metal detoxification is the reduction of metal ions to their elemental state. The observation that bacterial cells growing in the presence of tellurite accumulate elemental tellurium (Te^0) crystallites (Taylor 1999) led to the hypothesis that reduction was carried out as a detoxification mechanism. This hypothesis was strengthened by the presence of polypeptides predicted to be integral membrane proteins in all Te^R determinants and by the observation that overexpression of membrane-bound nitrate reductases, which can reduce tellurite, resulted in a resistant phenotype (Avazeri *et al.* 1997). However, none of the cloned sequences showed homology to reductases. Moreover, it was also observed that the deposition of Te^0 occurs in sensitive strains and that Te^R without metal accumulation occurred in several bacterial species, thus suggesting that tellurite resistance is not directly and strictly linked to tellurite reduction (Yurkov *et al.* 1996). A frequent biological response to tellurite is the chemical modification via methylation. In selenium metabolism, methylation of inorganic anions is considered as a detoxification mechanism, given that methylated forms are volatile and much less toxic than Se(VI) and Se(IV) oxyanions (Frankenberger and Arshad 2001). It is thought that biological transformations of Te may follow similar pathways to selenium, which require reductive steps along with transfer of methyl groups (Challenger 1945). Indeed, organoselenium and organotellurium compounds have been detected in bacterial gas phases during growth in the presence of selenium and tellurium salts. Selenium compounds detected include dimethyl selenide (DMSe), dimethyl diselenide (DMDS₂) and dimethyl selenyl sulfide (DMSeS) while tellurium derivatives include dimethyl telluride (DMTe) and dimethyl ditelluride (DMDT₂) (reviewed in Chasteen and Bentley 2003). These volatile compounds emit a distinct garlic odour, that is also emanated from humans intoxicated with tellurite (Cervenka and Cooper 1961, Kron *et al.* 1991) and is characteristic of *Ps. pseudoalcaligenes* KF707 growing in the presence of

potassium tellurite. Among the tellurite resistance determinants isolated, only *tehAB* and *tpm* were found to be associated with a possible methylase activity. The TehB protein sequence was observed to contain regions homologous to the S-adenosyl-L-methionine (SAM) binding site motifs present in non-nucleic acid methyltransferases (Liu *et al.* 2000). TehB was found to bind SAM with tellurite (Liu *et al.* 2000, Dyllick-Brenzinger *et al.* 2000) and SAM-dependent depletion of tellurite was observed, although no volatile organotellurium compounds were detected in the gas headspace of cultures expressing the *teh* determinant. The other element of the *teh* system, the TehA protein, displayed homology to the small multidrug resistance (SMR) protein family and was observed to be able to transport quaternary ammonium compounds, common substrates for SMR proteins (Turner *et al.* 1997). On the basis of the observation that DMTe and DMDTe were non detected in the gas phase of cultures expressing TehAB and considering the requirement of GSH for the function of this system, the authors hypothesized that TehB methylase could detoxify tellurite into a non volatile methylated derivative, such as GSTeCH₃, that could then be exported by the TehA carrier. To date, the detoxification mechanism of TehAB system is not completely understood but the methylation of tellurite oxyanions is a distinct feature of the detoxification pathway. The other tellurite resistance determinant that has been associated with methylation is the *tpm* gene, isolated from the tellurite resistant pathogen *Pseudomonas syringae* pathovar *pisi* (Cournoyer *et al.* 1998). The *tpm* gene encodes for a SAM-dependent thiopurine methyltransferase (TPM) enzyme but it does not show sequence similarity to the *tehB* determinant. Thiopurine methyltransferase (TMP) belongs to the small molecule SAM-dependent methyltransferase protein family, that also includes catechol-*O*-methyltransferase (COMT), glycine-*N*-methyltransferase (GNMT), phenylethanolamine-*N*-methyltransferase (PNMT) and histamine-*N*-methyltransferase (HNMT) (Scheuermann *et al.* 2003). The endogenous distinct role of TPM enzymes is unknown, although in humans the TPM enzyme has been shown to be involved in the metabolism of 6-thiopurine drugs (Weinshilboum 2001, Krynetski and Evans 2000, Coulthard and Hall 2001). 6-thiopurine medications are commonly used for immune suppression in autoimmune diseases

and transplantations and for the treatment of acute lymphoblastic leukemia (ALL) (Elion 1989). They are pro-drugs that require the transformation by the cellular metabolic system into active 6-thioguanine nucleotides. S-methylation by TPM absorb part of the activated 6-thiopurine molecules, thus causing the reduction of the efficacy of the administered dose. Orthologues of the human TPM enzyme have been identified in different organisms, ranging from primates to plants and bacteria (Attieh *et al.* 2000, Krynetski and Evans 2000). However, the selective pressure(s) responsible for the conservation of TPM enzyme activity in distantly related organisms is presently unknown.

In bacteria, TPM was observed to mediate resistance not only to tellurite but also to sodium biselenite, selenite and selenate (Ranjard *et al.* 2002). In the presence of selenium salts, DMSe and DMDS₂ were detected in the gas phase of *E. coli* cells and their production was observed to be strictly dependent on the expression of the TPM enzyme (Ranjard *et al.* 2002). In order to understand the genetic basis of *Ps. pseudoalcaligenes* KF707 resistance to potassium tellurite, previous studies have investigated the presence of *tehAB*, *terZABCDEF* and *telAtelBkilA* Te^R determinants in the genome of the KF707 strain by means of Southern blot hybridization analyses. These operons were not found in the KF707 genome (unpublished results). For this reason, the presence of the *tpm* gene was analyzed in this study and the possible role of this gene in mediating bacterial resistance to potassium tellurite was investigated.



Trends in Microbiology

Figure 5.1. Cloned tellurite resistance determinants. Origins of proteins identified as having some similarity with the various determinants are shown beneath each protein. The level of tellurite resistance, recorded as the minimal inhibitory concentration (MIC), is shown on the right (from Taylor 1999).

Materials and methods

Bacterial strains and growth conditions

Ps. pseudoalcaligenes KF707, and *E. coli* DH5 α strains harbouring pUC18, pTPM and pTPMKO were used in this study (see General materials and methods for relevant genotype features and plasmid characteristics). Bacterial strains were grown in LB medium. The composition of the media and growth conditions are described in the General materials and methods chapter.

MIC determination

For MIC determination, *E. coli* cultures were grown overnight in LB broth and then diluted in the same medium to OD₆₆₀ ~ 1, corresponding to ~ 10⁸ CFU/ml. 20 μ l aliquots were spot plated onto LB agar plates containing increasing concentrations of potassium tellurite. Plates were incubated at 37 °C for 1-2 days.

Amplification of a tpm gene fragment from Ps. pseudoalcaligenes KF707 genome

Ps. pseudoalcaligenes KF707 genomic DNA was extracted as described in the General materials and methods chapter. PTCF2 and PTCR2 (Favre-Bronté *et al.* 2005) primers were used to PCR-amplify a sequence of approximately 250 bp from *Ps. pseudoalcaligenes* KF707 genomic DNA. PTCF2 and PTCR2 primers were designed on the *Ps. syringae* pv. *pisi* *tpm* sequence in order to cover the conserved domains VPLCGK from position 43 and YDRAAM from position 121 of the *tpm* sequence (Favre-Bronté *et al.* 2005, Cournoyer *et al.* 1998). Reaction mixtures (50 μ l) contained 5 μ l of 10 \times PCR buffer containing Mg²⁺, 0.3 pmol of each primer, 0.2 mM of each dNTP, 1 U Taq DNA polymerase (Roche) and 50 ng of template KF707 genomic DNA. Amplification was performed in a Biometra-T gradient thermalcycler after a hot start at 95 °C for 4 minutes followed by 35 cycles consisting of 95 °C for 30 sec, 62 °C for 40 sec and 72 °C for 30 sec and a final extension of 8 minutes at 72 °C. PCR products were separated by electrophoresis on 1.5 % agarose gels and fragments of the expected size (250 bp) were purified using the QIAquick gel extraction kit (QIAGEN). PCR purified fragments were cloned in the pCR 2.1-TOPO plasmid using the TOPO TA

cloning kit (Invitrogen) and sent for sequencing to the BMR-genomics service of the University of Padova (Padova, Italy).

Shotgun cloning strategy for the isolation of the *tpm* full-length gene sequence

The 250 bp fragment amplified with PTCF2 and PTCR2 primers was labelled with [³²P]dCTP as described in the General materials and methods chapter and used for Southern blot analysis of KF707 genomic DNA digested with *EcoRI*, *KpnI*, *PstI*, *Sall* and *SacI* restriction enzymes. A fragment of ~ 900 bp hybridizing with KF707 genomic DNA digested with *EcoRI* was subsequently cloned in pUC18 cloning vector and transformed in *E. coli* DH5 α competent cells. Positive clones were transferred by tooth-picking on LB plates containing ampicillin (50 μ g/ml) to form ordered grids. Bacterial colony blots were prepared from LB agar plates on nylon membranes as described by Sambrook *et al.* (1989). Hybridization analysis was performed as described in the General materials and methods chapter with the 250 bp *tpm* radioactive-labelled probe. Plasmid DNA was isolated from positive clones using the PureLink™ Quick Plasmid Miniprep kit (Invitrogen) and ‘false positive’ clones were detected by PCR-amplification, using plasmid DNA as a template and PTCF2-PTCR2 primers. Plasmids positive to the hybridization and giving the expected 250 bp amplification product were sent for sequencing. The *tpm* full-length sequence was thus isolated (pTPM plasmid).

Screening of KF707 genomic DNA library and *tpm* subcloning

Approximately 1000 cosmid clones of the KF707 genomic library, prepared as described in the General materials and methods chapter, were screened by *tpm* colony blot hybridization using the full-length *tpm* sequence as a probe. Bacterial colony blots were prepared on nylon membranes as described by Sambrook *et al.* (1989). Cosmid DNA was extracted from positive clones with the Midi-prep kit (QIAGEN) and subjected to restriction analysis with *BamHI*, *BglII*, *HindIII*, *XhoI*, *KpnI*, *PstI* and *Sall* restriction enzymes. Digested cosmid DNA was transferred to a nylon membrane and analysed by Southern blot. Restriction fragments positive to the hybridization with the *tpm* full-length probe were

subcloned in pUC18. Subcloned plasmid DNA was extracted with Mini-prep kit (QIAGEN) and sequenced with M13 Forward and M13 Reverse primers.

Northern blot analysis of tpm gene expression

Exponentially growing *Ps. pseudoalcaligenes* KF707 cells were treated with 2.5 and 5 ug/ml (10-20 μ M) tellurite, 6.3 mM selenite and 2 mM paraquat and collected after 10 and 30 minutes. Total RNA preparation and blotting conditions are described in the General materials and methods chapter. The full-length gene was used as the *tpm* probe for hybridization analysis.

Insertional mutagenesis of the tpm gene

The KF707 *tpm* gene contains an *EcoRV* restriction site. A kanamycin resistance cassette was isolated from the pUTmini-Tn5-Km plasmid by *NotI* digestion and gel purification of the 1.5 Kb restriction fragment corresponding to the Km cassette. A blunt end kanamycin resistance cassette was obtained by treating the *NotI* Km cassette with the Klenow enzyme (Promega). The blunt-end Km cassette was ligated into the blunt-end *EcoRV* restriction site of pTPM plasmid producing the pTPMKO plasmid, in which the *tpm* coding sequence was interrupted by the Km resistance cassette. In order to obtain a conjugative plasmid for insertional mutagenesis of the KF707 chromosomal *tpm* gene, the insertion cassette thus formed was ligated into the pRK415 conjugative plasmid and the resulting construct was conjugated into the KF707 wild type strain. Double cross-over recombinants were isolated by plating KF707 exconjugants on LB plates containing kanamycin plus tetracycline (50 μ g/ml and 20 μ g/ml respectively) and kanamycin only. Exconjugants that showed resistance to kanamycin but not to tetracycline were isolated as possible *tpm::Km* insertion mutants. The integration of the Km cassette into the *tpm* sequence was verified by both southern blot analysis and sequencing of flanking DNA genomic regions.

Results

Isolation and characterization of Ps. pseudoalcaligenes KF707 tpm sequence

When growing in the presence of potassium tellurite, KF707 cultures emanate a strong garlic odour, that is characteristic of the production of organotellurium compounds (i.e. DMTe and DMDTe). Therefore, *tpm* universal primers PTCF2 and PTCR2, covering a highly conserved region of bacterial thiopurine methyltransferase sequences (Cournoyer *et al.* 1998, Favre-Bronté *et al.* 2005), were used to verify the presence of a *tpm* Te^R determinant in the genome of KF707. A 250 bp fragment was successfully amplified, whose sequence showed high homology (74 %) to the *tpm* sequence of *Ps. putida* KT2440. The full length *tpm* sequence was isolated by the shotgun cloning strategy and cloned in the pUC18 cloning vector as a 900 bp *EcoRI* restriction fragment (pTPM construct). The ORF Finder program was used to search the cloned sequence for the presence of open reading frames (ORF). Frame -1 was found to correspond to a 218 aminoacid ORF (from position 91 to 744 of the insert of pTPM plasmid), containing the 250 bp PCR-amplified fragment. Sequence analysis with the RBS Finder search program (TIGR) of the sequence presented in Figure 5.2, showed the presence of a ribosome binding site (RBS) upstream of the ATG start codon.

```

1  NNNTCTCGGTNGAGCCGGGCATCATCCGAGCTGGAACATATCGGTTTCCAGCATAAATAGTT      60
61  GGGCAATTTGATCGAATCGATGGAGGCATCATGGAGGAAAGTTTCTGGCAGGCGCGCTGG      120
121 GCGGAGAACCAGATCGGTTTCCATCAGCGGGAAACCAATCCGTATCTGGAGCGCTACTGG      180
181 TCGCGGCTGGGCCTGCCGGCAGGGTGCCAGGTGCTGGTCCCCTTGTGCGGCAAGAGCCTG      240
241 GACCTGCTCTGGCTGGCGGGCAGGGATATCGGGTGCTGGGCGTCGAGCTGGCGGAGCGG      300
301 GCGGTGCTGGACTTCTTCGCCGAGCAGGGCCTGGAGCCCGTCGTGACCGGACAGGGGGCG      360
361 CTGCGTGCCTTCAGCGCCGGCAGATCGAGATCCTCCAGGGTGACTTCTTCGCCCTGGAG      420
421 CCGGCCGATGTGGCGGACTGCCGTGCGCTCTACGACCGCGCCGCGATCATCGCGCTGCCG      480
481 CCGGCCATGCGCCGGGACTACGTGGCGCACCTGGCGCGCATCCTGCCCCGCCCTGCGAT      540
541 GGCCTGATGGTGACCCTGGACTACGAGCAGGCGCGTCTGGACGGCCCGCGTTCTCGGTG      600
601 CCGGAGCGGAGGTGCGCGAGCGCCTCGAGGGGAGCTGGGAGGTGGAGTTGCTGGAGCGT      660
661 TGGGATGTGCTGGAGAAGAAGTGAAGTTCGCTTCCCGGGGCTGGACAGCCTGCATGAG      720
721 CCGGCGTTCCGCCTGCATCGGAAGTAGGGGGATCGGTGTAGGGATGCAGGGTGCGCCGTT      780
781 CGCATAAGGGCCCTGCCGGACAAAAAGGTTTCATCGCGGATTATCGG

```

Figure 5.2. DNA sequence of the 900 bp *EcoRI* genomic fragment containing the KF707 *tpm* coding sequence in the pTPM plasmid. The start codon and the stop codon are coloured in red and blue respectively. The putative *tpm* ORF covers the region from position 91 to 744 of the sequence (underlined with a black line in the figure).

The protein sequence deduced from the translation of the putative ORF DNA sequence was used to search the Conserved Domain Database (CDD at the NCBI database) in order to verify the presence of conserved domains in the sequence. A domain typical of TPM methylases was found and Figure 5.3 shows the alignment of the translated sequence of the putative KF707 *tpm* ORF with the consensus sequence of the thiopurine methyltransferase conserved protein family.

pfam05724, TPMT, Thiopurine S-methyltransferase (TPMT). This family consists of thiopurine S-methyltransferase proteins from both eukaryotes and prokaryotes. Thiopurine S-methyltransferase (TPMT) is a cytosolic enzyme that catalyses S-methylation of aromatic and heterocyclic sulphhydryl compounds, including anticancer and immunosuppressive thiopurines..

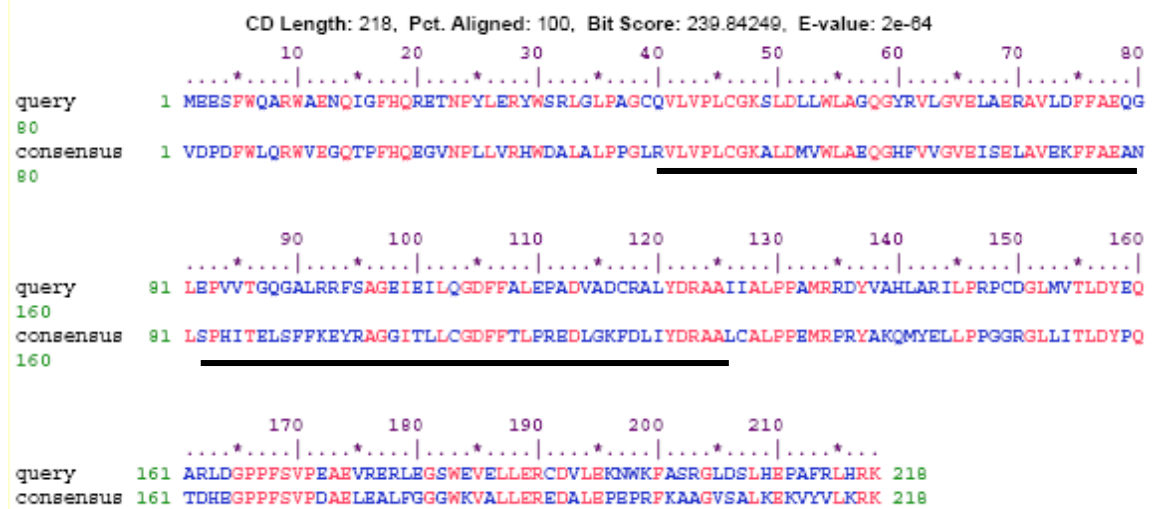


Figure 5.3. Alignment of the ORF -1 translated sequence of the pTPM plasmid with the consensus sequence of the TPM conserved protein family. The translated sequence of ORF -1 shows a 47.2 % homology to the TPM consensus sequence in the CDD database. Black bars underline the portion of the sequence amplified with the *tpm* universal primers. These primers cover two highly conserved regions (VLVPLCGK, from position 41 and YDRAA, from position 126) of TPM sequences, that are also conserved in the KF707 translated sequence.

A BLASTX search of the NCBI protein database showed that ORF -1 displayed high homology to the *tpm* genes of other bacterial species, such as *Azotobacter vinelandii* AvOP (accession number ZP00417432, 62 %), *Pseudomonas fluorescens* PfO-1 (accession number YP349713, 58 %), *Pseudomonas entomophila* L48 (accession number YP607250, 58 %), and *Pseudomonas putida* KT2440 (accession number NP744025, 57 %) and *Pseudomonas aeruginosa* PAO1 (accession number NP251522, 57 %).

Figure 5.4 shows a multiple alignment of protein sequences homologous to the putative KF707 *tpm* ORF. Sequences with at least 47 % homology were included. It can be noted that the aligned sequences present highly conserved aminoacid regions such as VLVPLCGKSLD (from position 40, corresponding to the PTCF2 primer), GDFFAL (from position 105), YDRAA (from position 121, corresponding to PTCR2 primer) and GPPFSVP (from position 166).

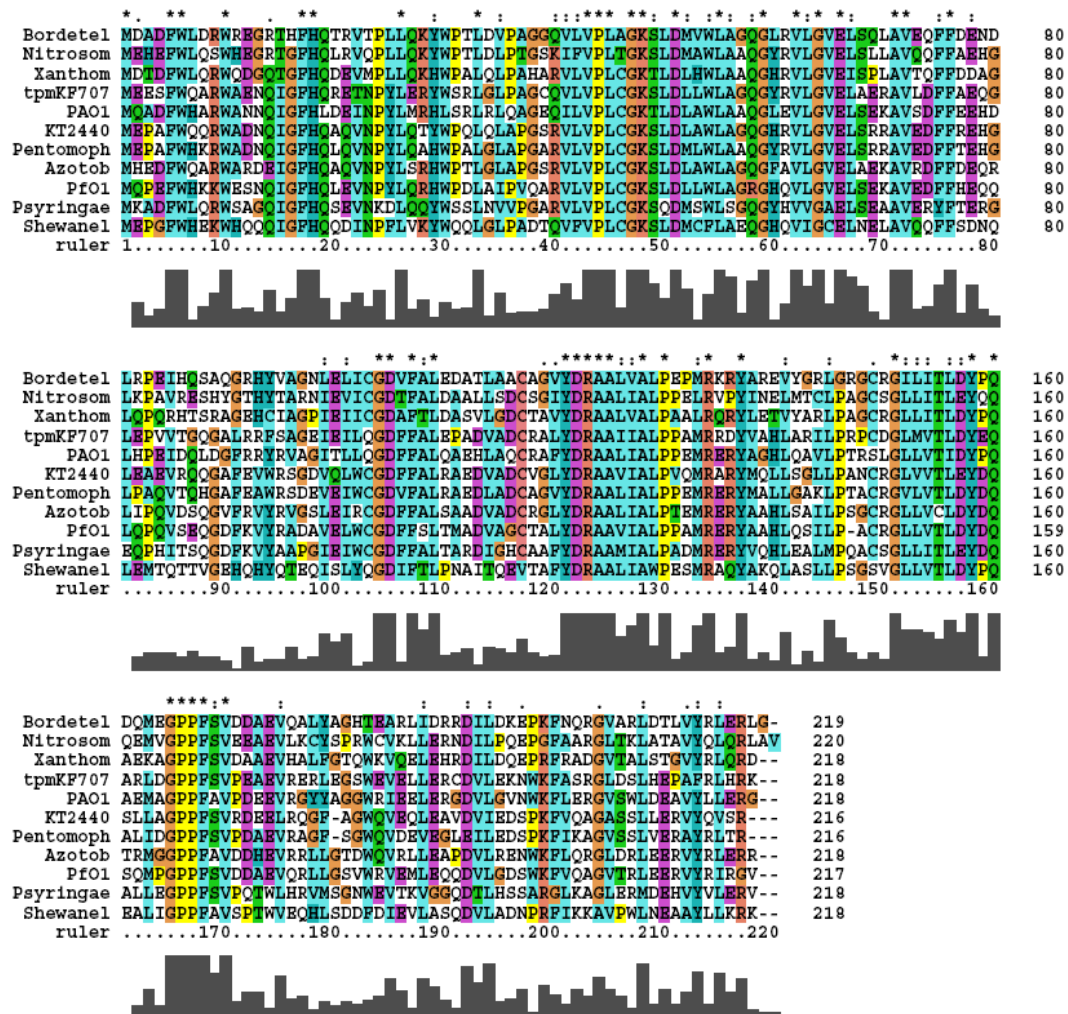


Figure 5.4. Multiple alignment of thiopurine methyltransferases sequences. Sequences were aligned using ClustalW program. Nomenclature and DNA sequence accession numbers are as follows: Bordetel, *B. pertussis* (YP748454); Nitrosom, *N. eutropha* (NP879683); Xanthom, *X. campestris* pv. *Campestris* (NP636768); tpmKF707, *Ps. pseudoalcaligenes* KF707 ORF -1 deduced sequence; PAO1, *Ps. aeruginosa* PAO1 (NP251522); KT2440, *Ps. putida* KT2440 (NP744025); Pentomoph, *Ps. entomophila* L48 (YP607250); Azotob, *A. vinelandii* AvOP (ZP00417432); Pfo1, *Ps fluorescens* Pfo-1 (YP349713); Psyringae, *Pseudomonas syringae* pv. *psi* (YP236687); Shewanel, *S. baltica* OS155 (ZP01433693).

The tertiary structure (3D) of the bacterial TPM from *Pseudomonas syringae* pv. *pisi*, that is coded by the *tpm* Te^R determinant isolated by Cournoyer and colleagues (1998), has been recently determined using NMR spectroscopy (Scheuermann *et al.* 2003). The 3D structure of the bacterial TPM enzyme revealed a classical SAM-dependent methyltransferase topology, consisting of a seven-stranded β -sheet flanked by α -helices on both sides (Figure 5.5 C) (Scheuermann *et al.* 2003). On the basis of aminoacid sequence and 3D structure of the TPM enzyme of *Pseudomonas syringae* pv. *pisi*, a model of *Ps. pseudoalcaligenes* KF707 TPM putative protein 3D structure was produced using Modeller program (Marti-Renom *et al.* 2000, <http://salilab.org/modeller>) (Figure 5.5 A). This structure corresponds well with the 3D structure and topology of *Ps. syringae* pv. *pisi* TPM enzyme (psTPM, Figure 5.5 C). In both psTPM and KF707 putative TPM structure, an extended N-terminus is present. These N-terminal residues were found to be critical for psTPM activity and are considered to play a role in substrate recognition (Scheuermann *et al.* 2003). Moreover, similarly to psTPM protein, the modelled 3D structure of KF707 putative TPM protein contains two additional β -strands and one α -helix that are characteristic of psTPM topology (Figure 5.5 C). The two loops and β -strands coloured in dark blue in Figure 5.5 A are proposed to belong to the SAM binding site in psTPM (Scheuermann *et al.* 2003) and correspond to the aminoacidic residues highly conserved among TPM sequences (Figure 5.4). Important conserved cysteine residues are shown in yellow (Figure 5.5 A). The analysis of the KF707 putative *tpm* ORF suggested that the isolated *EcoRI* fragment in the pTPM plasmid is likely to code for a *tpm* Te^R resistance determinant.

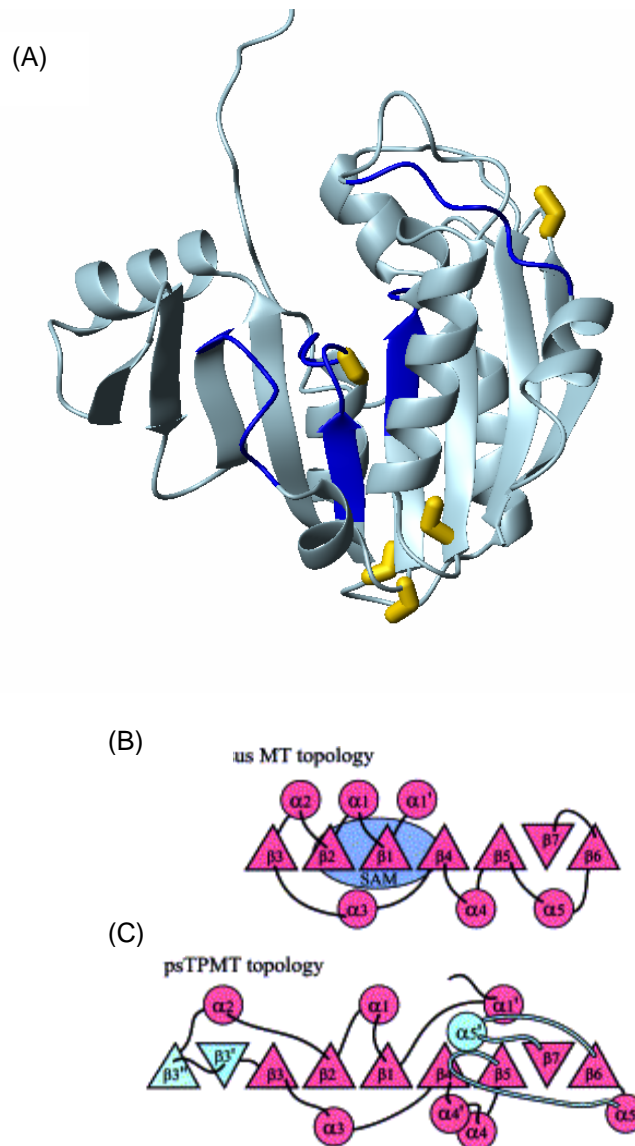


Figure 5.5. Model of the 3D structure of *Ps. pseudoalcaligenes* KF707 putative TPM enzyme (A). The topology of *Ps. syringae* pv. *pisi* protein (psTPM) (C) is shown and compared to the consensus topology of classical SAM-dependent methyltransferases (B) (MT consensus from Wang *et al.* 2000). Elements of the common core fold are in pink while the inserted elements of psTPM, putatively shared with KF707 TPM modelled structure, are in cyan. Topological graphs in B and C panels are from Wang *et al.* 2000 and Scheuermann *et al.* 2003.

***Role of Ps. pseudoalcaligenes* KF707 TPM enzyme in tellurite resistance**

The MIC of potassium tellurite linked to the activity of KF707 putative TPM enzyme was measured in LB medium containing increasing concentration of potassium tellurite. MIC determination was carried out for *E. coli* DH5 α cells harboring pTPM, pTPMKO and pUC18 plasmids. pTPM contains the 900 bp

EcoRI genomic fragment coding for the KF707 *tpm* putative ORF, pTPMKO contains the same KF707 genomic fragment in which the ORF was inactivated by the insertion of a Km resistance cassette and pUC18 is the control cloning vector. As a control, the MIC of TeO_3^{2-} of wild type *E. coli* DH5 α was also measured. The presence of the pTMP plasmid increased tellurite MIC from 1 ~ $\mu\text{g/ml}$ to more than 25 $\mu\text{g/ml}$. The inactivation of the *tpm* putative ORF caused the MIC to decrease to the value of wild-type *E. coli* DH5 α cells and those transformed with pUC18 cloning vector, thus abolishing the protection from tellurite toxicity conferred by KF707 TPM putative enzyme. These observations confirmed that the pTPM plasmid codes for a tellurite resistance determinant. It is interesting to note that the presence of the pTPM plasmid in *E. coli* DH5 α cells caused the emanation of a strong garlic odour. Notably, *E. coli* colonies formed on LB agar plates containing tellurite were not subjected to blackening during the first 24 h of growth, suggesting that the presence of TPM enzyme activity may prevent the interaction of tellurite with its cellular targets and the reduction to the elemental form.

In an attempt to assess the role of the isolated *tpm* Te^{R} determinants in KF707 resistance to tellurite, we tried to isolate a KF707 *tpm::Km* mutant strain. The *tpm::Km* insertion cassette was cloned in the pRK415 conjugative plasmid that was transferred into KF707 wild-type cells. Several double-crossover recombinants were isolated but none of them displayed the expected Km cassette insertion into the *tpm* gene region (as confirmed by both PCR and Southern blot). Therefore, the role of the *tpm* gene in KF707 resistance to tellurite could not be assessed. Also, the role of the highly conserved TPM enzyme in KF707 physiology could not be investigated and is presently unknown. Work is in progress, aimed at the isolation of *tpm* mutants constructed by *tpm* gene replacement.

Expression of the tpm gene in Ps. pseudoalcaligenes KF707 cells exposed to tellurite and selenite

The transcriptional activity of the KF707 *tpm* gene was assayed under conditions of exposure to tellurite and selenite. Exponentially growing cells of KF707 were treated with 6.3 mM selenite and 10 μ M tellurite and total RNA was extracted after 0, 10 minutes and 30 minutes of exposure (Figure 5.6). As shown in Figure 5.6, *tpm* expression was not increased during the first 30 minutes of tellurite and selenite exposure, while a garlic odour was already emanated from 10 minute-exposed cultures. So, the expression of the *tpm* gene was not induced by tellurite and selenite oxyanions but TPM activity was already present in non-treated cultures, suggesting a constitutive expression of the TPM enzyme in KF707 cells. The hypothesis that the TPM enzyme plays a role in the basal metabolism will be investigated in future experiments.

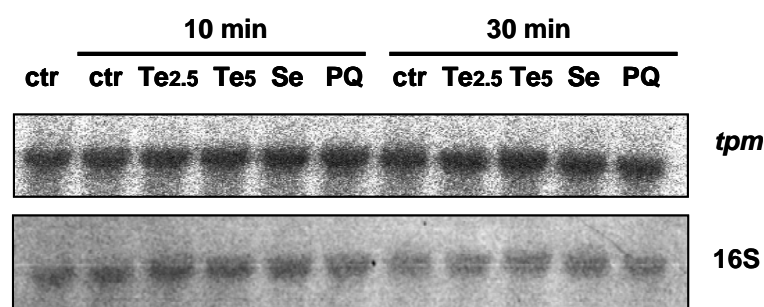


Figure 5.6. Transcriptional analysis of *tpm* gene expression in response to tellurite and selenite. Total RNA was isolated from cells treated with 2.5 and 5 μ g/ml TeO_3^{2-} (Te2.5, Te5), 6.3 mM SeO_3^{2-} (Se) and 2 mM paraquat (PQ) for 0, 10 and 30 minutes. The Northern blot was stripped with hot 0.1 % SDS and then hybridized with 16S DNA radiolabelled probe for loading calibration.

Discussion

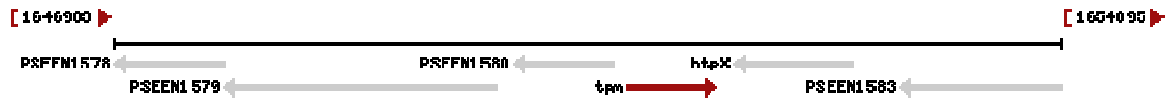
In this study, a tellurite resistance determinant was isolated from the tellurite resistant bacterium *Ps. pseudoalcaligenes* KF707, encoding for a SAM-dependent thiopurine methyltransferase highly homologous to the *tpm* Te^R resistance determinant of *Pseudomonas syringae* pv. *pisi* (Figure 5.1).

In bacteria, TPM was first isolated as a Te^R resistance determinant able to confer cross-resistance to selenium salts (Cournoyer *et al.* 1998). Bacterial TPM was then shown to be involved in the methylation of selenite and selenate into organoselenium compounds (DMSe and DMDS_e) (Ranjard *et al.* 2002). TPM activity was also detected in freshwater natural environments not subjected to selenium contamination, suggesting that the ability to methylate selenium compounds is a widespread feature of natural microbial communities (Ranjard *et al.* 2002). This observation is not surprising because the ability to counteract toxic metals is a widely distributed property in natural bacterial environments and is generally not a consequence of recent pollution from anthropogenic sources. In this respect, microbial natural communities are a precious source for their useful detoxification capabilities, that can be exploited to remediate hazardous polluted sites. As an example, microbial methylation of toxic Se salts is a well-accepted bioremediation strategy for the clean-up of contaminated areas (reviewed in Frankenberg and Arshad 2001) as it leads to the production of volatile DMSe and DMDS_e forms that are 500-700 times less toxic than other derivatives (Ganther *et al.* 1966).

The identification of a *tpm* determinant in *Ps. pseudoalcaligenes* KF707 is the first genetic evidence of the presence of a metal-resistance determinant in this bacterium. The research conducted so far has shown that the KF707 strain is highly tolerant to metalloids oxyanions such as selenite, arsenite and tellurite (see Chapter 2). Recent results show that the KF707 *tpm* sequence is adjacent to a *htpX* gene, coding for a 293 aminoacid heat-shock protein. The *tpm* and *htpX* genes are closely associated in other pseudomonads, thus suggesting that the genomic region in which these two genes are located could be involved in bacterial

adaptation to metalloids, as proposed also by Ranjard and colleagues (2003) (Figure 5.7).

Pseudomonas entomophila L48

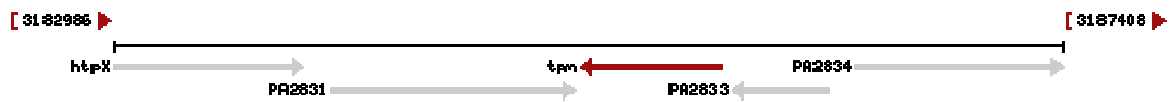


PSEEN1580: aromatic ring-opening dioxygenase

htpX: heat shock protein

PSEEN1583: aminotransferase

Pseudomonas aeruginosa PAO1



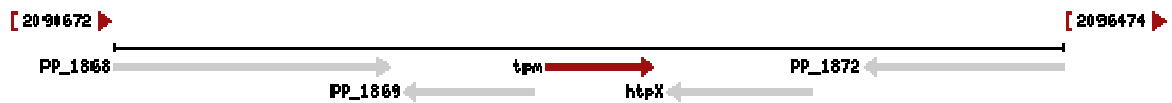
htpX: heat shock protein

PA2831: Predicted carboxypeptidase

PA2833: USP-like; Usp universal stress protein family

PA2834: LysR; Transcriptional regulator

Pseudomonas putida KT2440



PP_1868: ATP-dependent RNA helicase, DEAD box family

htpX: heat shock protein

PP_1872: aspartate aminotransferase

Pseudomonas syringae pv *psis*



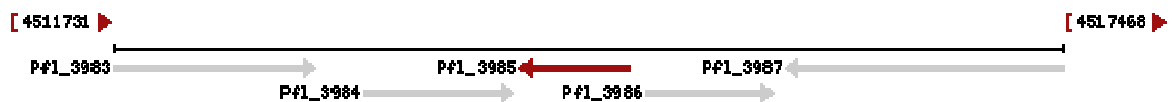
Psy_3615: aspartate aminotransferase

Psy_3616: heat shock protein HtpX

Psy_3618: Catalytic LigB subunit of aromatic ring-opening dioxygenase

Psy_3619: Helicase, C-terminal:DbpA, RNA-binding:DEAD/DEAH box helicase, N-terminal

Pseudomonas fluorescens PFO-1



Pfl_3983: Aminotransferase, class I and II

Pfl_3984: heat shock protein HtpX

Pfl_3986: Exradiol ring-cleavage dioxygenase, class III enzyme, subunit B

Figure 5.7. Analysis of genomic regions containing the *tpm* Te^R determinant in related pseudomonads.

However, we have observed that *tpm* gene expression is not induced by selenite and tellurite oxyanions and seems to be constitutive. This observation raises the question of whether this enzyme is specific to metalloid detoxification or, rather, if it is involved in other metabolic pathways. To this end, genomic regions of sequenced *Pseudomonas* genomes were searched in order to identify other gene functions commonly associated with *tpm* and *htpX* genes. Figure 5.7 shows that nucleic acid helicases, aromatic ring dioxygenases and aminotransferases are commonly and repetitively associated with the *tpm* gene. Recently, in cells of *R. capsulatus* B10 exposed to cadmium, the induction of aspartate aminotransferase and enzymes involved in basal metabolism was observed (El-Rab *et al.* 2006). Moreover, resistance to arsenite in *Ps. aeruginosa* was found to be dependent on the global regulator of carbon metabolism, Crc, (Parvatiyar *et al.* 2005), that also regulates chromosomal catabolic pathways of aromatic compounds (Morales *et al.* 2004). In order to understand the role of TPM in tellurite resistance, a *tpm* KF707 mutant strain will be constructed. In this way it will be possible to investigate both the endogenous metabolic function of this highly represented gene and the hypothesis that resistance to tellurite results from a secondary function of TPM activity.

Conclusions

Life on Earth evolved sometime around 3.5 billion years ago in what can be defined as an 'extreme' environment, characterized by volcanic emissions and release of toxic metals. For as long as 2 billion years, bacteria were the Earth's only form of life, for which the ability to adapt to harsh conditions was the only possible strategy of survival. Therefore, it is likely that metal resistance determinants and complex metabolic pathways arose soon after life began and not as a consequence of recent industrialization.

Knowledge of the mechanisms governing bacterial adaptation to an ever-changing environment has long been confined to the study of microorganisms as free-suspended cells. However, recent studies have revealed that bacteria can grow in association with surfaces and that this mode of growth, known as biofilm, is likely to affect bacterial physiology and to improve survival in stressful conditions. By exploiting the adaptable nature of bacteria and their ability to form resilient multicellular communities, it may be possible to resolve the increasing problem arising from pollution, which today derives from environmental and anthropogenic activities.

In the past decades, numerous xenobiotic compounds have been found to be susceptible to microbial degradation and in most cases the catabolic pathways and their regulation have been characterized. *Pseudomonas pseudoalcaligenes* KF707 was isolated from a site heavily polluted by polychlorinated biphenyls in Kyushu island in Japan. Previous studies have focused on the biochemistry and genetics of PCB metabolism in strain KF707 (reviewed in Furukawa and Kimura 1995) but did not take into account other aspects of the bacterium's physiology that can improve the overall result of degradation processes.

The studies detailed in this thesis were aimed at extending what is known about the physiology of *Ps. pseudoalcaligenes* KF707 beyond its ability to degrade toxic xenobiotics. In particular, the following aspects were investigated:

- I. Biofilm formation, nutritional requirements and involvement of the CheA-regulated signalling pathway in the development of a mature structure (Chapter 1).

- II. Tolerance to toxic metals in both planktonic and biofilm mode of growth (Chapter 2).
- III. Global analysis of the effects of tellurite on bacterial physiology and of the cellular factors involved in KF707 tolerance to this metalloid oxyanion (Chapter 3-5).

I-II. Biofilm formation and tolerance to toxic metals

The formation of *Pseudomonas pseudoalcaligenes* KF707 biofilm communities follows a general four-step developmental model, in which cell aggregates display distinct morphological traits at each step. Biofilm formation in KF707 is metabolically regulated. Minimal media compositions and high salinity trigger the production of dense multicellular structures that are less subjected to dispersal and more tolerant to biocides in comparison to biofilms formed in rich media. This response to different media compositions and high osmolarity may reflect the natural habitat to which this species is adapted. In this respect, the driving force for biofilm formation could be the colonization of favourable environmental niches. In natural environments, surfaces preferentially accumulate proteins, polysaccharides and other molecules, forming a nutritionally rich zone that is metabolically favourable for bacterial cells (Lengeler *et al.* 1999). The ability to direct movement against the flow and towards these surfaces via chemotaxis could be required for the successful colonization. Chemotaxis has been shown to be important during colonization and biofilm formation in both the human host and the environment (de Weert *et al.* 2002, Foyne *et al.* 2000, Kirov *et al.* 2004, Stelmach *et al.* 1999). However, chemotaxis was considered to be dispensable for biofilm formation in bacterial species such as *E. coli* (Pratt and Kolter 1998). The analysis of biofilm formation in the KF707 *cheA* chemotactic mutant shows that the CheA-regulated signalling pathway plays a role in the progression of biofilm formation from the early stage of microcolony to the production of a mature structure. Chemotaxis could be required not only for swimming towards the plastic surface but also for coordinating the aggregation of microcolonies. This work adds evidence to the observation that the molecular requirements for biofilm formation are different and differentially regulated in a

species-specific manner (Stanley and Lazazzera 2004). Chemotaxis has proven to be a selective advantage for the environmental fitness of degradative bacteria (reviewed in Pandey and Jain, 2002). Therefore, future studies will be aimed at the characterization of chemotaxis towards biphenyl and of the ability of KF707 cells to form biofilms in the presence of biphenyl as the sole carbon source. Given that biofilm growth in minimal media provides KF707 with increased tolerance to antibiotics and metals, it would be interesting to analyze KF707s' ability to cope with PCB toxicity in both biofilm and planktonic modes of growth. The tolerant state of KF707 cells within a biofilm could provide physiological, metabolic and genetic responses overcoming PCBs toxic effects.

Numerous factors have been shown to contribute to the increase of biofilm tolerance to antimicrobial killing (Lewis 2001, Harrison *et al.* 2005c). An open question is whether highly structured biofilm communities are more resilient than flat biofilms. The analysis of KF707s' tolerance to antibiotics has shown that cellular metabolism, more than structure, plays a key role in the development of KF707 biofilm tolerance. Indeed, biofilms grown in minimal medium are highly tolerant to antibiotics soon after attachment to the surface, suggesting that cell adherence may cause a reprogramming of bacterial physiology. However, this adaptation of bacterial cells during the surface-associated mode of growth was not apparent in rich medium. One may argue that, somehow, growth in LB results in the uncoupling of the attachment to a surface with the development of antimicrobial tolerance. It would be interesting to understand to what extent this effect is encoded by the genome, dependent on signalling circuits that affect protein activities or associated to a specific metabolic state.

Unlike what has been observed for tolerance of KF707 biofilms to antibiotics, cell attachment to the plastic surface did not provide increased tolerance to metal toxicity. Moreover, biofilms growing in minimal medium were at most two times more resistant than planktonic cells. These data indicate that biofilm tolerance to antibiotics and to metals is likely to originate from different mechanisms. However, it is interesting to note that low nutrient availability not only does not limit KF707 ability to form a biofilm, but also this condition provides KF707 biofilms with a tolerant phenotype to environmental stresses.

From the data obtained in this study we may expect KF707 to be able to maintain a metabolic potential in metal-polluted sites. In particular, KF707 tolerance to selenite and arsenite oxyanions seems promising for decontamination of polluted and co-polluted soil. The potential beneficial effects of the use of this metal-tolerant strain in the remediation of areas polluted by both PCB and heavy metals will be the object of further experimental work.

III. Effects of tellurite on bacterial physiology and analysis of cellular factors involved in KF707 tolerance

The mechanisms of tellurite toxicity to bacterial cells have been recently defined as ‘an ancient enigma’ which is in the process of being unravelled (Pérez *et al.* 2007). The work produced in this study has contributed to a better understanding of tellurite toxicity. We have shown for the first time that tellurite causes the release of reactive oxygen species in the cytosol and we suggest that these ROS are mainly superoxide anions. Indeed, Pérez and colleagues have recently shown that tellurite toxicity to *E. coli* is linked to the release of $O_2^{\cdot-}$ by the direct observation of the inactivation of superoxide sensitive [Fe-S] enzymes such as aconitase, increased carbonyl content in cellular proteins and also generation of superoxide radicals during *in vitro* enzymatic reduction of potassium tellurite (Pérez *et al.* 2007). We have observed that exposure to tellurite results in the oxidation of cellular reduced thiols but also that the inhibition of the first enzyme for glutathione synthesis relieves tellurite toxicity. It could be hypothesized that the interaction of tellurite with glutathione may be a source of ROS. Therefore, the inhibition of glutathione synthesis could result in a reduction of the release of ROS and hence reduced toxicity. However, our data tend to show that the kinetics of ROS production and RSH oxidation are not strictly related. Experiments aiming to elucidate other targets of tellurite reactivity and the role of glutathione in the reduction of tellurite and ROS release are in progress. In this context, the role of the plasma membrane redox complexes as other possible targets for tellurite toxicity but also as ROS generators will be investigated.

In KF707, exposure to tellurite does not cause a strong activation of SOD activity. Moreover, non-lethal doses of tellurite show a synergistic effect on the

toxicity of oxidant agents as well as other metalloids oxyanions, such as selenite and arsenite. In this respect, it is possible to conclude that tellurite is extremely toxic to bacterial cells and that the main cellular response to an acute exposure is cell death rather than the activation of response systems. Indeed, we show that the activation of both heat shock and superoxide stress responses increase tolerance to tellurite, suggesting that multiple cellular functions may be affected by tellurite toxicity. During chronic exposures, a long lag phase is observed before cellular growth and adaptation occur. We have not identified yet the genetic nature of the population growing in the presence of tellurite, that is, it is not clear whether these cells are spontaneous resistant mutants or specialized survival cells with a wild-type genetic background. However, the adaptation is not lost when cells are grown for 5-10 generations in the absence of the metalloid. Experiments are in progress aimed at elucidating this aspect of KF707s' response to tellurite and the nature of cellular adaptation. We have isolated an hyper-resistant tellurite mutant which is able to grow in the presence of high concentrations of the oxyanion without displaying any initial lag phase. We have observed that this mutant has a very low rate of tellurite uptake, its membrane potential is less perturbed by tellurite exposure and the rate of thiol oxidation during exposure to tellurite is extremely low in comparison to wild-type cells. A possible explanation is that this adapted mutant has a reduced permeability to the oxyanion. The tellurite hyper-resistant mutant was observed to be more resistant to SDS and biocides such as cetylpyridinium chloride. Resistance to such substances is often linked to a different LPS and outer membrane protein compositions (Nakamura 1968, Hirai *et al.* 1987, Tattawasart *et al.* 2000). The hypothesis that adapted cells have a different outer membrane structure and reduced permeability will be further investigated.

Finally, we have identified a tellurite resistance determinant in KF707, coding for a thiopurine methyltransferase (TPM). The identification of the *tpm* determinant is the first genetic evidence of the presence of a metal-resistance determinant in this bacterium. However, we have observed that the expression of the *tpm* gene is not induced by selenite and tellurite oxyanions and seems to be constitutive. This observation raises the question of whether this enzyme is

Conclusions

specific to metalloids detoxification or if it is involved in other metabolic pathways. The construction of a *tpm* KF707 mutant strain has not been successful. This result may suggest that the TPM activity may be required for KF707 survival. A knock-in/knock-out strategy could be used to investigate the endogenous metabolic function of this gene, which is highly conserved from bacteria to man. In addition, the hypothesis that resistance to tellurite may result from a secondary function of TPM activity will be considered. Overall, the data collected in this study may suggest that *Pseudomonas pseudoalcaligenes* KF707 is able to withstand tellurite toxicity because of its innate biochemical makeup, which renders this microorganism intrinsically resistant. The slow rate of tellurite uptake and the presence of a TPM enzyme may be contributing factors raising KF707 resistance to tellurite above the levels of sensitive strains.

References

- Allesen-Holm M., Barken KB., Yang L., Klausen M., Webb JS., and Kjelleberg S. (2006) *Mol Microbiol* **59**: 1114-1128.
- Angle JS., and Chaney RL (1989) *Appl Environ Microbiol* **55**: 2101-2104.
- Apontoweil P., and Berends W. (1975) *Biochim Biophys Acta* **399**: 1-9.
- Arrigo AP. (1998) *Biol Chem* **379**: 19-26.
- Ascon-Cabrera MA., Ascon-Reyes DB. and Lebeault JM. (1995) *J Appl Bacteriol* **79**: 617-624.
- Attieh J., Sparace SA., and Saini HS. (2000) *Arch Biochem Biophys* **380**: 257-266.
- Avazeri C., Turner RJ., Pommier J., Weiner JH., Giordano G., and Vermeglio A. (1997) *Microbiology* **143**: 1181-1189.
- Baath E. (1989) *Water Air Soil Poll* **47**: 335-379.
- Babich H., and Stotzky G. (1983) *Adv Appl Microbiol* **29**: 6782-6790.
- Banjerdkij P., Vattanaviboon P., and Mongkolsuk S. (2005) *Appl Environ Microbiol* **71**: 1843-1849.
- Bébian M., Lagniel G., Garin J., Touati D., Verméglio A., and Labarre J. (2002) *J Bacteriol* **184**: 1556-1564.
- Beloin C., Valle J., Latour-Lambert P., Faure P., Kzreminski M., Balestrino D., Haagensen J., Molin S., Prensier G., Arbeille B., and Ghigo J-M. (2004) *Mol Microbiol* **51**: 659-674.
- Beloin C., and Ghigo J-M. (2005) *Trends Microbiol* **13**: 16-19.
- Bernas Y., Asem EK., Robinson JP., and Dobrucki JW. (2005) *Photochem Photobiol* **81**: 960-969.
- Beyenal H. and Lewandowski Z. (2004) *Water Res* **38**: 2726-2736.
- Bigger JW. (1944) *Lancet* **11**: 497-500.
- Boles JO., Cisneros RJ., Weir MS., Odom JD., Villafranca JE., and Dunlap RB. (1991) *Biochemistry* **30**: 11073-11080.
- Boles JO., Lewinski K., Kunkle MG., Hatada M., Lebioda L., Dunlap RB., and Odom JD. (1995) *Acta Cryst D Biol Crystal* **51**: 731-739.
- Bollinger N., Hassett DJ., Iglewski BH., Costerton JW., and McDermott TR. (2001) *J Bacteriol* **183**: 1990-1996.
- Borriello G., Werner E., Roe F., Kim AM., Ehrlich GD., and Stewart PS. (2004) *Antimicrob Agents Chemother* **45**: 2659-2664.
- Borsetti F., Tremaroli V., Michelacci F., Borghese R., Winterstein C., Daldal F., and Zannoni D. (2005) *Res Microbiol* **156**: 807-813.

References

- Borsetti F., Toninello A., and Zannoni D. (2003) *FEBS Letters* **554**: 315-318.
- Boyer HW., and Rolland-Dussoix D. (1969) *J Mol Biol* **41**: 459-472.
- Bradley DE. (1985) *J Gen Microbiol* **131**: 3135-3137.
- Branda SS., Chu F., Kearns DB., Losick R., and Kolter R. (2006) *Mol Microbiol* **59**: 1229-1238.
- Branda SS., Vik S., Friedman L., and Kolter R. (2005) *Trends Microbiol* **13**: 20-26.
- Bröer S., Ji G., Bröer A., and Silver S. (1993) *J Bacteriol* **175**: 3480-3485.
- Budisa N., Karnbrock W., Steinbacher S., Humm A., Prada L., Neuefeind T., Moroder L., and Huber R. (1997) *J Mol Biol* **270**: 616-623.
- Budisa N., Huber R., Golbik G., and Weyher E. (1998) *Eur J Biochem* **253**: 1-9.
- Caiazza NC., and O'Toole GA. (2004) *J Bacteriol* **186**: 4476-4485.
- Cánovas D., Cases I., and de Lorenzo V. (2003) *Environ Microbiol* **5**: 1242-1256.
- Carmel-Harel O., and Storz G. (2000) *Annu Rev Microbiol* **54**: 439-461.
- Carvalho MF., Vasconcelos I., Bull AT., and Castro PM. (2001) *Appl Microbiol Biotechnol* **57**: 419-426.
- Ceri H., Olson ME., Stremick C., Read RR., Morck DW., and Buret AG. (1999) *J Clin Microbiol* **37**: 1771-1776.
- Cervantes C., Ji G., Ramírez JL. Silver S. (1994) *FEMS Microbiol Rev* **15**: 355-367.
- Cervenka EA., and Cooper WC. (1961) *Arch Environ Health* **3**: 71-82.
- Challenger F. (1945) *Chem Rev* **36**: 315-361.
- Chasteen TG., and Bentley R. (2003) *ChemicalReviews* **103**: 1-25.
- Chavez FP., Lunsdorf H., and Jerez CA. (2004) *Appl Environ Microbiol* **70**: 3064-3072.
- Chourey K., Thompson MR., Morrell-Falvey J., VerBerkmoes NC., Brown SD., Shash M., Zhou J., Doktycz M., Hettich RL., and Thompson DK. (2006) *Appl Environ Microbiol* **72**: 6331-6344.
- Cochran WL., McFeters GA., and Stewart PS. (2000) *J Appl Microbiol* **88**: 22-30.
- Costerton JW., Lewandowski Z., Caldwell D., Korber D., and Lappin-Scott HM. (1995) *Annu Rev Microbiol* **49**: 711-745.
- Costerton JW., Lewandowski Z., de Beer D., Caldwell D., Korber D., and James G. (1994) *J Bacteriol* **176**: 2137-2142.
- Costerton JW., Cheng K-J., Geesey GG., Ladd T., Nickel JC., Dasgupta M., and Marrie T. (1987) *Annu Rev Microbiol* **41**: 435-464.
- Costerton JW. (2001) *Trends Microbiol* **9**: 50-52.
- Costerton JW., Stewart PS., and Greenberg EP. (1999) *Science* **284**: 1318-1322.

- Coulthard SA., and Hall AG. (2001) *Pharmacogenomics J* **1**: 254-261.
- Cournoyer B., Watanabe S., and Vivian A. (1998) *Biochim Biophys Acta* **1397**: 161-168.
- Crooke E., and Wickner W. (1987) *Proc Natl Acad Sci USA* **84**: 5216-5220.
- Crow JP. (1997) *Nitric Oxide Biol Chem* **1**: 145-157.
- Danese PN., Pratt LA., and Kolter R. (2000) *J Bacteriol* **182**: 3593-3596.
- Das JR., Bhakoo M., Jones MV., and Gilbert P. (1998) *J Appl Microbiol* **85**: 852-858.
- Davies DG., Parsek MR., Pearson JP., Iglewski BH., Costerton JW., and Greenberg EP. (1998) *Science* **280**: 295-298.
- Davies DG., Chakrabarty AM., and Geesey, GG. (1993) *Appl Environ Microbiol* **59**: 1181-1186.
- Davies DG., and McFeters GA. (1988) *Microbial Ecology* **15**: 165-175.
- de Beer D., Stoodley P., and Lewandowski Z. (1994) *Biotechnol Bioeng* **43**: 1131-1138.
- de Lorenzo V., Herrero M., Jacobzik U., and Timmis KN. (1990) *J Bacteriol* **172**: 6568-6572.
- de Lorenzo V. (1994) *Trends Biotechnol* **12**: 2-5.
- de Lorenzo V., and Timmis KN. (1994) *Methods Enzymol* **235**: 386-405.
- de Weert S., Vermeiren H., Mulders IHM., Kuiper I., Hendrickx N., Bloemberg GV., Vanderleyden J., De Mot R., and Lugtenberg BJJ. (2002) *Mol Plant-Microbe Interact* **15**: 1173-1178.
- Dejonghe W., Boon N., Seghers D., Top EM., and Verstraete W. (2001) *Environ Microbiol* **3**: 649-657.
- Deuerling E., Patzelt H., Vorderwülbecke S., Rauch T., Kramer G., Schaffitzel E., Mogk A., Schulze-Specking A., Langen H., and Bukau B. (2003) *Mol Microbiol* **47**: 1317-1328.
- Dey S., and Rosen BP. (1995) *J Bacteriol* **177**: 385-389.
- Di Tomaso G., Fedi S., Carnevali M., Manegatti M., Taddei C., and Zannoni D. (2002) *Microbiol* **148**: 1699-1708.
- Diels L., Spaans PH., Van Roy S., Hooyberghs L., Ryngaert A., Wouters H., Walter E., Winters J., Macaskie L., Finlay J., Pernfuss B., Woebking H., Pümpel T., and Tsezos M. (2003) *Hydrometallurgy* **71**: 235-241.
- Diels L., Sadouk A., and Mergeay M. (1989) *Toxicol Environ Chem* **23**: 79-89.
- Diels L., and Mergeay M. (1990) *Appl Environ Microbiol* **56**: 1485-1491.
- Diorio C., Cai J., Marmor J., Shinder R., and DuBow MS. (1995) *J Bacteriol* **177**: 2050-2056.
- Donahue JL., Moses-Okpodu C., Cramer CL., Grabau EA., and Alsscher RG. (1997) *Plant Physiol* **113**: 249-257.

References

- Donlan RM., and Costerton JW. (2002) *Clin microbiol Rev* **15**: 167-193.
- Dunne WM., Mason EO., and Kaplan SL. (1993) *Antimicrob Agents Chemother* **37**: 2522-2526.
- Dyllick-Brenzinger M., Liu M., Winstone TL., Taylor DE., and Turner RJ. (2000) *Biochem Biophys Res Comm* **277**: 394-400.
- Elion GB. (1989) *Biosci Rep* **9**: 509-529.
- El-Rab SMFG., Shoreit AA., and Fukumori Y. (2006) *Biosci Biotechnol Biochem* **70**: 2394-2402.
- Evans RC., and Holmes CJ. (1987) *Antimicrob Agents Chemother* **31**: 889-894.
- Ewalt KL., Hendrick JP., Houry WA., and Hartl FU. (1997) *Cell* **90**: 491-500.
- Favre-Bronté S., Ranjard L., Colinin C., Prigent-Combaret C., and Cournoyer B. (2005) *Environ Microbiol* **7**: 153-164.
- Ferianc P., Farewell A., and Nyström T (1998) *Microbiology* **144**: 1045-1050.
- Figurski D., and Helinski D. (1979) *Proc Natl Acad Sci USA* **76**: 1648-1652.
- Fisher SL., Jiang W., Wanner BL., and Walsh CT. (1995) *J Biol Chem* **270**: 23143-23149.
- Fletcher M. (1996) in *Bacterial Adhesion: Molecular and Ecological Diversity*. Fletcher M. (ed.) John Wiley and sons, NY, pp. 1-24.
- Foynes S., Dorrel N., Ward SJ., Stabler RA., McColm AA., Rycroft AN., and Wren BW. (2000) *Infect Immun* **68**: 2016-2023.
- Frankenberger WT., and Arshad M. (2001) *BioFactors* **14**: 241.
- Frazzon J., and Dean DR. (2001) *Proc Natl Acad Sci USA* **98**: 14751-14753.
- Fridovich I. (1995) *Annu Rev Biochem* **64**: 97-112.
- Furukawa K., and Kimura N. (1995) *Environ Health Perspect* **103**: 21-23.
- Furukawa K., and Miyazaki T (1992) *J Bacteriol* **166**: 392-398.
- Fux CA., Costerton JW., and Stoodley P. (2005) *Trends Microbiol* **13**: 34-40.
- Ganther HE. (1971) *Biochemistry* **10**: 4089-4098.
- Ganther HE., Levander OA., and Sauman CA. (1966) *J Nutr* **88**: 55-60.
- Gérard-Monnier D., and Chaudière J. (1996) *Pathol Biol* **44**: 77-85.
- Ghiorse WC., and Wilson JJ. (1988) *Adv Appl Microbiol* **33**: 107-172.
- Gilbert P., Das J., and Foley I. (1997) *Adv Dent Res* **11**: 160-167.
- Gilson E., Alloing G., Schmidt T., Claverys J-P., Dudler R., and Hofnung M. (1988) *EMBO J* **7**: 3971-3974.
- Gjermansen M., Ragas PC., Sternberg C., Molin S., and Tolker-Nielsen T. (2005) *Mol Microbiol* **7**: 894-906.
- Griffith OW., and Meister (1979) *J Biol Chem* **254**: 7558-7560.

- Griffith PC., and Fletcher M. (1991) *Appl Environ Microbiol* **57**: 2186-2191.
- Gristina AG., Hobgood CD., Webb LX., and Myrvik QN. (1987) *Biomaterials* **8**: 423-426.
- Hanahan D., (1983) *J Mol Biol* **166**: 557-580.
- Harrison JJ., Turner RJ., and Ceri H. (2005a) *BMC Microbiol* **5**: 53.
- Harrison JJ., Turner RJ., and Ceri H. (2005b) *Environ Microbiol* **7**: 981-994.
- Harrison JJ., Ceri H., Roper NJ., Badry EA., Sproule KM., Turner RJ (2005d) *Microbiol* **151**: 3181-3195.
- Harrison JJ., Ceri H., Yerly J., Stremick C., Hu Y., Martinuzzi R., and Turner RJ. (2006) *Biol Proced Online* **8**: 194-215.
- Harrison JJ., Ceri H., Stremick., and Rurner RJ. (2004a) *Environ Microbiol* **6**: 1220-1227.
- Harrison JJ., Ceri H., Stremick., and Rurner RJ. (2004b) *FEMS Microbiol Lett* **235**: 357-362.
- Harrison JJ., Turner RJ., and Ceri H. (2005c) *Rec Res Devel Microbiol* **9**: 33-55.
- Hassen A., Saidi N., Cherif M., and Boudabous A. (1998) *Biores Technol* **64**: 7-15.
- Heim S., Ferrer M., Heuer H., Regenhardt D., Nimtz M., and Timmis KN. (2003) *Microbiology* **5**: 1257-1269.
- Hellmann CO., Schweitzer O., Gerke C., Vanittanakom N., Mack D., and Gotz F. (1996) *Mol Microbiol* **20**: 1083-1091.
- Henis Y. (1987) in *Survival and dormancy of bacteria*, Henis Y. (ed.), John Wiley and sons, NY, pp. 1-108.
- Henrichsen J. (1972) *Bacteriol Rev* **36**: 478-503.
- Henrichsen J. (1983) *Annu Rev Microbiol* **37**: 81-93.
- Hentzer M., Teitzel GM., Balzer GJ., Heydorn A., Molin S., Givskov M., and Parsek MR. (2001) *J Bacteriol* **183**: 5395-5401.
- Herrero M., de Lorenzo V., and Timmis KN. (1990) *J Bacteriol* **172**: 6557-6567.
- Hesterkamp T., and Bukau B (1996) *FEBS Lett* **389**: 32-34.
- Higgins CF., Hyde SC., Mimmack MM., Gileadi U., Gill DR., and Gallagher MP. (1990) *J Bioenerg Biomembr* **22**: 571-592.
- Highsmith AK., and Abshire RL. (1975) *Appl Environ Microbiol* **36**: 596-601.
- Hinsa SM., Espinosa-Urgel M., Ramos JL., and O'Toole GA. (2003) *Mol Microbiol* **49**: 905-918.
- Hirai K., Suzue S., Irikura T., Iyobe S., and Mitsushashi S. (1987) *Antimicrob Agents Chemother* **31**: 582-586.
- Hoch JA. (2000) *Curr Opin Microbiol* **3**: 165-170.
- Hogan D., and Kolter R. (2002) *Curr Opin Microbiol* **5**: 472-477.

References

- Houry WA., Frishman D., Eckerskorn C., Lottspeich F., and Hartl FU. (1999) *Nature* **402**: 147-154.
- Huang C-T., Yu FP., McFeters GA., and Stewart PS. (1995) *Appl Environ Microbiol* **61**: 2252-2256.
- Igo MM., Ninfa AJ., and Silhavy TJ. (1989) *Genes Dev* **3**: 598-605.
- Ischiropoulos H., Gow A., Thom S., Kooy NW., Royall JA., and Crow JP. (1999) *Methods Enzymol* **301**: 367-373.
- Ji G., and Silver S. (1992) *Proc Natl Acad Sci USA* **89**: 7974-7978.
- Kalmokoff M., Lanthier P., Tremblay T-L., Foss M., Lau PC., Sanders G., Austin J., Kelly J., and Szymanski CM. (2006) *J Bacteriol* **188**: 4312-4320.
- Kataran E., Duncan TR., and Watnick PI. (2005) *J Bacteriol* **187**: 7434-7443.
- Kazy SK., Sar P., Singh SP., Sen AK., and D'Souza SF. (2002) *World J Microbiol Biotechnol* **18**: 583-588.
- Keasling JD., and Bang SW. (1998) *Curr Opin Biotechnol* **9**: 135-140.
- Keen NT., Tamaki S., Kobayashi D., and Trollinger D. (1988) *Gene* **70**: 191-197.
- Keren I., Shah D., Spoering A., Kaldalu N., and Lewis K. (2004a) *J Bacteriol* **186**: 8172-8180.
- Keren I., Kaldalu N., Spoering A., and Lewis K. (2004b) *FEMS Microbiol Lett* **230**: 13-18.
- Kessi J. (2006) *Microbiol* **152**: 731-743.
- Kessi J., and Hanselmann KW (2004) *J Biol Chem* **279**: 50662-50669.
- Kho DH., Yoo SB., Kim JS., Kim EJ., and Lee JK. (2004) *FEMS Lett* **234**: 261-267.
- Kim SK., Wilmes-Riesenberg MR., and Wanner, BL. (1996) *Mol Microbiol* **22**: 135-147.
- Kirisits MJ., and Parsek MR. (2006) *Cellular Microbiol* **8**: 1841-1849.
- Kirov SM., Castrision M., and Shaw JG. (2004) *Infect Immun* **72**: 1939-1945.
- Kitagawa M., Matsumura Y., and Tsuchido T. (2000) *FEMS Microbiol Lett* **184**: 165-171.
- Kitagawa M., Matsumura Y., and Tsuchido T. (2002) *Eur J Biochem* **269**: 2907-2917.
- Klausen M., Heydorn A., Ragas PC., Lambertsen L., Aaes-Jørgensen A., Molin S., and Tolker-Nielsen T. (2003) *Mol Microbiol* **48**: 1511-1524.
- Köhler T., Kocjancic Curty L., Barja F., van Delden C., and Pechère J-C. (2000) *J Bacteriol* **182**: 5990-5996.
- Korber DR., Lawrence JR., and Caldwell DE. (1994) *Appl Environ Microbiol* **60**: 1421-1429.
- Kosower NS., and Kosower EM. (1995) *Methods Enzymol* **251**: 123-133.

- Kramer GF., and Ames BN. (1988) *Mutat Res* **201**: 169-180.
- Kron T., Hansen C., and Werner E. (1991) *Trace Elem Electrolytes Health Dis* **5**: 239-244.
- Krynetski EY., and Evans WE. (2000) *Pharmacology* **61**: 136-146.
- Kuiper I., Bloemberg GV., Noreen S., Thomas-Oates JE., and Lugtenberg BJJ. (2001) *Mol Plant-Microbe Interact* **14**: 1096-1104.
- Labrenz M., and Banfield JF. (2004) *Microb Ecol* **47**: 205-217.
- Landry RM., An D., Hupp JT., Singh PK., and Parsek MR. (2006) *Mol Microbiol* **59**: 142-151.
- Langford PR., Sansone A., Valenti P., Battistoni A., and Kroll JS. (2002) *Methods Enzymol* **349**: 155-166.
- Lauber WM., Carroll JA., Dufield DR., Kiesel JR., Radabaugh MR., and Malone JP. (2001) *Electrophoresis* **22**: 906-918.
- Leichert LI., Scharf C., and Hecker M (2003) *J Bacteriol* **185**: 1967-1975.
- Lengeler JW., Drews G., and Schlegel HG. (1999) in *Biology of Prokaryotes*. Stuttgart: Blackwell Science.
- Lewis K. (2001) *Antimicrob Agents Chemother* **45**: 999-1007.
- Lewis K. (2005) *Biochemistry (Moscow)* **70**: 327-336.
- Liu M., Turner RJ., Winstone TL., Saetre A., Dyllick-Brenzinger M., Jickling G., Tari LW., Weiner JH., and Taylor DE. (2000) *J Bacteriol* **182**: 6509-6513.
- Lowry OH., Rosebrough NJ., Farr AL., and Randall RJ. (1951) *J Biol Chem* **193**: 265-275.
- Mah CT-H., and O'Toole GA. (2001) *Trends Microbiol* **9**: 34-39.
- Malik A. (2004) *Environ Int* **30**: 261-278.
- Marshall E., Stout R., and Mitchell R. (1971) *J Gen Microbiol* **68**: 337-348.
- Marti-Renom MA., Stuart A., Fiser A., Sánchez R., Melo F., and Sali A. (2000). *Annu Rev Biophys Biomol Struct* **29**: 291-325.
- Matsubara M., and Mizuno T. (1999) *Biosci Biotechnol Biochem* **63**: 408-414.
- McCord J., and Fridovich I. (1969) *J Biol Chem* **244**: 6049-6055.
- McFeters GA., Egli T., Wilberg E., Alder A., Schneider R., Suozzi M., and Giger W. (1990) *Water Res* **24**: 875-881.
- McKeehan WL., Hamilton WG., and Ham RG. (1976) *Proc Natl Acad Sci USA* **73**: 2023-2027.
- Meister A. (1974) in *The enzymes*, Boyer P. (ed), Academic New York, 3rd Ed., pp. 671-697.
- Mergeay M., Nies D., Schlegel HG., Gerits J., Charles P., and van Gijsegem F. (1985) *J Bact* **162**: 328-334.

References

- Mogk A., Tomoyasu T., Goloubinoff P., and Bukau B. (2001) *Mol Microbiol* **40**: 397-413.
- Mongkolsuk S., Vattanaviboon P., and Praitau W. (1997) *FEMS Microbiol Lett* **146**: 217-221.
- Morales G., Linares JF., Beloso A., Albar JP., Martinez JL., and Rojo F. (2004) *J Bacteriol* **186**: 1337-1344.
- Morgan R., Kohn S., Hwang S-H., Hassett DJ., and Sauer K. (2006) *J Bacteriol* **188**: 7335-7343.
- Morrison GM., Batley GE., and Florence TM. (1989) *Chem Britain* **8**: 791-795.
- Nakamura H. (1968) *J Bacteriol* **96**: 987-996.
- Newton GL., and Fahey RC. (1989) Viña J ed. CRC Press, Boca Raton FL, pp 69-77.
- Nickel JC., Ruseska I., Wright JB., and Costerton JW. (1985) *Antimicrob Agents Chemother* **27**: 619-624.
- Nies DH. (2000) *Extremophiles* **4**: 77-82.
- Nies DH. (1999) *Appl Microbiol Biotechnol* **51**: 730-750.
- Ninfa AJ., Ninfa EG., Lupas AN., Stock AM., Magasanik B., and Stock JB. (1988) *Proc Natl Acad Sci* **85**: 5492-5496.
- O'Toole GA., and Kolter R. (1998a) *Mol Microbiol* **28**: 449-461.
- O'Toole GA., and Kolter R. (1998b) *Mol Microbiol* **30**: 295-304.
- O'Toole GA., Gibbs KA., Hager PW., Phibbs PV., and Kolter R. (2000a) *J Bacteriol* **182**: 425-431.
- O'Toole GA., Kaplan H., and Kolter R. (2000b) *Annu Rev Microbiol* **54**: 49-79.
- Palleroni NJ. (1984) in *Bergey's Manual of Systematic Bacteriology*. Krieg NR. and Holt JG. (eds.) Williams and Wilkins, Baltimore, MD, USA, vol. 1, pp. 141-199.
- Pandey G., and Jain R. (2002) *Appl Environ Microbiol* **68**: 5789-5795.
- Pandza M., Baetens CH., Park T. Au, Kehyan M., and Martin A. (2000) *Mol Microbiol*. **36**: 414-423.
- Parkins MD., Ceri H., and Storey D. (2001) *Mol Microbiol* **40**: 1215-1226.
- Parvatiyar K., Alsabbagh EM., Ochsner UA., Stegemeyer MA., Smulian AG., Hei Hwang S., Jackson CR., McDermott TR., and Hassett DJ. *J Bacteriol* **187**: 4853-4864.
- Pérez JM., Calderón IL., Arenas FA., Fuentes DE., Pradenas GA., Fuentes EL., Sandoval JM., Castro ME., Elias AO., and Vásquez CC. (2007) *PLoS ONE* **2**: e211.
- Peterson GL. (1977) *Anal Biochem* **83**: 346-356.
- Pratt LA., and Kolter R. (1999) *Curr Opin Microbiol* **2**: 598-603.

- Pratt LA., and Silhavy TJ. (1995) in *Two component signal transduction*, Hoch JA. and Silhavy TJ. (eds), American Society for Microbiology Press, Washington, DC, pp. 105-127.
- Pratt LA., and Kolter R. (1998) *Mol Microbiol* **30**: 285-293.
- Prigent-Combaret C., Brombacher E., Vidal O., Ambert A., Lejeune P., Landini P., and Dorel C. (2001) *J Bacteriol* **183**: 7213-7223.
- Privalle CT., Kong SE., and Fridovich I. (1993) *Proc Natl Acad Sci USA* **90**: 2310-2314.
- Prosser BL., Taylor D., Dix BA., and Cleeland R. (1987) *Antimicrob Agents Chemother* **31**: 1502-1506.
- Puhakka JA., Melin ES., Järvinen KT., Koro PM., Rintala JA., Hartikainen P., Shieh WK., and Ferguson JF. (1995) *Water Sci Technol* **31**: 227-235.
- Ranjard L., Nazaret S., and Cournoyer B. (2003) *Appl Environ Microbiol* **69**: 3784-3790.
- Ranjard L., Prigent-Combaret C., Nazaret S., Cournoyer B. (2002) *J Bacteriol* **184**: 3146-3149.
- Rashid MH., and Kornberg A. (2000) *Proc Natl Acad Sci USA* **97**: 4885-4890.
- Reisner A., Haagensen MA., Schembri EL., Zechner EL., and Molin S. (2003) *Mol Microbiol* **48**: 933-946.
- Ren D., Bedzyk LA., Thomas SM., Ye RW., and Wood TK. (2004) *Appl Microbiol Biotechnol* **64**: 515-524.
- Sambrook J., Fritsch EF., and Maniatis T. (1989) in *Molecular cloning: a laboratory manual*, 2nd ed. Cold Spring Harbor Laboratory Press, Cold Spring Harbor, NY.
- Sandrin TR., Chech AM., and Maier RM. (2000) *Appl Environ Microbiol* **66**: 4585-4588.
- Sandrin TR., and Maier RM (2003) *Environ Health Perspect* **111**: 1093-1101.
- Sauer K., Camper KA., Ehrlich GD., Costerton JW., and Davies DG. (2002) *J Bacteriol* **184**: 1140-1154.
- Sauer K. (2003) *Genome Biol* **4**: 219.
- Schembri MA., Kjærgaard K., and Klemm P. (2003) *Mol Microbiol* **48**: 253-267.
- Scheuermann TH., Lolis E., Hodsdon ME. (2003) *J Mol Biol* **333**: 573-585.
- Schilderman PA., Maas LM., Pachen DM., de Kok TM., Kleinjans JC., and van Schooten FJ. (2000) *Environ Mol Mutagen* **36**: 79-86.
- Shamberger RJ. (1983) in *The biochemistry of selenium*. Plenum Press Inc, New York, NY.
- Shrout JD., Chopp DL., Just CL., Hentzer M., Givskov M., and Parsek MR. (2006) *Mol Microbiol* **62**: 1264-1277.

References

- Silhavy TJ., Berman ML., and Enquist LW. (1984) in *Experiments with gene fusions*. Cold Spring Harbor Laboratory, Cold Spring Harbor, N.Y.
- Silver S., and Phung LT. (1996) *Annu Rev Microbiol* **50**: 753-789.
- Silver S. (1998) *J Ind Microbiol Biotechnol* **1**: 1-12.
- Simon R., Priefer U., and Pühler A. (1983) *Biotechnology* **1**: 784-791.
- Singh R., Paul D., and Jain RK. (2006) *Trends Microbiol* **14**: 389-397.
- Southey-Pillig CJ., Davies DG., and Sauer K. (2005) *J Bacteriol* **187**: 8114-8126.
- Springael D., Diels L., Hooyberghs L., Kreps S., and Mergeay M. (1993) *Appl Environ Microbiol* **59**: 334-339.
- Springael D., Diels L., and Mergeay M. (1994) *Biodegradation* **5**: 343-357.
- Stanley NR., and Lazazzera B. (2004) *Mol Microbiol* **52**: 917-924.
- Stelmack PL., Gray MR., and Pickard MA. (1999) *Appl Environ Microbiol* **65**: 163-168.
- Stephen JR., Chang YJ., Macnaughton SJ., Kowalchuk GA., Leung KT., Flemming CA., and White DC. (1999) *Appl Environ Microbiol* **65**: 95-101.
- Stewart PS. (2002) *Int J Med Microbiol* **292**: 107-113.
- Stewart PS., and Costerton JW. (2001) *Lancet* **358**: 135-138.
- Stock JB., Lukat GS., and Stock AM. (1991) *Annu Rev Biophys Biophys Chem* **20**: 109-136.
- Stock JB., Ninfa AJ., and Stock AM. (1989) *Microbio Rev* **53**: 450-490.
- Storz G., Tartaglia LA., Farr SB., and Ames BN. (1990) *Trends Genet* **6**: 363-368.
- Summers AO., and Jacoby GA. (1977) *J Bacteriol* **129**: 276-281.
- Sutherland IW. (2001) *Microbiology* **147**: 3-9.
- Tabares LC., Bittel C., Carrillo N., Bortolotti A., and Cortez N. (2003) *J Bacteriol* **185**: 3223-3227.
- Taira K., Hirose H., Hayashida S., and Furukawa K. (1992) *J Biol Chem* **267**: 4844-4853.
- Tantaleán JC., Araya MA., Saavedra CP., Fuentes DE., Pérez JM., Calderón IL., Youderian P., and Vásquez CC. (2003) *J Bacteriol* **185**: 5831-5837.
- Tattawasart U., Maillard J-Y., Furr JR., and Russell AD. (2000) *Int J Antimicrob Agents* **16**: 233-238.
- Taylor DE. (1999) *Trends Microbiol* **7**: 111-115.
- Teitzel G., and Parsek MR. (2003) *Appl Environ Microbiol* **69**: 2313-2320.
- Thormann KM., Saville RM., Shukla S., Pelletier DA., Spormann AM. (2004) *J Bacteriol* **186**: 8096-8104.

- Tolker-Nielsen T., Brinch UC., Ragas PC., Andersen JB., Jacobsen CS., and Molin S. (2000) *J Bacteriol* **182**: 6482-6489.
- Travieso L., Pellon A., Bentez F., Sanchez E., Borja R., O'Farrill N., and Weiland P. (2002) *Biochem Eng J* **12**: 87-91.
- Tremaroli V., Fedi S., and Zannoni D. (2007) *Arch Microbiol* **187**: 127-135.
- Tremoulet F., Duche O., Namane A., Martinie B., and Labadie JC. (2002) *FEMS Microbiol Lett* **210**: 25-31.
- Trutko AM., Akimenko VK., Suzina NE., Anisimova LA., Shlyapnikov MG., Baskunov BP., Duda VI., and Boronin AM. (2000) *Arch Microbiol* **173**: 178-186.
- Tseng AL., Srikhanta Y., McEwan AG., and Jennings MP. (2001) *Mol Microbiol* **40**: 1175-1186.
- Tuomanen E., Cozens R., Tosch W., Zak O., and Tomasz A. (1986) *J Gen Microbiol* **132**: 1297-1304.
- Turner RJ., Weiner JH., and Taylor DE. (1997) *Antimicrob Agents Chemother* **41**: 440-444.
- Turner RJ., Weiner JH., and Taylor DE. (1992a) *Anal Biochem* **204**: 292-295.
- Turner RJ. (2001) *Recent Res Dev Microbiol* **5**: 69-77.
- Turner RJ., Aharonowitz Y., Weiner J., and Taylor DE. (2001) *Can J Microbiol* **47**: 33-40.
- Turner RJ., Weiner JH. and Taylor DE. (1995) *Can J Microbiol* **41**: 92-98.
- Turner RJ., Aharonowiwitz Y., Weiner JH., and Taylor DE. (2001) *Can J Microbiol* **47**: 33-40.
- Turner RJ., Weiner JH., and Taylor DE. (1999) *Microbiology* **145**: 2549-2557.
- Turner RJ., Weiner JH., and Taylor DE. (1998) *BioMetals* **11**: 223-227.
- Turner RJ. Hou Y., Weiner J., and Taylor DE. (1992b) *J Bacteriol* **174**: 3092-3094.
- Valls M., Atrian S., de Lorenzo V., and Fernandez LA. (2000) *Nat Biotechnol* **18**: 661-665.
- Vandevivere P., and Kirchman DL. (1993) *Appl Environ Microbiol* **59**: 3280-3286.
- Verhamme DT., Arents JC., Postma PW., Crielaard W., and Hellingwerf KL. (2002) *Microbiology* **148**: 69-78.
- von Canstein H., Li Y., Timmis KN., Deckwer W-D., and Wagner-Döbler I. (1999) *Appl Environ Microbiol* **65**: 5279-5284.
- Wadhams GH., and Armitage JP. (2004) *Nature Rev* **5**: 1024-1037.
- Walters MC., Roe F., Bugnicourt A., Franklin MJ., and Stewart PS. (2003) *Antimicrob Agents Chemother* **47**: 317-323.

References

- Wang H., Boisvert d., Kim KK., Kim R., and Kim SH. (2000) *EMBO J* **19**: 317-323.
- Wanner BL. (1992) *J Bacteriol* **174**: 2053-2058.
- Watnick PI., and Kolter R. (1999) *Mol Microbiol* **34**: 586-596.
- Weinshilboum R. (2001) *Drug Metab Dispos* **29**: 601-605.
- Wen ZT., Suntharaligham P., Cvitkovitch D., and Burne RA. (2005) *Infect Immun* **73**: 219-225.
- Wentland EJ., Stewart PS., Huang C-T., and McFeters GA. (1996) *Biotechnol Prog* **12**: 316-321.
- Westenberg D., and Guerinot M. (1997) *Adv Genet* **36**: 187-238.
- Whitchurch CB., Tolker-Nielsen T., Ragas PC., and Mattick JS. (2002) *Science* **295**: 1487.
- White C., and Gadd GM. (1998) *Microbiology* **144**: 1407-1415.
- White C., and Gadd GM. (2000) *FEMS Microbiol Lett* **183**: 313-318.
- Yaku H., Kato M., Hakoshima T., Tsuzuki M., and Mizuno T. (1997) *FEBS Lett* **408**: 337-340.
- Yildiz FH., and Schoolnik GK. (1999) *Proc Natl Acad Sci USA* **96**: 4028-4033.
- Yu HS., and Alam M. (1997) *FEMS Microbiol Lett* **156**: 265-269.
- Yurkov V., Jappé J., Vermeglio A. (1996) *Appl Environ Microbiol* **62**: 4195-4198.
- Zanaroli G., Fedi S., Carnevali M., Fava F., and Zannoni D. (2002) *Res Microbiol* **153**: 353-360.

Sitography

TIGR database	http://tigrblast.tigr.org/cmz
NCBI database	http://www.ncbi.nlm.nih.gov
<i>Pseudomonas</i> database	http://www.pseudomonas.com
U.S. Environmental Protection Agency (EPA), Superfund sites	http://www.epa.gov/superfund
Agency for Toxic Substances & Disease Registry (ATSDR), CERCLA priority list of hazardous substances	http://www.atsdr.cdc.gov/cercla
Oak Ridge Field Research Centre (ORFRC)	http://www.esd.ornl.gov/nabirfrc
MASCOT search engine	http://www.matrixscience.com
ORF FINDER program	http://bioinformatics.org/sms2/orf_find.html
MODELLER program	http://salilab.org/modeller
DNA sequencing service	http://www.bmr-genomics.it